Table of Contents

Collaborating Departments and Institutions

Individuals from the following departments and institutions (listed alphabetically) collaborated with Center for Radiological Research staff in the above research abstracts (for individual attributions see specific reports):

Collaborating Columbia University Departments:

- **Department of Environmental Health Sciences, Joseph Mailman School of Public Health**
- **Department of Radiation Oncology**
- **Department of Ophthalmology, Eye Radiation & Environmental Health Laboratory**
- **Department of Urology**

Collaborating Institutions:

- **Albert Einstein College of Medicine, New York, NY**
- **Colorado State University, Dept. of Environmental and Radiological Health Sciences, Fort Collins, CO**
- **Louisiana Accelerator Center, University of Louisiana at Lafayette, Lafayette, LA**
- **National University of Singapore, Department of Physiology, Singapore**
- **Pace University (undergraduate research trainee)**
- **Radiological Society of North America, Oak Brook, IL**
- **Southern Urals Biophysics Institute, Ozyorsk, Russia**
- **University of Tarapaca, Arica, Chile**
- **University of Wisconsin, Madison, WI**

Acknowledgments

Research at the Center for Radiological Research, College of Physicians & Surgeons of Columbia University, is supported by competitively awarded grants from:

- **American Cancer Society**
- **Avon**
- **Department of Energy, Low Dose Radiation Research Program, Biological & Environmental Research**
- **Department of Health and Human Services, National Institutes of Health:**
  - **National Cancer Institute [Program Project (PO1) and Individual Research Grants (RO1s)]**
  - **National Institute of Bioimaging and Bioengineering (P41)**
  - **National Institute of Environmental Health Sciences (RO1s)**
  - **National Institute of General Medical Sciences (RO1)**
- **Herbert Irving Comprehensive Cancer Center of Columbia University**
- **National Aeronautics and Space Administration**
- **Radiological Society of North America**

Web Sites

- **Center for Radiological Research** ..... **http://crr-cu.org**
- **Radiological Research Accelerator Facility** ..... **http://www.raraf.org**
- **Web-Rad-Train** ..... **http://www.web-rad-train.org**
- **Department of Radiation Oncology** ..... **http://cpmcnet.columbia.edu/dept/radoncology**
- **Radiation Safety Office** ..... **http://cpmcnet.columbia.edu/dept/radsafety**

Introduction

The Center for Radiological Research of Columbia University epitomizes a multidisciplinary approach toward understanding, at both basic and applied levels, the biological consequences of ionizing radiation exposures as they relate to human health.

The Center's staff includes an interdisciplinary mix of professional scientists from fields as diverse as molecular biology, cell biology, radiation physics, computational physics, engineering and radiation oncology, performing research in experimental biophysics, cellular and microbeam studies, molecular and chromatin studies, and physics and biology related to both low dose radiation and radiation therapy-modeling.

This report summarizes the principal research initiatives and academic activities during the past year. There are a number of major research initiatives that have borne fruit during the past year.

Evaluations of long-lived chromosomal changes in personnel exposed to low and/or high LET radiation at Mayak Production Association, in Ozersk, Russia, were carried out using state-of-the-art FISH technology. High LET (Pu-α exposure) led to numerous complex chromosomal interchanges (as assessed by multiplex FISH) and to many chromosomal intrachanges (by m-band FISH). This latter category was sparse in gamma ray exposed individuals. Such changes may provide both dose and radiation specific biomarkers of past exposure.

The pursuit of the mechanisms of radiation carcinogenesis resulted in the identification of a novel tumor suppressor function of the Betaig-H3 gene in radiation induced tumorigenic human bronchial epithelial cells, as well as in a variety of human cancer lines.

The study of the RAD9 gene has led to the construction of knockout mouse cells and whole animals, as well as the demonstration that this mammalian gene plays a key role in the cellular response to DNA damage, the maintenance of genomic integrity, and is essential for proper embryonic development.

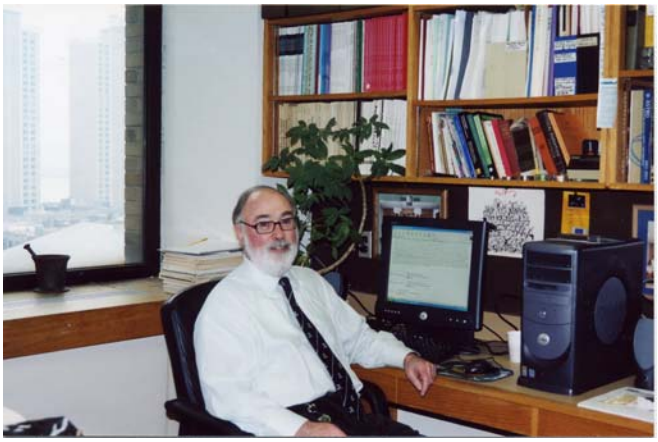

Dr. Charles R. Geard in his office hard at work.

Left to right: Dr. David J. Brenner, Dr. Tom K. Hei and Dr. Eric J. Hall at the Center's annual holiday party.

During the year we were able to complete studies which demonstrate unequivocally that AT heterozygotes are sensitive to radiation. This applies to radiation induced cataracts in mice as well as to radiation induced oncogenic transformation in mouse embryo fibroblasts.

Some of the most exciting research involved the single particle microbeam facility and the "Bystander Effect," referring to biological effects in cells not themselves hit by an α-particle, but in close proximity to hit cells. The bystander effect has been demonstrated for a wide range of biological endpoints, including chromosomal aberrations, cell lethality, mutation, oncogenic transformation and gene expression. Attention now focuses on the mechanism(s) of this important effect, and the relative importance of direct cell-cell communication versus communication via released cytofactors.

The Center continues to be prolific in terms of producing a steady stream of scientific papers to peer-reviewed journals, including a few in high profile journals.

Faculty are often involved in organizing national and international meetings, and are frequently called upon to serve as consultants, reviewers or site visitors by government bodies.

The teaching activities of the Center include the teaching of radiation biology and radiation physics to undergraduates, medical students, graduate students in the School of Public Health, and residents in Radiation Oncology at Columbia-Presbyterian Medical Center, as well as a City-wide course for residents in Radiology.

The Center continues to enjoy cordial relations with our clinical colleagues in the Department of Radiation Oncology. Three residents completed research electives in the Laboratory, and laboratory researchers joined clinicians in preparing a renewal request for the program in Radiation Physics and Biology in the Herbert Irving Comprehensive Cancer Centers. CRR

CENTER FOR RADIOLOGICAL RESEARCH FACULTY AND STAFF

Front row (*l-r*): Ms. Diana Morrison, Dr. David Brenner, Dr. Howard Lieberman, Ms. Monique Rey, Dr. Eric Hall, Ms. Mary Coady, Dr. Charles Geard, Dr. Tom Hei.

2nd row: Dr. Yuxin C. Liu, Mr. Gary Johnson, Dr. Su-Xian Liu, Ms. Alison Groome, Mrs. Cui-Xia Kuan, Dr. Peng He, Ms. Heidy Hernandez, Ms. Xiaojian Wang, Ms. Marni Hall, Dr. Aiping Zhu, Dr. Gloria Calaf, Ms. Gloria Jenkins-Baker, Dr. Catherine Mitchell, Dr. Alan Bigelow, Ms. Annerys Rodriguez, Mr. Kurt Michel.

3rd row: Mr. Carl Elliston, Dr. Yuxin Yin, Dr. Haiying Hang, Mr. Robert Archigian, Dr. Debasish Roy, Mr. Ronald Baker, Dr. Stephen Mitchell, Mr. David Cuniberti, Dr. Chang-Qing Piao, Dr. Jianli Wang, Dr. Fu-ru Zhan, Dr. Adayabalam Balajee.

Back row: Mr. Moshe Friedman, Dr. Lubomir Smilenov, Dr. Rudranath Persaud, Dr. Brian Ponnaiya, Mr. Stephen Marino, Mr. Kevin Hopkins, Mr. Gregory Ross, Dr. Gerhard Randers-Pehrson, Dr. Oleg Belyakov, Dr. Yong-Liang Zhao, Dr. Hongning Zhou.

CENTER FOR RADIOLOGICAL RESEARCH FACULTY AND STAFF

FACULTY

ERIC J. HALL, D.Phil., D.Sc., FACR, FRCR, Higgins Professor of Radiation Biophysics, Professor of Radiology and Radiation Oncology, Chairman of Joint Radiation Safety Committee – ***CRR Director***

CHARLES R. GEARD, Ph.D., Professor of Clinical Radiation Oncology – ***CRR Associate Director***

DAVID J. BRENNER, Ph.D., D.Sc., Professor of Radiation Oncology and Public Health (Environmental Health Science) – ***RARAF Director***

TOM K. HEI, Ph.D., Professor of Radiation Oncology and Public Health (Environmental Health Science)

HOWARD B. LIEBERMAN, Ph.D., Professor of Radiation Oncology

HAIYING HANG, Ph.D., Assistant Professor of Radiation Oncology

YUXIN YIN, M.D., Ph.D., Assistant Professor of Radiation Oncology

RESEARCH STAFF

GERHARD RANDERS-PEHRSON, Ph.D., Research Scientist

ADAYABALAM BALAJEE, Ph.D., Associate Research Scientist

ALAN BIGELOW, Ph.D., Associate Research Scientist

GLORIA CALAF, Ph.D., Associate Research Scientist

BRIAN PONNAIYA, Ph.D., Associate Research Scientist

LUBOMIR SMILENOV, Ph.D., Associate Research Scientist

YONG-LIANG ZHAO, Ph.D., Associate Research Scientist

HONGNING ZHOU, M.D., Associate Research Scientist

KEVIN HOPKINS, M.S., Senior Staff Associate

STEPHEN A. MARINO, M.S., Senior Staff Associate

CHANG-QING PIAO, M.D., Senior Staff Associate

CARL ELLISTON, M.S., Staff Associate

SU-XIAN LIU, M.D., Staff Associate

AIPING ZHU, M.D., Staff Associate

POST-DOCTORAL FELLOWS

OLEG BELYAKOV, Ph.D., Post-Doctoral Research Scientist

PENG HE, Ph.D., Post-Doctoral Research Scientist

YUXIN C. LIU, Ph.D., Post-Doctoral Research Scientist

CATHERINE R. MITCHELL, Ph.D., Post-Doctoral Research Scientist

STEPHEN A. MITCHELL, Ph.D., Post-Doctoral Research Scientist

RUDRANATH (Ravi) PERSAUD, Ph.D., Post-Doctoral Research Scientist

DEBASISH ROY, Ph.D., Post-Doctoral Research Scientist

JIANLI WANG, Ph.D., Post-Doctoral Research Scientist

FU-RU ZHAN, Ph.D., Post-Doctoral Research Scientist

PRE-DOCTORAL FELLOWS

MARNI HALL, M.S., Staff Associate

DESIGN AND INSTRUMENT SHOP

GARY W. JOHNSON, A.A.S., Senior Staff Associate – ***Design & Instrument Shop Director***

DAVID CUNIBERTI, B.A., Instrument Maker

ROBERT ARCHIGIAN, Instrument Maker

TECHNICAL STAFF

GLORIA JENKINS-BAKER, B.A., Research Worker

XIAOJIAN WANG, M.S., Research Worker

RONALD BAKER, B.S., Sr. Technician

CUI-XIA KUAN, Technical Assistant

ADMINISTRATIVE AND SECRETARIAL STAFF

MONIQUE REY, B.A., Center Administrator

MARY COADY, Administrative Coordinator

MOSHE FRIEDMAN, B.A., Administrative Assistant

HEIDY HERNANDEZ, Jr. Accountant

DIANA MORRISON, Administrative Assistant

ANNERYS RODRIGUEZ, Clerk Typist

Center for Radiological Research Staff News

Dr. Eric Hall is currently President of the International Association of Radiation Research. He continues to serve as Senior Biology Editor of the *International Journal of Radiation Oncology, Biology, Physics.*

Dr. Hall has been awarded a renewal of the RSNA World Wide Web-Based Educational Program Grant from the Radiological Society of North America Research and Education. This grant is designed to provide an opportunity for scientists and physicians in the radiological sciences to develop educational materials specifically for widespread distribution via the Internet. The subject of Dr. Hall's project is "*Web-Based Educational Program for Diagnostic and Interventional Radiologists: Radiobiology, Radiation Protection, and Risks vs. Benefits*" (see p. 63 of this report for details).

Dr. Hall gave the Neuhauser Memorial Lecture sponsored by the Society of Pediatric Radiology and was elected a Fellow of that organization.

Drs. Hall and Brenner are both Councilors of the National Council on Radiological Protection. Dr. Brenner serves on NCRP Committee 12, on the use of ionizing radiations to combat terrorism. Dr. Brenner gave the Jean Ray Memorial Lecture to the Canadian Society of Radiation Therapists.

Dr. Howard B. Lieberman was promoted to Professor of Radiation Oncology. Dr. Lieberman still serves as a Member of the Scientific Advisory Panel of the Israel Cancer Research Fund, a private organization that supports biomedical research related to cancer. He is also a member of the basic and preclinical Subcommittee C of the NCI Initial Review Group.

Dr. Tom K. Hei has been appointed External Examiner at the University of Hong Kong where he will evaluate graduate and undergraduate training programs for the next three academic years. He continues to serve as adjunct professor and doctorate student mentor at the Chinese Academy of Sciences, Beijing, China.

Miss Hitomi Yoshida, a third year medical student from the Okayama Medical University spent three months in Dr. Hei's laboratory studying differentially expressed genes in breast cancer cells as part of a physician-scientist training program.

Dr. Tom Hei and his colleague, Dr. Yong-Liang Zhao, have been awarded a provisional patent by the US patent office for the tumor suppressor function of the Betaig-H3 gene, first identified in their pursuit of the mechanism of radiation induced cancer.

Dr. Tom Hei was the keynote speaker at the twelfth meeting of the American Association of Radon Scientists and Technologists in Reno, NV.

The year 2002 was a year of solid achievements and productivity. Half-way through the cycle of our major funding (the Program Project grant and the P41 grant in support of RARAF), we were able to concentrate on research unencumbered by the preparation of major grant proposals or site-visits.

Center staff changes included:

- Dr. Tej K. Pandita moved his Laboratory to Washington University, St. Louis, MO.
- Dr. Prakash Hande left the Center to take a position with the Faculty of Medicine at the National University of Signapore.
- Dr. Alexander Dymnikov, who was here as a visiting scientist, left the Center to take a position with the Louisiana Accelerator Center, University of Louisiana at Lafayette, Lafayette, LA.
- Drs. Alan Bigelow and Hongning Zhou were promoted to Associate Research Scientists.
- The Center has several new Post-Doctoral Fellows, Drs. Oleg Belyakov, Peng He, Catherine Mitchell, Stephen Mitchell, Rudranath Persaud, Jian Li Wang, and Fu-Ru Zhan, and one new Pre-Doctoral Fellow, Marni Hall.

Dr. Howard B. Lieberman (left), with members of his research group, Mr. Kevin Hopkins, Ms. Xiaojian Wang, Dr. Aiping Zhu, and Dr. Haiying Hang.

Dr. Yong-Liang Zhao, who together with Dr. Tom Hei, was awarded a provisional patent by the US patent office for the tumor suppressor function of the Betaig-H3 gene.

The Columbia Colloquium and Laboratory Seminars

At approximately one month intervals during the academic year the Center for Radiological Research is pleased to welcome accomplished specialists from around the world to present formal seminars and/or spend time discussing ongoing research. These seminars are attended by Center and RARAF professional staff, senior technical staff and graduate students, as well as doctors and scientists from other departments of the College of Physicians & Surgeons interested in collaborative research. Attention has focused on recent findings and future plans, with special emphasis on the interdisciplinary nature of our research effort.

Dr. Howard Lieberman organized these sessions and scheduled the speakers from 1999 through 2001. Presently Dr. Yuxin Yin has taken over these responsibilities.

During 2002 the speakers included Drs.:

- Sally A. Amundson, National Institutes of Health, Bethesda, MD
- Marina Cholewa, GSI, Darmstadt, Germany
- P. Uma Devi, Jawaharlal Nehru Cancer Hospital, Bhopal, India
- Guy Garty, Weizmann Institute, Rehovot, Israel
- Kirk T. Kitchin, Environmental Carcinogenesis Division, U.S. Environmental Protection Agency, Research Triangle Park, NC
- Arthur Ko, Department of Radiation Oncology, Columbia University, N.Y., NY
- Kenshi Komatsu, Department of Genome Repair Dynamics, Kyoto University, Japan
- Qamar Rahman, Industrial Toxicology Research Center, Lucknow, India
- Elaine Ron, Radiation Epidemiology Branch, National Institutes of Health, Bethesda, MD
- Giuseppe Schettino, Gray Cancer Institute, Northwood, Middlesex UK
- Susan Smith, Skirball Institute of Biomolecular Medicine, New York University School of Medicine, N.Y., NY
- Guillermo E. Taccioli, Department of Microbiology, Boston University, Boston, MA

Dr. Yuxin Yin with Dr. Elaine Ron, who spent three months at the Center as a visiting scientist and gave a Colloquium presentation. Dr. Ron is Chief of the Radiation Epidemiology Branch of the National Institutes of Health, Bethesda, MD, and an Adjunct Professor of Radiation Oncology at Columbia University. Dr. Eric Hall appears in the center of the picture in the background.

Sample Targeting During Single-Particle Single-Cell Irradiation

Alan W. Bigelow, Gerhard Randers-Pehrson, Kurt A. Michel, David J. Brenner and Alexander D. Dymnikov[1]

The Radiological Research Accelerator Facility (RARAF) at Columbia University is frequently used by biologists to study the effects of radiation on individual mammalian cells. For these experiments an apertured microbeam line was developed to perform controlled single-particle single-cell irradiation. In this highly regulated situation, a biologist can prescribe that a certain percentage of stained cells be irradiated with a certain number of particles, including only one.

Presently, the apparatus employs a stepping motor-driven stage. Experimental protocol acquires images through a 4× optical microscope lens of cells plated in a dish mounted to this stage and records their position. During irradiation cell images are acquired again but through a 40× lens and each targeted cell within that frame is sequentially positioned above a 5 μm dia. exit aperture window to a vertical ion beam. This stage positioning has worked well with experiments thus far as it can target the nucleus of a cell; however, overall positioning error would be a handicap according to upgrade plans for a focused microbeam with submicrometer resolution. Hence, a new sample stage has been developed that meets the next generation resolution requirements. The new stage, dubbed a voice coil stage, utilizes principles similar to those found within sound wave transducers such as microphones or audio speakers. In addition, frictionless position measurement devices are wired into a closed feedback loop on the voice coil stage to further enhance position accuracy and precision. This new stage will play an important role to satisfy the biology research community's interest in targeting subnuclear cellular components

In order to draw an adequate comparison between the stepping motor stage and the voice coil stage, a review of the stepping motor stage is useful. The x-y stepping motor-driven stage that is routinely used (Daedal, Inc., Harrison City, PA) was designed to move 0.1 μm per step. Although the stage was designed for making submicron steps, positioning limitations are inherent to this type of stage, even after performing an involved optimization of tuning parameters.

Positioning error testing using a similar stepping motor stage from Ludl Corporation measured the location of a fixed object for 50 consecutive 1 μm steps. The overall positioning error of ±0.5 μm for the Ludl stage compared to ±0.2 μm for the voice coil stage. In this comparison test, both stages were operating in an open loop mode, without feedback.

The voice coil stage pictured in fig. 1 was developed at Columbia University and weighs about 1 kg. Most of the stage and its frame were made from aluminum. And when possible, excess material was removed from moving components to reduce inertia without compromising rigidity. Flexure mounts hold together the moving parts; they are robust to the load and the smooth elastic bending motion is favorable to other systems such as bearings. The flexure mount springs are simply thin steel plates; 0.004 in. and/or 0.015 in. thickness. Novel aspects of the voice coil stage are infinitesimal position variability and frictionless position monitors incorporated into a closed feedback loop.

For this stage, the voice coil concept applies in that each voice-coil drive unit consists of a driving arm with a coil at one end that is set between permanent magnets. When a current flows through the coil, the interaction between the field produced by the coil and that of the permanent magnets causes the arm to move until this force is balanced by the tension in the flex springs connected to the arm. Each coil is approximately rectangular, with inner dimensions of 15 x 17.5 mm and outer dimensions of 40 x 43 mm. They consist of about 400 windings of 34 AWG wire trapped between two aluminum plates attached at the ends of two pivot arms. These current controlled actuators are attractive for their continuous positioning, however, when operated in an open-loop configuration, they are not precise because of hysteresis effects on the flexure mounts.

Closed-loop operation of the voice coil stage is possible with position monitors and feedback circuitry. For this stage, a linear variable differential transformer (LVDT) measures the angular position of a pivot arm. An LVDT has a primary

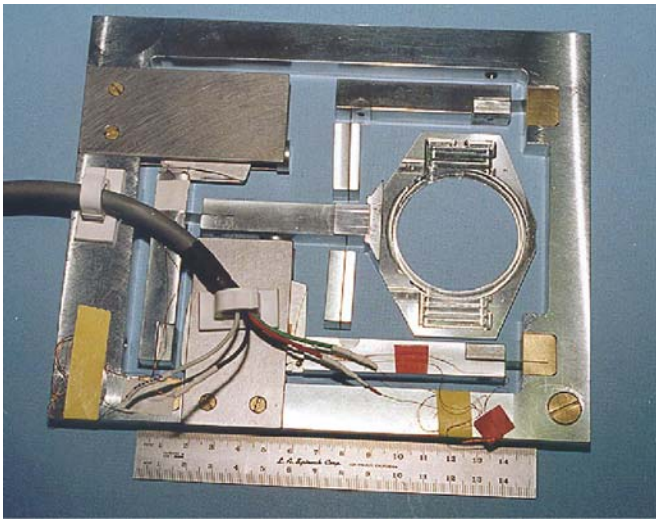

Fig. 1. Photograph of the voice coil stage.

[1] *Presently at Louisiana Accelerator Center, University of Louisiana at Lafayette, Lafayette, LA.*

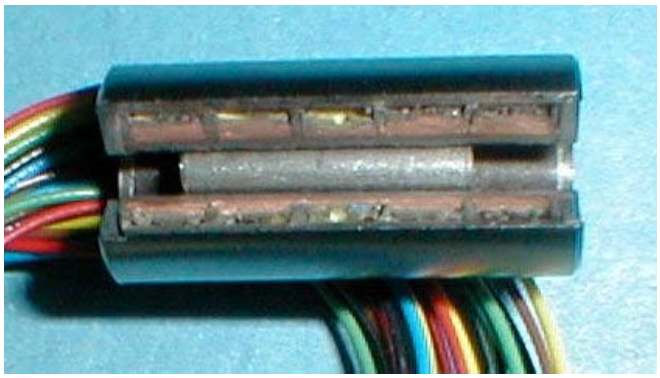

Fig. 2. Quarter section removed from an LVDT (Schaevitz model 050 MHR) reveals windings, excess inner wall material, and a close fit for the original 0.5 inch long core.

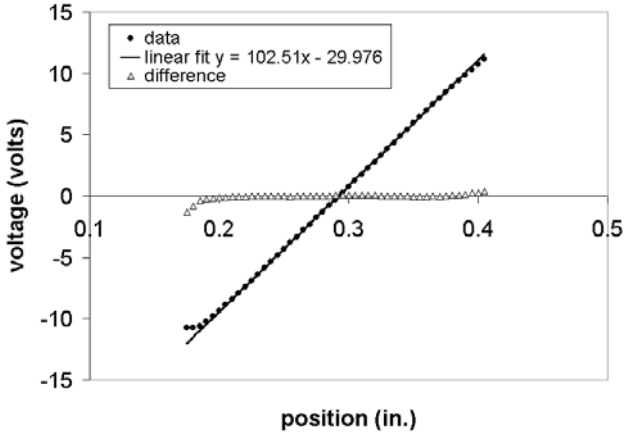

Fig. 3. Plot of an LVDT short-core response curve using a 150 kW gain resistor. The response of this configuration was measured at 3.22 mV/㎜.

coil centered between two secondary coils, all about a shared axis. A magnetic core positioned within these coils translates an oscillating signal in the primary coil to the secondary coils. The pick-up signal ratio in the secondary coils is a function of the core position. From the dissected view of the LVDT pictured in fig. 2, it was obvious that some physical modifications were necessary to adapt this linear measuring device to a system with angular motion. It was also made clear that there was room to safely enlarge the inner diameter of the coil sensor housing without damaging the windings. So to meet the stage's angular acceptance requirements, half of the coil form material thickness was removed and the core length was shortened to 0.125 in., despite the vendor's insistence that the cores not be modified.

Position response tests for a variety of core lengths were conducted by mounting an LVDT core and sensor to caliper measuring tips. For a series of core positions (0.005 in. increments), voltage signals were read using an AD598, a complete, monolithic LVDT signal conditioning subsystem (Analog Devices). Initial subsystem interconnections followed the data sheet design procedure. For the original core, the LVDT responded linearly across ±0.050 in., the advertised measurement range. At the range ends, the electronics saturated at just beyond ±10 volts. On the other hand, signal from the shorter core test tended to stray from linearity at range ends. An increase in the gain resistance on the AD598 circuit optimized the linear response range for the short core.

To more accurately view the LVDT linear response, a linear fit of the response curve mid section was plotted along with the measurements and the difference between the fit and the measurements. This response curve shown in fig. 3 also portrays an added benefit, an increase in measurement range.

The AD598 data sheet included an electronics schematic for a set-point controller. This circuit was used as a model for the voice coil stage closed loop feedback system; the principle feature is an op amp with negative feedback. Work in progress on this circuit is expected to minimize the stage settling time. Mechanical variables such as spring thickness and eddy current damping (aluminum plates contain the voice coil windings) are important considerations for tuning the feedback system. Under one set of mechanical conditions (0.015 in. thick springs and the use of eddy current damping) the settling time was approximately 100 ns, three times faster than for the present stepping motor stage. Figures 4 and 5 show the frequency response of the AD598 LVDT signal conditioner for the condition mentioned above.

A precision evaluation of the voice coil stage stressed the importance for closed loop feedback. One stage control arm was alternately pulled to the side and released. Without feedback, there were significant elastic hysteresis effects. The feedback system improved the positioning error of this

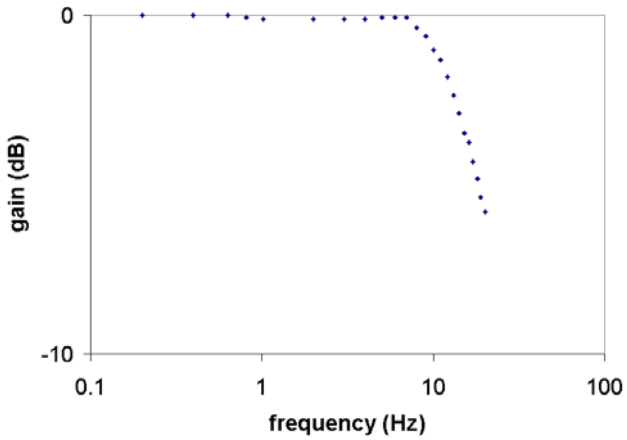

Fig. 4. Gain characteristics vs. frequency.

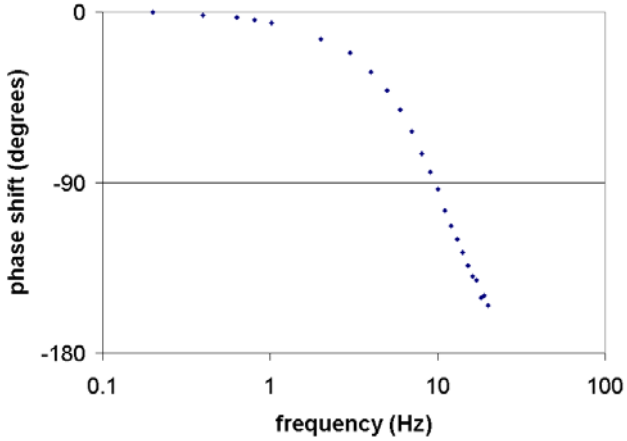

Fig. 5. Phase characteristics vs. frequency.

alternate-pull test from ±2.6 mm to ±0.12 mm, meeting a goal for sub-micron resolution using thin springs (0.004 in.).

Plans for the voice coil stage incorporate its use in on-line and off-line microscopes. Ideal imaging capabilities require that the stage operate consistently under either microscope. The stage frame is designed with a kinetic mount for precision placement each time it is moved between microscopes. The LVDT monitor sets within the walls of the stage frame. And, the plan for the electronics is that they will be imbedded in the frame wall, dedicating one control and feedback circuit for the stage. Again, the overall design goal for this voice coil stage is sub-micron resolution.

Laser Ion Source Simulations for the Columbia University Microbeam

Alan W. Bigelow, Gerhard Randers-Pehrson and David J. Brenner

At Columbia University's Radiological Research Accelerator Facility (RARAF), fundamental investigations into the radiobiological effects on mammalian cells are conducted through broad beam and through controlled single-particle single-cell microbeam irradiation (1). Recent upgrade plans to our 4.2 MV Van de Graaff particle accelerator include implementation of a laser ion source. The laser-ablation based ion source will produce highly charged heavy ions that will extend the linear energy transfer (LET) range of our experiments. Presently, our duoplasmatron ion source can ionize atoms from the gaseous phase, namely from hydrogen and helium. These ions are suitable for particle irradiation experiments with an LET range of 9.5 to 210 keV/μm. Expectations are that the laser ion source will enable a range of ions from hydrogen to iron with an approximate LET range of 10 to 4,500 keV/μm.

In the field of laser ion sources, two common modes of ion production are laser ablation and resonance ionization spectroscopy, a species-selective technique that requires tunable lasers (2). The operational mechanism of our laser ion source is plasma generation through laser ablation of a solid target. Focused Nd:YAG laser pulses supply the power density required to create a plasma plume (3). The plasma ions have distributions over charge state, energy, and angle. To then reduce the beam load on the accelerator vacuum system, an electrostatic analyzer (ESA) selects ions with a particular energy per charge.

The design development procedures for our laser ion source originated with a prototype based on the laser operated ion source acquired from Hughes at the University of Arkansas (4). Ion trajectories in this source experienced in turn, 70 cm of plasma expansion drift, a 180± cylindrical ESA, two Einzel lenses, and a final drift distance to a detector whose position would effectively be the location of the 3.18 mm diameter entrance aperture of the particle accelerator. Dimension details of the original laser operated ion source have been provided elsewhere (5). Furthermore, the following simulation results complement a previous document of our laser ion source development (6).

Ion trajectories through the laser ion source prototype were simulated with the ion optics package, SIMION (7). In SIMION, the potential at points outside electrodes and poles is determined by solving the Laplace equation by finite difference methods (8). Virtual ion optical components are constructed and arranged on an ion optics workbench. Ions flown through such an optical system retain characteristic information useful for generating phase space patterns for simulated ion source emittance measurements.

The ion optics workbench setup for the laser ion source prototype required constructing virtual ion optical elements that paralleled as much as possible the physical configuration. The optical elements were constructed with a grid resolution of 1 mm/grid unit. To project an optical element into three dimensions, SIMION supports both planar and cylindrical symmetries. Planar geometry was used for the cylindrical ESA. And, cylindrical geometry was used for the Einzel lenses. Initial characteristics of the ions flown through the simulation were mass, charge state, position, energy, angle, and a random function applied, within certain bounds, to offsets about the energy and the angle. Typical ion parameters were: aluminum, singly charged positive, origin about a circular area representing the ablation crater (0.25 mm diameter), 400 eV mean energy, and normal emission with a random divergence within a 0.2± cone angle. Voltage settings on the optical elements during the simulation were 69.35V across the analyzer, -200V on the first Einzel lens and 100V on the second Einzel lens.

Emittance results emerged from analysis of the ion flight data. In a typical case, the vertical extent of the ion beam was acceptable for input to the accelerator aperture. However, the horizontal ion beam component extends beyond the aperture boundary, suggesting reduced ion transmission. For other voltage settings on the Einzel lenses, a variety of spot patterns were produced, but none could match the aperture size constraints in the vertical and in the horizontal direction simultaneously. This limitation to the ion source prototype was an artifact of the ion optical geometry.

A double focusing, spherical ESA with point-to-point focusing in both the horizontal and vertical planes offered an attractive solution for our laser ion source design constraints.

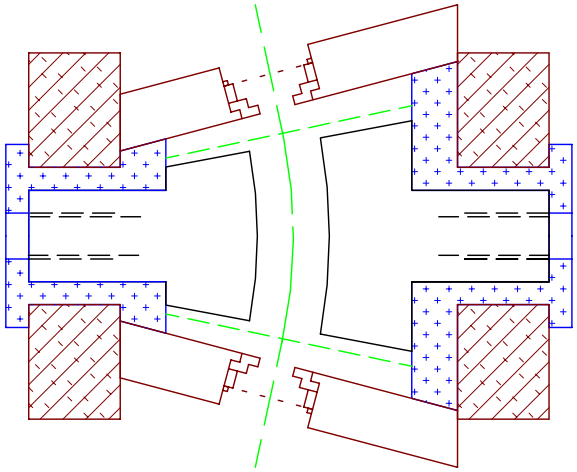

Fig. 1. Top view cross section diagram of the 24± ESA.

With this one ion optical element, laser plasma plume ions are both E/z analyzed and focused at the accelerator entrance aperture. The footprint of this option fit well within the accelerator terminal. Einzel and quadrupole lens options were also considered, but their linear arrangements would require structural modifications of the accelerator terminal frame.

Guided by spatial limitations in the particle accelerator and by a desired plasma expansion drift distance of 70 cm, (3) the ESA dimensions were narrowed to a 24± bend with a 2.7 inch radius. This geometrical solution was found by applying Barber's rule; the object point, the center of curvature, and the image point lie on a straight line (9).

Spherical ESA theory and fringing field effects are well documented in Wollnick's treatment of electrostatic prisms (10). Wollnick's guidelines for fringing field termination provided additional dimension details to the ESA. Electrode spacing and field-terminating diaphragm dimensions were set similar to those in the prototype's ESA. For a 10 mm space between electrodes, a 5 mm arc length from the ESA electrodes to the diaphragm, and a 5 mm diam diaphragm aperture, the 24± ESA would have a 21.32± arc for the physical electrodes and a 29.68± arc for the diaphragm. The ideal field boundary would, in theory, have a 24± arc. A top view cross section diagram of the 24± ESA is shown in Fig. 1.

For the simulation of the 24± ESA, the ion optics workbench set up in SIMION was similar to the one presented in the prototype simulation section. However, an increased resolution (0.2 mm/grid unit) was used for the 24± analyzer. Again, the component dimensions in the simulation paralleled as much as possible the intended "real world" case. To insure that the electric field lines were fully terminated in the ESA element, an ideal grounded mesh was wrapped about the ESA diaphragm material at a 5 mm offset distance from the inside of the diaphragm.

For the proposed laser ion source, the simulated spot size is shown in Fig. 2. Horizontal and vertical histograms across this ion spot are shown in Fig. 3. The improvements are clear; the spot size is smaller and the ions tend to focus in both the horizontal and the vertical directions. The structure in the emittance patterns is due to aberrations that arose from the use of a spherical optical element. However, upright ellipse envelopes about the emittance patterns do still imply a focus at the entrance aperture to the particle accelerator. One more note is that the simulation results suggest an energy resolution compatible with input requirements of a six-element electrostatic quadrupole lens with Russian symmetry that is under development. To tune the resolution, interchangeable diaphragms are available for the ESA.

An interest in the fabrication of the ESA is to match the simulation geometry as best as possible. The physical dimensions used in the simulation will be retained except for one feature. The spherical ESA design in SIMION utilized a slot diaphragm. During the simulation, a virtual round diaphragm was realized by limiting the cone angle of the incident ions. The construction will incorporate circular diaphragms.

In constructing the laser ion source, alignment issues are crucial. In particular, the ESA must be placed in its designated position and the electrode orientation should be optimized. The construction will utilize a self-aligning technique to insure proper placement. During the electrode machining process, flat surfaces and alignment holes for indexing pins incorporated into the outsides of the electrodes will allow them to accurately rest in a frame mount.

Electrode surface treatment will also be an issue. A thin layer of carbon will be deposited on the electrodes in order to reduce patch potentials. This should lead to a smoother electric field within the ESA.

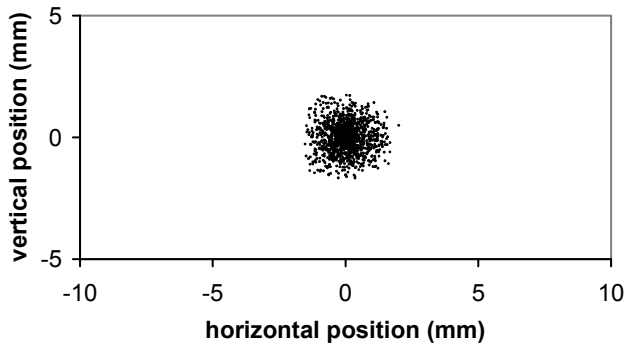

Fig. 2. Spot pattern of proposed laser ion source. Focus is acceptable.

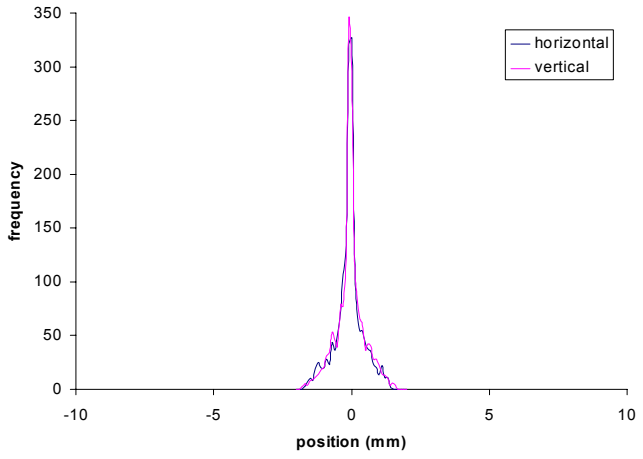

Fig. 3. Intensity histograms across the ion spot pattern shown in fig. 2.

References

1. Randers-Pehrson G, Geard CR, Johnson G, Elliston CD, and Brenner DJ. The Columbia University single-ion microbeam. *Radiat Res* **156**:210-4, 2001.
2. Brown IG, in *The Physics and Technology of Ion Sources* (Wiley, New York, 1989), p. 299.
3. Sharkov B, in *Handbook of Ion Sources*, edited by B. Wolf (Chemical Rubber, Boca Raton, 1995), pp. 149-51.
4. Miller RD, Wattuhewa G, Hughes RH, Pederson DO, and Ye XM. Remnant charge of slow multicharged ions scattered from a gold surface. *Phys Rev B* **45**:12019-27, 1992.
5. Miller RD, Ph.D. thesis, The University of Arkansas, 1990.
6. Bigelow AW, Randers-Pehrson G, and Brenner DJ. *Rev Sci Instrum* in press.
7. Idaho National Engineering and Environmental Laboratory, Idaho Falls, ID 83415
8. Dahl DA, in *SIMION 3D Version 7.0 User's Manual* (Idaho National Engineering and Environmental Laboratory, Idaho Falls, ID, 2000), p. 2-1.
9. Wollnik H, in *Optics of Charged Particles* (Academic Press, Inc., San Diego, 1987), p. 98.
10. Wollnik H, in *Focusing of Charged Particles*, edited by A Septier (Academic Press, Inc., Orlando, 1967), pp. 163-202.

(*l-r*): Dave Cuniberti, Robb Archigian and Gary Johnson, the Design & Instrument Shop team in their machine shop.

Intra-Nuclear Dynamics of Phospho-p53 Protein in Human Cells Following Microbeam Irradiation of α-Particles

Adayabalam S. Balajee and Charles R. Geard

Ionizing radiation (IR) induces a wide spectrum of lesions involving DNA single strand breaks (SSBs), double strand breaks (DSBs), base damage and DNA-protein cross links. Recent studies have indicated that the spectrum of lesions induced in the interphase nuclei largely depends both on the quality of radiation exposure and on the chromatin structure. Among IR induced DNA lesions, DSBs are considered to be very lethal as they lead to genomic instability and cell mortality if left unrepaired. Two major pathways exist in eukaryotic cells to remove DSBs from the genomic DNA: (i) non-homologous end joining repair pathway and (ii) the recombinational repair pathway. Both these repair pathways involve a number of proteins, which have dual roles in repair and DNA metabolic activities, interact with each other and sequentially assemble at the site of DNA lesions. Although substantial progress has been made in understanding the functional complexities of the various proteins in response to DNA damage, the precise participation of each of these proteins in the nuclear environment remains to be characterized. As compared to conventional gamma and X-ray irradiation, introduction of a minimum number of lesions at the defined sub-cellular compartments by microbeam irradiation would greatly enable us to understand the precise mode of action of the various protein complexes in DSB repair. Using such a facility developed at RARAF for microbeam α-particle irradiation, we have set out to examine the intra-nuclear dynamics phosphorylated p53 protein in human cells in response to DNA strand breaks. P53 is a dynamic protein that is induced and phosphorylated at several serine/threonine residues in response to DSBs. However, role of phosphorylated p53 protein and its association with other DSB factors remain largely unknown. Knowledge on the intranuclear dynamics of phosphor-p53 protein in response to IR would enable us to understand its role in DSB repair.

Human primary fibroblast cells lines from Normal (MRC5) and ataxia telangiectasia (AT, GM8391A) patients used in this study were procured from Coriell Cell repository, Camden, New Jersey. The layout and microbeam irradiation procedure have been previously described (Hei et al., 1997). Briefly, plateau phase cells were trypsinized and approximately 500-600 cells were seeded in dishes specially designed for microbeam irradiation. The cells were stained with a 50 nM solution of Hoechst 33342 for 30 min prior to irradiation. The cells were irradiated with 0, 1, 2, 4, 8 and 12 α-particles and the cells were either fixed immediately in ice-cold methanol or allowed to recover for various lengths of time (30 min, 2hr, 4hr, 8hr and 24 hr). The cells that were stained with Hoechst 33342 and exposed to UV served as control. Antibody for p53 (Ser15) was procured from Cell Signaling Technology, USA. Procedure for immunodetection of phosphop53 was done essentially as described before. Following immunofluorescence, cells were washed in TBST and dehydrated in 70% and 95% ethanol. DNA was counterstained with DAPI (0.1μg/ml prepared in Vectashield mounting medium; Vector laboratories) and covered with a

Fig. 1A

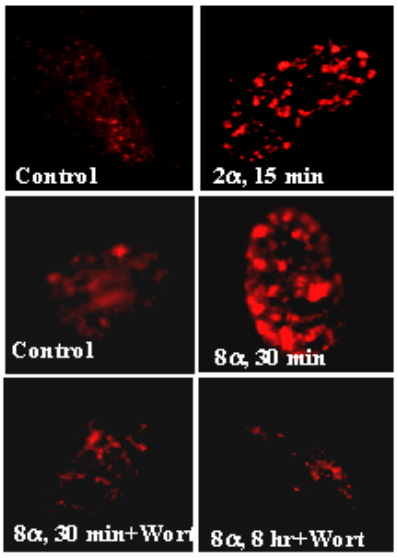

Fig. 1B

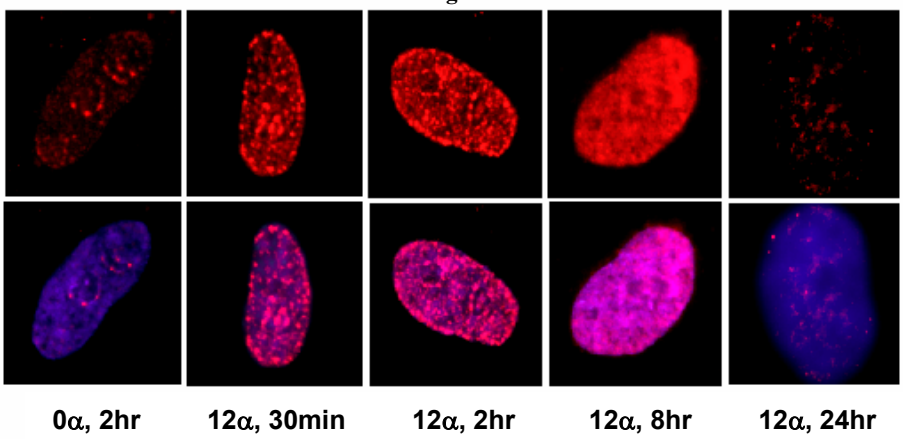

Fig.1. Intranuclear dynamics of $p53^{ser15}$ protein in microbeam irradiated human cells. MRC5 cells treated with defined number of α-particles were post-incubated for different recovery times. Cells were fixed in ice-cold methanol, immunostained for Phospho-p53 and detected with Texas red conjugated streptavidin antibody.

cover glass.

In unirradiated control cells, $p53^{ser15}$ staining was very faint. In contrast to control cells, irradiated cells showed a dose dependent increase in the intensity of phospho-p53 protein (Fig. 1A). In cells treated with 2α-particles, 20-25 focal sites of p53 induction were observed. The number of focal sites did not drastically increase after exposure to 8α-particles but the focal sites became much denser and showed increased fluorescence intensity probably suggestive of clustered induction of DNA lesions (1A). It should be noted that the sites of $p53^{ser15}$ foci bears no relationship to the nuclear centroid site of particle traversals (nuclear centroid ± μms). Treatment of cells with 20 μM of phosphatidylinositol kinase (PI-3) inhibitor, Wortmannin for 30 min prior to α-particle irradiation completely abolished $p53^{ser15}$ formation in the nuclei (Fig.1A) indicating that the $p53^{ser15}$ phosphorylation is mediated by PI-3 kinases such as ATM and DNA dependent protein kinase (DNA-PK). Time course kinetics of phospho-p53 foci formation analyzed in cells treated with nuclear irradiation of 12 α-particles showed the rapid induction of phospho-p53 at the earliest time point of analysis (15 minutes after IR). The punctuated pattern of p53 foci formation observed during the initial hours of IR became more homogenous at 8 hr after irradiation. Distinct focal sites of p53 appearing like a string of beads were observed after IR at the nuclear membrane as well as at the perinucleolar regions (Fig. 1B). These regions probably represent the sites of DSB repair. The specific enrichment of p53 protein at the perinucleolar regions in response to microbeam irradiation is under investigation.

Preliminary studies have indicated the lack of p53 phosphorylation in AT cells harboring mutations in the ATM gene product. Using a combination of known DSB repair factors, efforts are underway to determine whether the sites of phospho-p53 protein represent the sites of DSB repair. The specific enrichment of p53 at the nuclear membrane as well as at the perinucleolar regions suggests that the repair events occur in specific nuclear compartments in a non-random manner. Studies are in progress to determine whether the focal phospho-p53 distribution in the nuclear environment depends on the quality of IR.

Identification of Signal Transduction Pathway(s) Involved in Radiation Induced Bystander Response by cDNA Microarray Analysis

Adayabalam S. Balajee, Brian Ponnaiya and Charles R. Geard

"Bystander effect" (BE) is an intriguing phenomenon that has recently attracted a wide attention in radiation biology. BE is the result of the ability of the cells directly affected by an agent to convey the manifestation of the damage to neighboring cells that are not directly targeted thereby eliciting a response similar to that of targeted cells. BE can be triggered either through direct contact with the damaged cells or through the growth factors released from the targeted cells (1). Although the molecular basis for BE is largely unknown at this moment, this multifaceted phenomenon may have a significant impact on the radio- and chemotherapy of tumors. A better understanding of molecular steps involved in BE is pivotal for modulation and evaluation of the radiotherapy protocols designed to improve the efficacy of the radio and chemotherapy treatments. In an attempt to understand the molecular basis for BE, we have undertaken a cDNA microarray approach to identify the components of diverse signal transduction pathways that mediate the bystander response.

The primary fibroblast cell lines (MRC5 and WI38) derived from healthy individuals were obtained from Coriell Cell repository, Camden, New Jersey. All the cells were routinely maintained in 2X Eagle's minimal essential medium (E-MEM) supplemented with 15% fetal bovine serum, vitamins, essential amino acids, non-essential amino acids and antibiotics (Gibco BRL). The cultures were maintained at 37°C in a humidified 5% CO_2 atmosphere. MRC5 or WI38 cells in plateau phase were irradiated with 10 Gy of γ-rays using a ^{137}Cs source delivering a dose rate of 0.98 Gy/min (Gamma cell 40, Atomic Energy of Canada, Canada). The cells were kept at 37°C for 1 hr and the conditioned medium from irradiated cells was transferred to plateau phase MRC5 cells. Cells treated with irradiated medium alone without cells served as a positive control. The cells were incubated for different recovery times and the total RNA was isolated from control, direct hit and bystander cells according to manufacturer's instructions (Invitrogen). Alternatively, cells were seeded on double-sided Mylar dishes and the dishes were irradiated only on one side with different doses of track segment alpha particles. The protocol for preparation and irradiation of cells in double-sided Mylar dishes has been previously described (2). Total RNA was isolated from both irradiated and non-irradiated cells. cDNA synthesis was carried out using biotin-16-dUTP and the biotinylated cDNA samples were denatured and hybridized with cDNA signal transduction pathway finder array

procured from Super Array, MD, USA. This array contains 96 marker genes associated with 18 different signal transduction pathways (Mitogenic pathway, Wnt pathway, Hedgehog pathway, TGF pathway, Survival pathway, p53 pathway, stress pathway, NFkB pathway, NFAT pathway, CREB pathway, Jak-Stat pathway, Estrogen Pathway, Androgen pathway, calcium and Protein kinase C pathway, phospholipase C pathway, insulin pathway, LDL pathway and Retinoic acid pathway). After hybridization, the signal was detected using streptavidin-alkaline phosphatase as per the instructions of the manufacturers. The membranes were exposed to Kodak BiomaX light films. The digital images were generated using ScanAlyze2 programme (developed by Michael Eisen at Lawrence Berkeley National Laboratory). The analysis was done using GE array analyzer (Super Array). A representative example of hybridization patterns obtained for control and direct hit cells is shown in Fig. 1.

Preliminary studies have indicated that 20 genes out of a total of 96 belonging to stress, p53, survival, hedgehog, NFkB, jak-stat, calcium and protein kinase C, phospholipase C, LDL, androgen and estrogen pathways showed 2-4 fold increase in direct hit MRC5 cells as compared to unirradiated control cells. Interestingly, 26 genes out of 96 showed more than 2-fold increase in bystander cells as compared to control cells. Although increased expression of some of the genes such as Creb-2, p21, bax and DR5 were observed in both direct hit and bystander cells, there were distinct differences in the expression patterns of other genes between direct hit and bystander cells. These include hsp90, BMP2, BMP4, p27 Hoxa-1, p18, Leptin, mad3, VCAM1 and WISP3, which were specifically induced in bystander cells. Interestingly, increased expression of genes representing TGF, insulin, stress and Wnt pathways were observed only in bystander cells. The unique expression patterns observed for direct hit and bystander cells indicate that the factors triggering the signal transduction pathways differ between BE and radiation response. We are presently doing pathway specific arrays to confirm these initial observations. Additionally, efforts are underway to verify cDNA array results by western blotting and RT-PCR. It would be interesting to know whether the signal transduction pathways that mediate the bystander response are defective in radiosensitive mutants. We plan to use several human mutant cells defective in important DSB repair genes to determine whether DSB repair efficiency contributes to bystander response. This project will be soon initiated by culture of wild type and AT cells in double-sided Mylar dishes to determine the effect of ATM associated pathways in bystander response. Subsequently this will be extended to other DSB repair mutant cell lines.

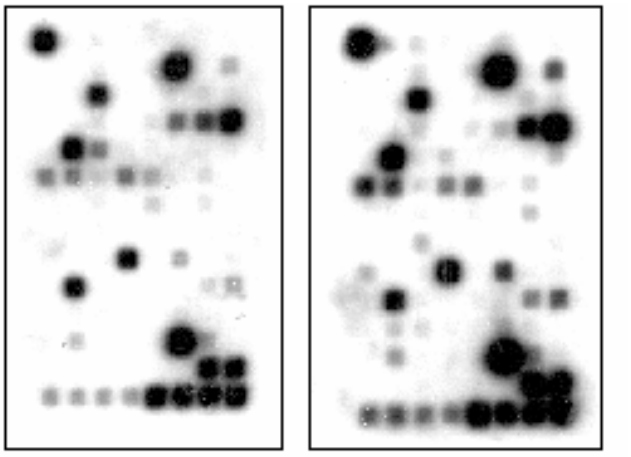

Fig. 1. Schematic cDNA expression profiling of genes associated with 18 signal transduction pathways in control and direct hit cells.

References

1. Iyer R and Lehnert BE. Effects of ionizing radiation in targeted and nontargeted cells. *Arch Biochem Biophys* **376**:14-25, 2000.
2. Geard CR, Jenkins-Baker G, Marino SA and Ponnaiya B. Novel approaches with track segment alpha particles and cell co-cultures in studies of bystander effects. *Radiat Prot Dosimet* **99**: 233-6, 2002.

Interaction of the Radiation Induced Bystander Effect and the Adaptive Response in Mammalian Cells

Hongning Zhou, Gerhard Randers-Pehrson, Eric J. Hall and Tom K. Hei

There are many reports on the role of bystander effect and adaptive response, two interesting and important phenomena, in low dose radiation effects (1-3). The bystander effect tends to exaggerate the effect of low doses, by elicit damage in non-irradiated cells, while the adaptive response presents resistance to a subsequent dose after a low initial priming dose. Although these two conflicting phenomena have attracted interest, there are only limited data available about the interaction of bystander effect and adaptive responses (4,5).

Using the Columbia University charged particle microbeam and the highly sensitive A_L cell mutagenic assay,

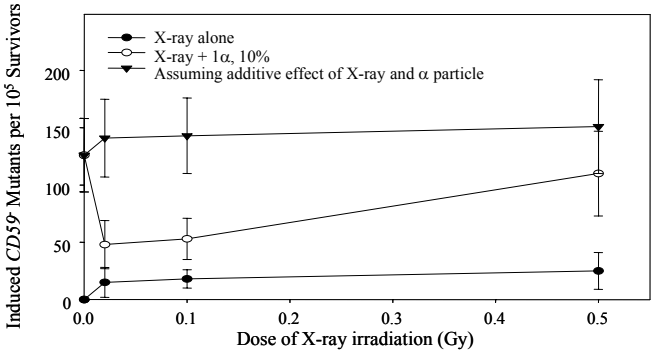

Fig. 1. Effect of the pretreatment X-ray dose on bystander mutagenesis in A_L cells. Cells were pretreated with graded doses of X-rays 4 hr before targeted nuclear irradiation of 10% of randomly selected cells with a single alpha particle. Pretreatment of cells with X-rays significantly reduced the bystander mutagenic effect across the whole spectrum of adaptive doses used. Data are pooled from four independent experiments. Bars represent ± SD.

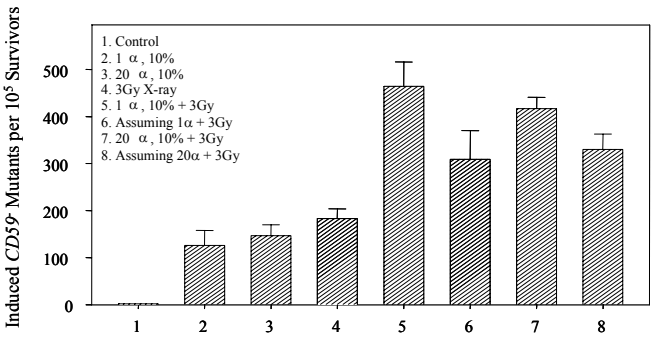

Fig. 2. Response of bystander cells to the followed challenging high dose radiation. 10% of randomly selected cells were irradiated with a single or 20 alpha particles, 4 hours later, the cells were exposed to a 3 Gy dose of X-ray. Data were pooled from 3 independent experiments. Error bars represent ± SD.

we reported previously that cells that had been lethally irradiated with alpha particles could induce mutagenesis in neighboring cells not directly hit by the particles, and that mutant induction depended on cell-cell communication (6). Furthermore, the findings can also be extended to a single alpha particle radiation, and gap junction mediated cell-cell communication plays an important role in the process of bystander mutagenesis (7). In our present study, two related experiments were designed to explore the interaction of bystander effect and adaptive responses. First, we asked whether low dose radiation decreased bystander mutagenesis. AL cells were plated in microbeam dishes two days before treatment as described previously (6,7). Cells were exposed to graded, low doses of X-rays. Four hours later, 10% of randomly selected cells were irradiated with a single or 20 alpha particles using the Columbia precision particle microbeam. Second, we examined the response of the bystander cells to a subsequent, high dose radiation. 10% of randomly selected cells in microbeam dishes were irradiated with 1 or 20 alpha particles. 4 hours later, the cells were irradiated with a subsequent, challenging 3 Gy dose of X-rays. After the second irradiation, the cells were kept in microbeam dishes for 2 days before replating in culture flasks. Determination of the mutant fraction and mutant spectra analysis was carried out as described (6,7).

Our data show that the mutant yield from the population where 10% of randomly selected cells were irradiated with single alpha particle decreased significantly if the cells were pretreated with a low dose of X-rays (Figure 1). Similar response was found if 10% of the cells were given 20 alpha particle traversal through nuclei (data not shown). The results indicate that after low dose radiation, bystander mutagenesis is decreased by the adaptive response. Though the mechanism(s) is unclear, it is likely that when cells are exposed to low doses X-ray, they initiate a series of self-preservation mechanisms that diminish their ability to respond to bystander signaling. What is the response of bystander cells to a challenging dose of radiation? We found that when 10% of randomly selected cells were irradiated with 1 or 20 alpha particles 4 hours before the cells were irradiated with 3Gy X-rays, the mutant yield in the whole population was significantly higher than the yield assuming an additive effect of alpha particle and X-ray irradiation (Figure 2). These data point out that bystander cells show an increase in sensitivity following a subsequent, challenging dose of X-rays. The mutant spectra analysis is ongoing. These results are of importance in reassessing the potential genotoxic effect of low dose radiation and suggest a reconsideration of the current model in risk estimation for low dose radiation.

References

1. Mothersill C and Seymour C. Radiation-induced bystander effects: past history and future directions (Review). *Radiat Res* **155**:759-67, 2001.
2. Upton AC. Radiation hormesis: data and interpretations (Review). *Toxicol* **31**:681-95, 2001.
3. Rigaud O and Moustacchi E. Radioadaptation for gene mutation and the possible molecular mechanisms of the adaptive response (Review). *Mutat Res* **358**:127-34, 1996.
4. Sawant SG, Randers-Pehrson G, Metting NF and Hall EJ. Adaptive response and the bystander effect induced by radiation in C3H10T1/2 cells in culture. *Radiat Res*, **156**:177-80, 2001.
5. Iyer R and Lehnert BE. Alpha-particle-induced increases in the radioresistance of normal human bystander cells. *Radiat Res* **157**:3-7, 2002.
6. Zhou H, Randers-Pehrson G, Waldren CA, Vannais D, Hall EJ and Hei TK. Induction of a bystander mutagenic effect of alpha particles in mammalian cells. *Proc Natl Acad Sci (USA)* **97**:2099-104, 2000.
7. Zhou H, Suzuki M, Randers-Pehrson G, Vannais D, Chen G, Trosko JE, Waldren CA, Hei TK. Radiation risk to low fluences of alpha particles may be greater than we thought. *Proc Natl Acad Sci (USA)* **98**:14410-5, 2001.

The Bystander Effect in Radiation Oncogenesis: Effect of Cell Density on the Magnitude of Bystander Response

Stephen A. Mitchell, Fu-ru Zhan, Gerhard Randers-Pehrson, David J. Brenner and Eric J. Hall

Previous work using the Columbia University microbeam has demonstrated a reproducible bystander effect for the endpoints of clonogenic survival and oncogenic transformation using C3H 10T½ cells. The aim of the present study was to assess the importance of gap junction communication between cells as a mediator of this bystander effect. To facilitate this, C3H 10T½ cells were plated at high and low cell concentrations and irradiated with high LET α-particles.

Approximately 18 hours prior to irradiation, exponentially growing C3H 10T½ cells (passage 9-12) were plated onto 3.8 μm polypropylene in the center of a series of 6.3 mm diameter mini-wells. Cells were plated to give a final concentration of either 200 or 2000 cells per dish. When viewed down the microscope the lower concentration resulted in isolated cells with very little cell to cell contact compared with the higher concentration where cells were approximately 90% confluent, allowing direct communication. The attached cells were stained for 0.5 h with a low concentration of Hoechst 33342, enabling individual nuclei to be identified and located with the optical image analysis system. Then 10% of the cells were randomly selected and irradiated with 6 MeV α-particles over a range of 1 to 12 α-particles per cell. The average stopping power of the α-particles traversing the cells was 90 keV/μm. After irradiation, the cells were trypsinized and replated at a low density of about 100 viable cells into 100 mm culture dishes and incubated for 2 weeks. Cells were then stained with 2% crystal violet and the resulting colonies (containing greater than 50 cells) scored to determine plating efficiencies and surviving fractions of the control and irradiated cells.

Figure 1 shows the results obtained. The lower solid line shows the observed survival when 100% of the cells are hit by various numbers of α-particles. The upper solid line shows the estimated surviving fraction when 10% of the cells are irradiated in the absence of a bystander effect. The extent to which the observed survival falls below this line indicates the magnitude of any bystander effect. At both cell densities, the surviving fraction falls progressively as the number of α-particles delivered per cell is increased and more cells have been inactivated than were actually traversed by α-particles. The fact that a bystander effect is evident even at the low cell concentration suggests that it is not dependent on cells being in direct contact. However, the bystander effect is greater among the cells plated at high density with an observed surviving fraction of 0.76 when 12 α-particles are delivered per cell, compared with 0.88 at the low cell density. This would suggest that when a cell is hit by radiation, a signal is transmitted through cell to cell contact to neighboring unirradiated cells, resulting in a larger bystander effect.

To further assess the importance of cell to cell communication in mediating the observed bystander effect we pretreated the cells with Filipin. Filipin disrupts lipid rafts present in the cell membrane, thereby inhibiting membrane signaling and interfering with gap junction-mediated intercellular communication. Cells plated at both high and low density were incubated with Filipin at a concentration of 1 μgml^{-1}

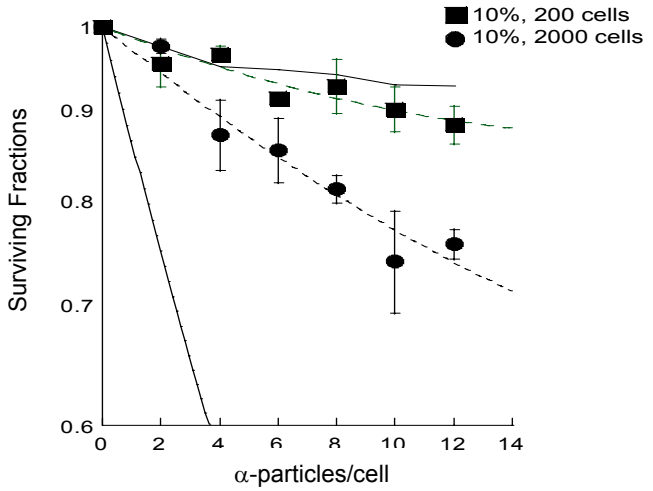

Fig. 1. Relationship between magnitude of bystander response and cell density in C3H 10T½ cells. The response seen at the high density (●) is significantly more sensitive than the low density (■)($p<0.0001$). Data points are the mean of three experiments (±SEM).

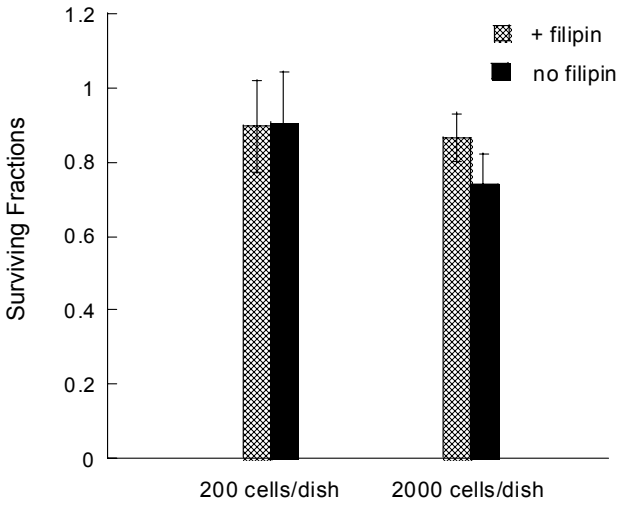

Fig. 2. Effect of Filipin on bystander response in C3H 10T½ cells.

for 1 h at 37ºC and 10% of the cells were then irradiated on the microbeam with 12 α-particles per cell. Preliminary results are shown in Figure 2. When cells are irradiated at low density, pre-incubation with Filipin had no effect on cell survival (SF of 0.90 +/– Filipin). However at the high cell density, pre-treatment of the cells with Filipin caused an increase in cell survival similar to the level seen in the low density cultures (SF of 0.87 (+ Filipin) vs. 0.74). This is further evidence for the importance of the cell membrane in the transmission of signals from hit to bystander cells.

The Bystander Effect in Radiation Oncogenesis

Stephen A. Mitchell, Stephen A. Marino, David J. Brenner and Eric J. Hall

We have used a novel irradiation set up to investigate the bystander effect in C3H 10T½ cells and its relationship with the adaptive response. Although both these phenomena are important at low doses, they have opposite effects on cell survival with the bystander effect transmitting damage from irradiated to non-hit cells while the adaptive response confers resistance to radiation following an initial low priming dose.

The system employed in this study consists of an outer and inner ring which fit together as shown on the left in Figure 1. The outer ring has a base of 6 μm mylar while the inner ring has several strips of 30 μm mylar on the base. Following sterilization with 70% ethanol, the rings are fitted together such that the mylar strips of the smaller ring sit directly on the mylar base of the larger ring. The cells can be plated at the desired concentration. In this way, cells attach to both the 6 μm mylar and the top surface of the 30 μm mylar strips. As the dishes are irradiated from underneath on the track segment facility, α-particles can penetrate the 6 μm mylar, irradiating cells attached to this layer but are unable to pass through the 30 μm mylar layer. Therefore cells growing on the strips are unirradiated but are in close physical proximity to irradiated cells. Following irradiation and further incubation the dishes can then be separated and the non-irradiated cells removed from the strips and examined for several endpoints.

C3H 10T½ cells (passage 9-12) were grown in Eagle's basal medium supplemented with 10% fetal calf serum and penicillin/streptomycin. Cells were plated in the dishes at two different concentrations (1×10^5 or 6×10^5 per dish) to investigate any potential influence of cell density on the magnitude of the bystander effect. The effect of irradiating media alone was also examined to investigate the contribution of factors which may be generated in the irradiated medium.

Cells were either sham irradiated or irradiated with α-particles to a total dose of 5 Gy using the track segment mode of the 4 MeV Van de Graff accelerator at RARAF. The dishes were then returned to the incubator for either 24 or 48 h before processing.

To assess radiation-induced oncogenic transformation and clonogenic survival, approximately 300 or 100 viable cells were plated into 10 cm dishes respectively. For transformation studies, culture medium was changed at 12 day intervals during the 7 week incubation. The cells were then fixed in formalin, stained with Giemsa and transformed foci types II and III scored. Cells plated for clonogenic survival were incubated for 2 weeks without medium change, stained with 2% crystal violet and colonies >50 cells scored.

Fig. 1. Apparatus used for investigation of bystander response.

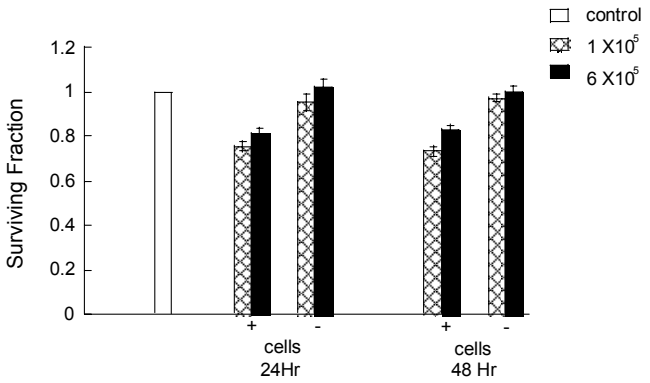

Fig. 2. Surviving fraction of non-irradiated C3H 10T½ cells co-cultured either with cells (+ cells) or media (- cells) irradiated with 5 Gy of α-particles. Data were pooled from three independent experiments (±SEM).

Table I

Oncogenic transformation in bystander cells

Irradiation conditions	Clonogenic surviving fraction (plating efficiency)	Number* of viable cells exposed/10^4	Number of transformants produced	Transformation frequency/10^4 surviving cells
Control	(0.44)	3.96	2	0.51
Bystander	0.79	2.50	11	4.4

*Estimated, accounting for plating efficiency and clonogenic survival.

As shown in Figure 2, a significant decrease in surviving fraction (SF~0.80; $p<0.05$) was observed in the non-irradiated cells following both 24 and 48 h co-culture with cells irradiated with 5 Gy of α-particles. These data indicate that the irradiated cells release cytotoxic factors into the medium that were toxic to the non-irradiated cells. However irradiating media alone had no effect on the survival of the non-irradiated bystander cells. A similar magnitude of bystander effect was seen when the cells were irradiated with 5 Gy of low LET X-rays (data not shown). It has been suggested that gap junction communication between cells is an important mediator of bystander effects. However, no difference was seen between the two cell densities examined. This may be because at the low density used in the present study, 30-40% of the cells are in contact after 24 h incubation and so it may be necessary to reduce the cell density further to study this effect.

Considering oncogenic transformation, preliminary results show that there is an increased transformation frequency in bystander cells compared with control cells (Table I).

To examine the interaction of the adaptive response with the bystander effect, cells were exposed to either 0 or 2 cGy of 250 kVp X-rays at 5 mA with 0.2 mm copper and 1 mm aluminum external filters. The absorbed dose rate was calculated at 8.5 $cGymin^{-1}$. Six hours after the initial exposure cells were then irradiated on the track segment facility as described above. The results are shown in Figure 3.

Cells exposed to the priming radiation dose 6 hours prior to being co-cultured with cells exposed to 5 Gy of α-particles showed an increase in surviving fraction at both 24 and 48 h post-irradiation compared with cells which did not receive the priming dose. These preliminary findings indicate that a dose of X-rays as low as 2 cGy can result in an adaptive response that cancels out the majority of the observed bystander effect.

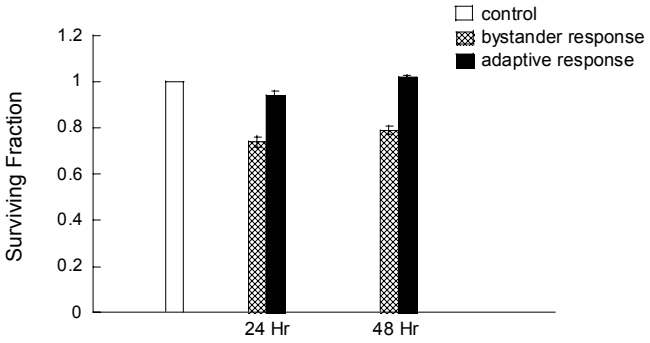

Fig. 3. Relationship between adaptive response and bystander effect in C3H 10T½ cells.

Analysis of Media for Factors Involved in the Initiation and Propagation of a Radiation-Induced Bystander Effect

Brian Ponnaiya, Fu-ru Zhan, Stephen A. Marino and Charles R. Geard

There is now a substantial amount of data in support of a radiation-induced bystander effect. However, little is know of the mechanisms involved in the initiation and propagation of the phenomenon. One hypothesis is that following irradiation, cells secrete certain factors into the media that diffuse through the media and affect the non-irradiated cells and are responsible for the initiation of the response in these bystander cells. To test this hypothesis, we have examined the media surrounding irradiated cells for alterations in the levels of cytokines using a previously described co-culturing protocol. We have previously demonstrated the presence of a radiation induced bystander effect using this protocol, where irradiated and bystander cells were cultured on two surfaces of mylar separated by media.

For these studies, normal human fibroblasts were cultured on both mylar surfaces (separated by serum-containing

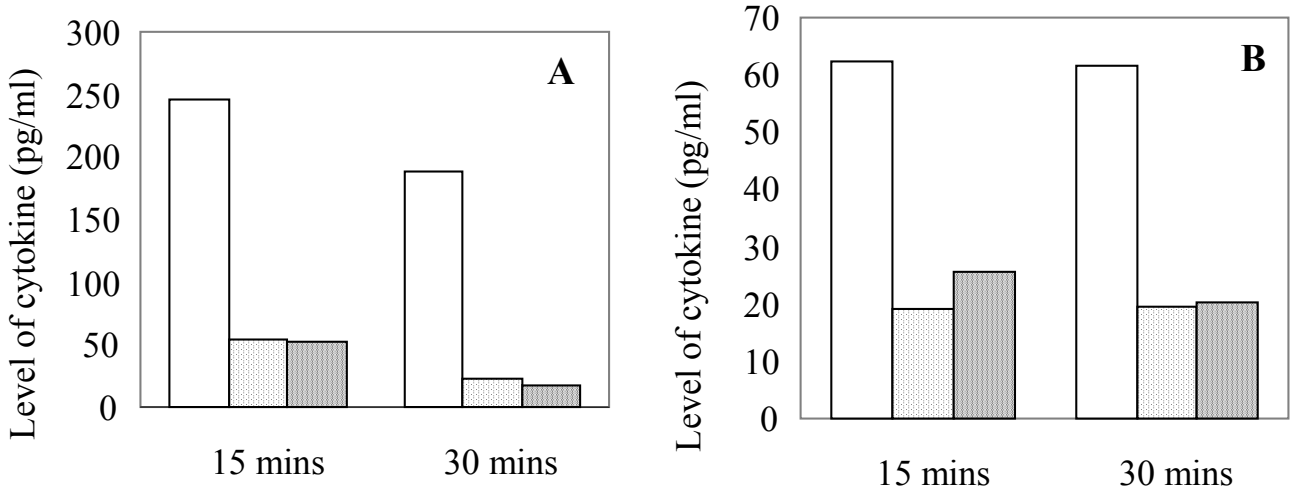

Fig. 1. Levels of IL2 (A) and IL4 (B) detected in media in unirradiated dishes (□), or following irradiation with 0.1 Gy (▨) or 1 Gy (▩) α-particles.

media) and cells on one side were irradiated with 0.1 or 1 Gy α-particles (an average of 1 and 10 particles per cell nucleus respectively). Following irradiation, dishes were returned to the incubator and 300 μl of media aliquots were removed from the dishes at the indicated time, spun down to remove any floating cells/debris, quick frozen in liquid N_2 and stored at -80 ^{o}C till they were analyzed. All cytokine analyses were conducted by Pierce Boston Technology Center, MA. The cytokines analyzed for were IL2, IL4, IL8, IL10, IL12, IL13, TNFα and INFγ.

As can be seen in the figure, in non-irradiated dishes the levels of IL2 and IL4 were around 200-250 and 60 pg/ml respectively. These levels were probably derived from the serum in the media. Following irradiation, levels of IL2 dropped to less that 50 pg/ml in as little as 15 minutes and remained there for the rest of the time points examined. In these repeat experiments the levels of the other 6 cytokines assayed were unchanged.

The decrease in levels of this cytokine were not dependent on the dose of α-particles delivered. Similar decreases were seen with IL4 levels. At 15 minutes post-irradiation, IL4 levels were down to between 20-25 pg/ml at both doses.

The rapid depletion of some cytokine levels following irradiation may be due to the activation of receptors on either the irradiated cells or bystander cells or both populations, which then results in the removal of these cytokines from the media. Alternatively, it is possible that the irradiation results in the excretion of molecules that either directly or indirectly degrade or alter the conformation of the cytokines. Studies are currently ongoing to examine these various possibilities. CRR

Alterations in Gene Expression in Bystander Normal Human Fibroblasts Following Microbeam Irradiation with α-Particles

Brian Ponnaiya, Gloria Jenkins-Baker, Gerhard Randers-Pherson and Charles R. Geard

Previous Microbeam studies of the radiation-induced bystander effect have indicated a lack of dose response, i.e. the amplitude of the response is independent of the dose (or fluence) delivered to the irradiated cells in the population. In addition, data suggest that the response seen in bystander cells is independent of the number of cells that are irradiated in the population. In fact, for a variety of end points including oncogenic transformation and mutation, irradiating a fraction of the population or the entire population with a defined number of a-particles, resulted in similar frequencies of events.

We have previously demonstrated the induction of p21/WAF1 in bystander normal human fibroblasts following Microbeam irradiation. These studies were conducted with

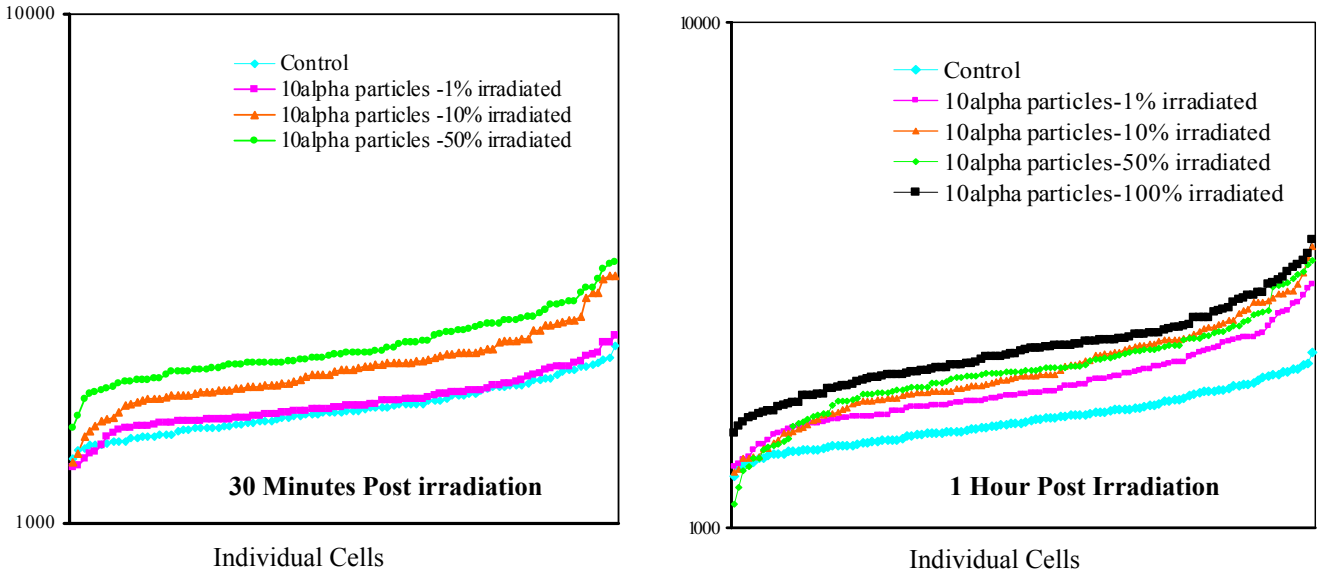

Fig. 1. Expression of p21/WAF1 expression as measured by fluorescence intensity/nucleus in individual cells of populations of control or microbeam irradiated populations where 1%, 10%, 50%, or 100% the cells were irradiated with 10 α-particles and assayed at 30 minutes and 1 hour post irradiation.

equal numbers of irradiated and bystander cells in the population, i.e. 50% of the cells in the population were irradiated and the other half were bystander cells. Here we present data of the induction of p21/WAF1 following microbeam irradiation of 1%, 10%, 50% and 100% of cells in the population.

Plateau phase normal human fibroblasts were seeded onto cell-tak coated dishes designed for Microbeam irradiation (~500 cells per dish). Cells were stained with 50 nM Hoechst 33342 for 30 minutes and then maintained in serum-supplemented media till the time of irradiation. A predetermined fraction of the cells on each dish were irradiated with 10 α-particles. Following irradiation, 2 ml of media was added to the dish, and incubated for indicated times after which dishes were rinsed briefly in Hanks balanced salt solution (HBSS) and fixed with 100% ice-cold methanol. In situ detection of p21/WAF1 protein induction in hit and bystander cells was performed as previously described, though with some modification. Briefly, methanol-fixed cells were air dried, rinsed in PBS and permeabilized with 4% neutral buffered formalin for 30 minutes at 37^{o}C followed by incubation with 6% BSA for 30 minutes. Slides were then washed and incubated with a mouse monoclonal antibody against p21/WAF1 (Santa Cruz) (10μg/ml in 1% BSA) at 37^{0}C for 30 minutes. Following three washes in PBS, cells were incubated with a FITC tagged sheep anti-mouse antibody (Sigma) (1mg/ml in 1% BSA). Slides were then washed and mounted in Vectashield (Vector Laboratories, Burlingame, CA) and visualized using fluorescent microscopy. Images of individual cell nuclei were obtained using a hamamatsu CCD camera and fluorescence intensity per individual nucleus was measured by ImagePro Plus.

The expression of p21/WAF1 in individual cell nuclei is given in figure 1. Individual cells have been arranged from lowest to highest fluoresence intensities in the population. As can be seen there was considerable variation in expression levels even in the control cells. This is in keeping with previous microbeam data of the variability in mRNA and protein levels. At 30 minutes post irradiation, the profile of the population with 1% irradiated cells was essential indistinguishable from that of the controls. As expected the 50% irradiated population had cells that were expressing much higher levels of p21/WAF1 protein. The profile of the 10% irradiated population was intermediate between the 50% and control profiles. At 1 hour post-irradiation the 1% irradiated population was significantly different from that of controls, and was approaching that of the 10% and 50% irradiated populations that were similar at that time point. Cells in the 100% irradiated population continued to express p21/WAF1 at much higher levels throughout.

The change in the profile of the population in which only 1% of the cells were irradiated, from that resembling controls at 30 minutes to that of 10% and 50% irradiated populations would indicate that there is some sort of measured response depending on the fraction of cells that are irradiated. It is possible that when only a few cells in the population are irradiated, the factors being released into the media are not at sufficiently high enough concentrations to provide as rapid a response. That is, the kinetics of the development of the response are slower if fewer numbers of cells are irradiated. However, with time the response is indistinguishable from that where larger numbers of cells are hit. This is in keeping with data of other endpoints which are assayed at days and even weeks after the irradiation. CRR

Studies of Bystander Effects in Artificial Human 3D Tissue Systems Using a Microbeam Irradiation

Oleg V. Belyakov, Eric J. Hall, Stephen A. Marino, Gerhard Randers-Pehrson and David J. Brenner

Introduction

According to the target theory of radiation-induced effects (1), a central tenet of radiation biology, DNA damage occurs during or very shortly after irradiation of the nuclei in targeted cells, and the potential for biological consequences can be expressed within one or two cell generations. A range of evidence has now emerged that challenges the classical effects resulting from targeted damage to DNA. These effects have also been termed "non-targeted" (2) and include radiation-induced bystander effects (3), genomic instability (4), adaptive response (5), low dose hyper-radiosensitivity (HRS) (6), delayed reproductive death (7) and induction of genes by radiation (8). An essential feature of "non-targeted" effects is that they do not require a direct nuclear exposure by irradiation to be expressed, and they are particularly significant at low doses. This evidence suggests a new paradigm for radiation biology that challenges the universality of target theory.

The radiation-induced bystander effect is the phenomenon whereby cellular effects such as sister chromatid exchanges, chromosome aberrations, apoptosis, micronucleation, transformation, mutations, differentiation and changes of gene expression are expressed in unirradiated neighboring cells near to an irradiated cell or cells (9). The bystander effect cannot be comprehensively explained on the basis of a single cell reaction. It is well known that an organism is composed of different cell types that interact as functional units in a way to maintain normal tissue function. Radiation effects at the tissue level under normal conditions prove that individual cells cannot be considered as an isolated functional unit within most tissues of a multicellular organism (10). Experimental models, which maintain tissue-like intercellular cell signaling and 3-D structure, are essential for proper understanding of the bystander effect. Only a few papers have been published on bystander effects in multicellular systems (11-15).

With the exception of abscopal effects (16) and clastogenic factors in the blood plasma of patients undergoing radiation therapy (17), little evidence of a bystander effect under *in-vivo* conditions is available. The only experimental work which deals with the bystander effect under *in-vivo* conditions is from Watson and coauthors (18), who utilized a bone marrow transplantation protocol to demonstrate that genomic instability could be induced in bystander cells; a mixture of irradiated and non-irradiated cells, distinguished by a cytogenetic marker, was transplanted into CBA/H mice, and genomic instability was demonstrated in the progeny of the non-irradiated cells.

Our rationale for the current project is that the bystander effect is likely to be a natural phenomenon, which should be studied in an *in-vivo*-like multicellular system with preserved 3-D tissue microarchitecture. This necessitates moving from purely *in-vitro* cell culture systems to a tissue-based system for *in situ* microbeam irradiation, allowing us to study bystander effects in samples with preserved 3-D microarchitecture and an intact tissue microenvironment.

Materials and Methods

Human Artificial Skin Tissue Systems

Our hypothesis is that the bystander effect is, at least in part, a natural protective phenomenon which can most usefully be investigated under *in-vivo* like conditions. We suggest here that the 3-D tissue microarchitecture and microenvironment are important for initiation and perpetuation of the bystander effect. In order to fulfill these requirements, yet maintain good reproducibility, we decided to use novel artificial human tissue systems, which are commercially available (MatTek Corporation, Ashland, MA). Artificial tissues reconstruct the normal tissue microarchitecture and preserve the *in-vivo* differentiation pattern. They are mitotically and metabolically active and release the relevant cytokines. Cells in these tissues also demonstrate the presence of gap junctions.

Artificial tissues are cultivated using an air-liquid interface tissue culture technique (Fig. 1A). Tissue is grown on a semi-permeable membrane and fed with a serum-free medium from below (Fig. 1B). The human skin artificial tissue systems are cultivated on Millicell-CM culture inserts (Millipore), using a 28 μm hydrophilic PTFE membrane. The surface of the tissue is exposed to the air, which stimulates differentiation. Artificial tissues consist of a few layers of cells. The diameter of the MatTek tissues is about 8 mm, and their lifetime is 2 to 3 weeks depending on the tissue type.

Artificial tissues are very stable and allow a high degree of reproducibility. This is a *crucial* advantage for microbeam experiments, which require a high degree of precision. On the other hand it is a very flexible system because many parameters including the type of cells, degree of differentiation and size can be controlled. The system is very cost effective, compared to working with primary explants, which requires an animal house.

We are using a few types of artificial tissues for microbeam bystander experiments. In this short communication we will concentrate on EpiDerm, which is a human artificial skin system. EpiDerm consists of normal, human epidermal keratinocytes, which have been cultured to form a multilayered, differentiated model of the human epidermis. It closely resembles human skin microarchitecture with *in-vivo* like morphological and growth characteristics, which are uniform and highly reproducible. We are using three modifications of

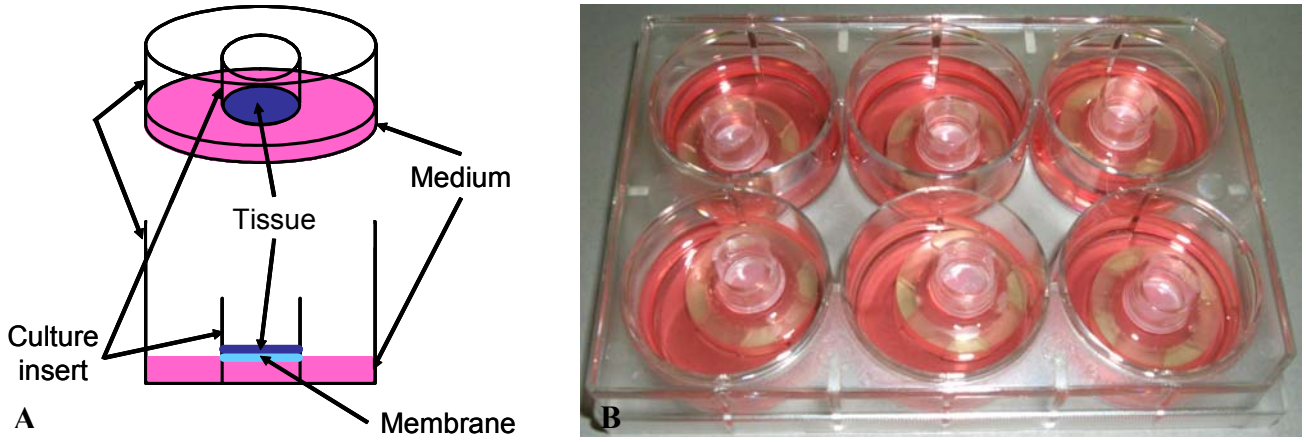

Fig. 1. Panel A, schematic representation of the Air-Liquid Interface tissue culture technique. Panel B, cultivation of an EpiDerm artificial human tissue system (EPI-200) in a multiwell dish. Millicell-CM culture inserts (Millipore) rest on plastic stands, which allow better medium supply. The diameter of these Millicell-CM culture inserts is 12 mm.

EpiDerm: EPI-200-3s, EPI-201 and EPI-200. EPI-200-3s (Fig. 2A) is a non-differentiated model; it consists of 1-2 cell layers and is not more than 10 μm thick. EPI-201 (Fig. 2B) is an intermediately-differentiated model; it consists of 3-5 cell layers and is 20-45 μm thick. Finally, EPI-200 (Fig. 2C) is a differentiated model of the epidermis; it consists of 10-12 cell layers and is 75-100 μm thick.

Various degrees of differentiation are important because we demonstrated recently the importance of differentiation as a major component of the bystander response in the urothelial explant model (19). On the other hand, both the EPI-200-3s and EPI-201 models, if cultured, eventually form a system similar to the fully differentiated EPI-200. This gives us the opportunity to irradiate the undifferentiated EPI-200-3s model and study delayed bystander effects 7 days later when a fully differentiated multilayer structure would be formed - a study on the bystander response in the progeny of irradiated cells.

Morphologically, EpiDerm consists of basal, spinous, granular, and cornified layers analogous to those found in an *in-vivo* epidermis. The system is mitotically and metabolically active (20). Markers of mature epidermis-specific differentiation such as pro-filaggrin, K1/K10 cytokeratin pair, involucrin, and type I epidermal transglutaminase are expressed in the EpiDerm system (21). Analysis of the tissue microstucture has proved the presence of keratohyalin granules, tonofilament bundles, desmosomes, and a multi-layered stratum corneum containing intercellular lamellar lipid layers arranged in patterns characteristic of an *in-vivo* epidermis (22).

Microbeam Irradiation

The Columbia University single-cell / single-particle microbeam was used for tissue irradiation. A detailed description of the Columbia University microbeam has been given by Randers-Pehrson and co-authors (23).

One of irradiation schedules we used was to microbeam irradiate each tissue sample in a known pattern, so that all the irradiated cells are in one plane. Ten α-particles (~7.2 MeV) per location were delivered every 20-100 μm along the irradiation plane. A tissue sample is 8 mm in diameter. The human skin artificial tissue system is cultivated on Millicell-CM culture inserts (Millipore), using a 28 μm hydrophilic PTFE membrane. The tissue samples are irradiated from below through the membrane that forms the base of the culture insert. After traversal of the membrane a 7.2 MeV α-particle beam would have a remaining energy of about 2 MeV. This is enough energy to traverse about 10-15 μm of tissue, a range sufficient to target the basal cellular layers of EPI-200 and EPI-201 and to traverse all layers of EPI-200-3s artificial tissues.

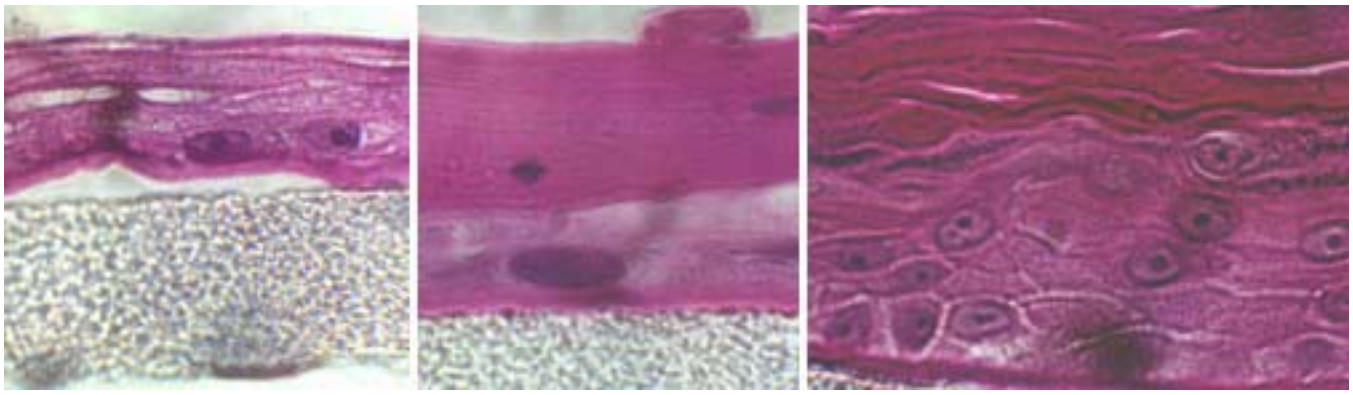

Fig. 2. Artificial epidermal human skin systems EPI-200-3s (A), EPI-201 (B) and EPI-200 (C), which have increasing levels of differentiation. Samples are formalin fixed, paraffin embedded, with H&E stained sections imaged through a transmission light microscope (400X).

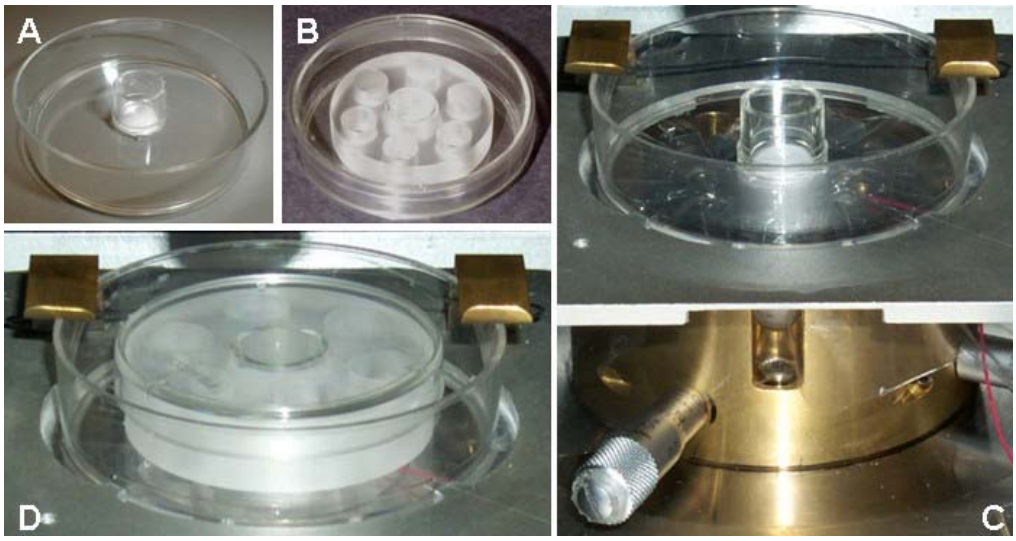

Fig. 3. Setup for microbeam irradiation of tissue fragments. The human skin artificial tissue system is cultivated on a Millicell-CM culture insert (Millipore), which utilizes a 28 µm hydrophilic PTFE membrane. For irradiation, the insert is positioned in a custom-designed holder (**A**) and is held down by a fixture (**B**) to maintain stability. The insert holder is positioned on the microbeam stage, and the tissue is irradiated from below. The full microbeam cell dish assembly is represented in **D**.

In order to maintain high precision, the culture insert is positioned in a custom-designed holder (Fig. 3A) and held with a fixture (Fig. 3B) to maintain stability. The holder is positioned on the microbeam stage (Fig. 3C), and the tissue is irradiated from below. The full microbeam cell dish assembly is represented in Fig. 3D. It is covered with a fixture to prevent contamination and drying-up during irradiation. The irradiation is fully automated, with a user-friendly interface to specify the number of protons per irradiation point and the separation between the irradiation points along the line of irradiation. Typical irradiation times vary from 1 to 4 minutes per tissue.

After microbeam irradiation, each tissue is returned to a multi-well dish filled with fresh medium and incubated at 36.5-37°C in a humidified atmosphere with 5% CO_2, prior to fixing for 3 days.

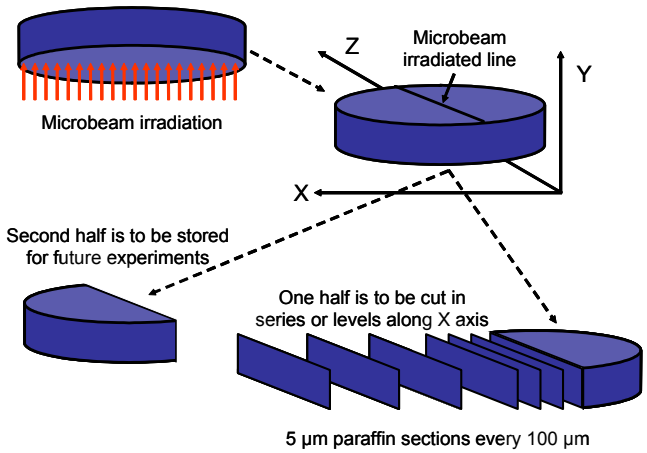

Fig. 4. After incubation, tissues were fixed in 10% neutral buffered formalin, paraffin embedded, and cut in 5 µm segments along the X axis to prepare histological sections.

Paraffin Histological Section Preparation

After incubation tissues were fixed in 10% neutral buffered formalin, paraffin embedded, and cut in 5 µm segments along the X axis (see Fig. 4) to prepare histological sections. We used vertical sectioning to physically isolate tissue fragments which contained directly irradiated cells from other fragments containing cells which had not been irradiated but were at known distances from irradiated cells. Figure 4 demonstrates our approach in detail.

Endpoints

After cutting and mounting on slides, sections were stained for the endpoints of interest. We performed a routine haemotoxylin-eosin (H&E) staining for every series of slides

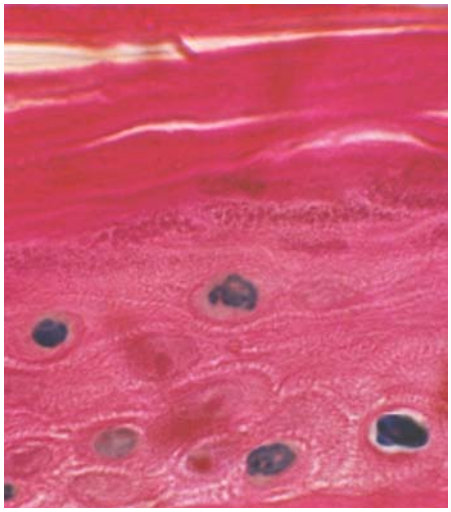

Fig. 5. Bystander-induced apoptosis in the artificial human skin system EPI-200 stained with the DermaTACS apoptosis kit. Positive apoptotic cells appear blue. Formalin fixed, paraffin embedded 5 µm histological sections are shown as imaged through a transmission light microscope (600X).

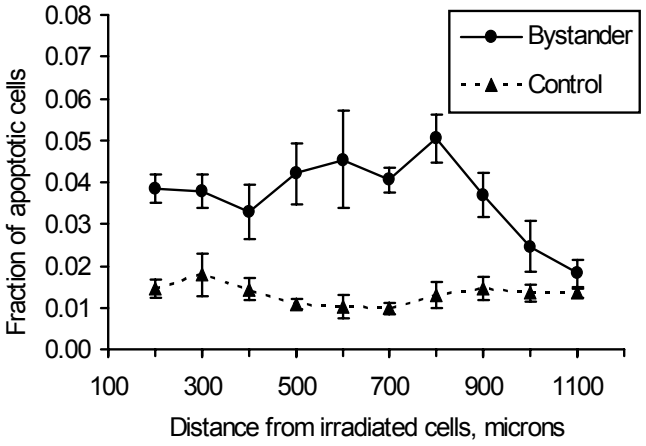

Fig. 6. Fraction of apoptotic cells (TUNEL assay) in unirradiated bystander cells at different distances from irradiated cells in 3-D human artificial skin tissue (EPI-200, 10 α-particles every 100 μm) on day 3 after irradiation. Error bars represent standard deviations of the means (SEM). Each point (and SEM) is derived from at least 3 repeat experiments.

to assess the tissue morphologically. The next step was a quantitative assessment of the apoptosis contribution to the bystander effect using a TUNEL enzymatic *in-situ* labeling kit (DermaTACS) optimized for paraffin sections (Figs. 5, 6). The fraction of apoptotic cells is counted and the spatial distribution recorded. We also studied bystander-induced differentiation under *in-situ* conditions using immunohistochemical markers such as pro-filaggrin, K1/K10 cytokeratin pair (data not shown).

Statistical Analysis

Each experiment was performed with at least three different tissues and repeated at least for 3 times. All individual tissues were number-coded and scored blindly. The mean and standard deviation were calculated for all endpoint-positive and control cases. Significance tests were performed using the Student's t test. In all statistical analyses, $P < 0.05$ was considered as statistically significant.

Results and Discussion

We have been working with MatTek human artificial tissues for over 9 months. During this period of time we have tested a variety of human artificial tissues. In addition to the skin models already discussed, we performed microbeam and broad-field experiments with two other human artificial tissue systems: a reconstruction of the tracheal/bronchial tissue of human respiratory tract EpiAirway (AIR-110) and a corneal model (OCL-200). During these pilot experiments we used the Columbia University charged particle microbeam system (α-particles, ~7.2 MeV) and broad-beam track-segment facility (3.3 MeV α-particles, 3.4-3.8 MeV protons). However, here we would like to concentrate on the preliminary results obtained with the EpiDerm human artificial skin models subjected to 7.2 MeV α-particles microbeam irradiation.

Human artificial skin systems have been carefully characterized; we performed extensive morphometric measurements and tested cultivation procedures for these models. We have developed unique techniques for broad-field and microbeam irradiations of human artificial tissue systems. We solved technical complications connected with the relatively short range of the beam. The nature of the bystander experiments also requires high precision in positioning and registration of the samples during and post-irradiation. We have designed, in collaboration with the Design & Instrument Shop of the Center for Radiological Research, a set of fixtures (Fig. 3), used for microbeam and broad-field irradiation as well as for cultivation and histological processing. In summary, we now have a well-tuned methodology for microbeam-based bystander experiments on 3-D tissue samples.

We further measured apoptosis using a TUNEL assay (DermaTACS kit) and demonstrated a pronounced bystander-induced apoptosis after microbeam irradiation in the EpiDerm human artificial skin systems (Fig. 5). Positive apoptotic cells appear bright blue (TACS Blue Label) on these photographs. These particular sections were located 500-700 μm from the irradiated line. Figure 6 demonstrates that there was an increased fraction of apoptotic cells versus control in the EPI-200 human artificial tissues. The fraction of apoptotic cells was measured at different distances, ranging from 200 to 1100 μm, away from the line of irradiated cells (10 α-particles every 100 μm) on day 3 after irradiation. The average fraction of apoptosis for all layers in irradiated samples is 3.7±0.6% versus 1.3±0.3% for all layers in control samples. Importantly, there are no statistically significant variations in the expression of bystander apoptosis over the 900 μm distance. This suggests that the bystander response has a long range and is propagated through 3-D tissues, possibly mediated by gap junctions.

We performed a few pilot experiments with morphological (relative ratio of the thicknesses of differentiated cornified layer to non-differentiated, malpighian layer of the epidermis) and immunohistochemical markers of differentiation (pro-filaggrin and cytokeratin 10) in microbeam-irradiated human artificial skin systems. We found a tendency (data not shown) of increased bystander differentiation in irradiated samples.

The main conclusion from the experiments described above is that the developed methodology can be successfully used for microbeam bystander-irradiation experiments. We demonstrated a pronounced bystander-induced apoptosis in human artificial skin systems after microbeam irradiation. There was also a tendency for increased bystander differentiation detected.

The final goal of this ongoing project is to develop a tissue-based hypothesis for the role of bystander responses in radiation-induced tissue responses and, ultimately, carcinogenesis. During this project we are testing hypotheses concerning the protective role of the bystander effects under tissue-like conditions.

References

1. Lea DE. *Actions of Radiation on Living Cells*. University Press, Cambridge, 1946.
2. Ward J. New Paradigms for Low-Dose Radiation Re-

sponse in Proceedings of the American Statistical Association Conference on Radiation and Health. San Diego, California, USA. June 14-17, 1998. *Radiat Res* **151**:92-117, 1999.
3. Iyer R and Lehnert BE. Effects of ionizing radiation in targeted and nontargeted cells. *Arch Biochem Biophys* **376**:1, 14-25, 2000.
4. Wright EG. Inducible genomic instability: new insights into the biological effects of ionizing radiation. *Med Confl Surviv*, **16**:117-30; discussion 131-3, 2000.
5. Wolff S. The adaptive response in radiobiology: evolving insights and implications. *Environ Health Perspect* **106 Suppl:**1277-83, 1998.
6. Joiner, M.C., Marples, B., Lambin, P., Short, S.C. and Turesson I. Low-dose hypersensitivity: current status and possible mechanisms. *Int J Radiat Oncol Biol Phys* **49**:379-89, 2001.
7. Seymour CB, Mothersill C and Alper T. () High yields of lethal mutations in somatic mammalian cells that survive ionizing radiation. *Int J Radiat Biol Relat Stud Phys Chem Med* **50**:167-79, 1986.
8. Hickman A, Jaramillo R, Lechner J and Johnson N. Alpha-particle-induced p53 protein expression in a rat lung epithelial cell strain. *Cancer Res* **54**:5797-800, 1994.
9. Mothersill C and Seymour C. Radiation-induced bystander effects: past history and future directions. *Radiat Res* **155**: 759-67, 2001.
10. Barcellos-Hoff MH and Brooks AL. Extracellular signaling through the microenvironment: a hypothesis relating carcinogenesis, bystander effects, and genomic instability. *Radiat Res* **156**:618-27, 2001.
11. Cummins RJ, Mothersill C, Seymour CB, Johns H and Joiner MC. The effect of microcolony size, at time of irradiation, on colony forming ability. *Int J Radiat Biol* **75**: 225-32, 1999.
12. Bishayee A, Rao DV and Howell RW. Evidence for pronounced bystander effects caused by nonuniform distributions of radioactivity using a novel three-dimensional tissue culture model. *Radiat Res* **152**: 88-97, 1999.
13. Bishayee A, Rao DV, Bouchet LG, Bolch WE and Howell .W. Protection by DMSO against cell death caused by intracellularly localized iodine-125, iodine-131 and polonium-210. *Radiat Res* **153**: 416-27, 2000.
14. Korystov Yu N, Shaposhnikova VV, Dobrovinskaya OR and Eidus L. Intercellular interactions in the interphase death of irradiated thymocytes. *Radiat Res* **134**:301-6, 1993.
15. Jen Y, West C and Hendry J. The lower radiosensitivity of mouse kidney cells irradiated in vivo than in vitro: a cell contact effect phenomenon. *Int J Radiat Oncol Biol Phys* **20**: 1243-8, 1991.
16. Nobler MP. The abscopal effect in malignant lymphoma and its relationship to lymphocyte circulation. *Radiology* **93**:410-2, 1969.
17. Hollowell JG Jr and Littlefield LG. Chromosome damage induced by plasma of x-rayed patients: an indirect effect of x-ray. *Proc Soc Exp Biol Med* **129**:240-4, 1968.
18. Watson GE, Lorimore SA, Macdonald DA and Wright EG. Chromosomal instability in unirradiated cells induced in vivo by a bystander effect of ionizing radiation. *Cancer Res* **60**:5608-11, 2000.
19. Belyakov OV, Folkard M, Mothersill C, Prise KM and Michael BD. Bystander-induced apoptosis and premature differentiation in primary urothelial explants after charged particle microbeam irradiation. *Radiation Protection Dosimetry* **99**:249-251, 2002.
20. Boelsma E, Gibbs S, Faller C and Ponec M. Characterization and comparison of reconstructed skin models: morphological and immunohistochemical evaluation. *Acta Derm Venereol* **80**: 82-8, 2000.
21. Zhao JF, Zhang YJ, Kubilus J, Jin XH, Santella RM, Athar M, Wang ZY and Bickers DR. Reconstituted 3-dimensional human skin as a novel in vitro model for studies of carcinogenesis. *Biochem Biophys Res Commun* **254**: 49-53, 1999.
22. Monteiro-Riviere NA., Inman AO, Snider TH, Blank JA and Hobson DW. Comparison of an in vitro skin model to normal human skin for dermatological research. *Microsc Res Tech* **37**:172-9, 1997.
23. Randers-Pehrson G, Geard CR, Johnson G, Elliston CD and Brenner DJ. The Columbia University single-ion microbeam. *Radiat Res* **156**: 210-4, 2001.

Ronald Baker preparing material for expression analyses of oncongenically transformed mouse embryo fibroblasts (MEF). (See the next article).

Oncogenic Transformation of MEF by Radiation: Characterization Using Gene and Protein Expression

Lubomir Smilenov, Ronald Baker and Eric J. Hall

Exposure to ionizing radiation can have somatic and genetic consequences. The most serious late effects following such exposure is the induction of malignant tumors. Almost all types of cancer have been associated with radiotherapy (1). The latent period between radiotherapy and the appearance of a second primary cancer ranges from a few years to several decades. The risk for a second primary cancer following radiotherapy or chemotherapy emphasizes the need for life-long follow-up of patients receiving such treatments. This is particularly the case in individuals with long life expectancy, for example, patients treated for a childhood neoplasm. The risk of radiation induced cancer following radiotherapy are relatively small in general (example - 0.3% in 5 years survivors (2), and the benefits of radiotherapy in oncology exceed the risks for second primary cancers. The risk can be reduced further by expanding our understanding of the mechanisms involved in cell transformation by radiation. In the recent decades our knowledge about cancer transformation expanded significantly. Many oncogenes and tumor suppressor genes were characterized in cancer models but cancer appears to be a much more complex disease than initially expected (3). In recent years gene expression profiling of cancers was viewed and developed as an important alternative to the classical histopathological characterization of cancers (4). Up to date some articles (5-9) showed altered gene expression patterns in cancer cells and show the possibility to link specific patterns of gene expression to particular tumors. The main problems in this kind of experiment arise from the complexity of tissues where many different types of cells are presented and each type contribute to the measured global gene expression. This combined with the insufficient knowledge of expression of many known and unknown genes makes the analysis of the final data difficult. These problems point to the need for a cell model where the initial and final stages of cancer could be characterized. During an extensive study of cell transformation by radiation we established such a model. The methodology included isolation of mouse embryo fibroblasts, irradiation and culturing of large numbers of cells and identification of transformed clones. In morphological analysis of more than 35000 clones, we isolated 200 clones, expanded them and checked some of them for tumorogenicity in nude mice. Four clones very aggressively formed tumors, five others did not and we considered them immortalized. As result we have stable cell lines and the parental normal cells from which the clones were derived. This represents a line of transformation as follows: Normal cells > Immortalized non-tumorgenic cells > Tumorgenic cells.

To study gene expression patterns in this system we used membrane based hybridization arrays spotted with tags representing 5024 mouse genes and EST's.

For gene expression experiments we used 6 cell lines – 2 normal, 2 immortalized by radiation and 2 transformed by radiation. The expression data was averaged for each type of cells and the comparisons were performed between normal cells, immortalized and cancer cells. The results show a complex pattern of gene expression changes and pointed to genes expressed only in specific stages of the transformation process.

A brief characteristic of the gene expression data follows:

Changes in gene expression in the transition of normal to immortalized: 1434 genes (1176 went up, and 157 went down).

Changes in gene expression in the transition of immortalized to cancer: 1440 genes (685 went up, 755 went down).

Changes in gene expression in the transition of normal to cancer – 1092 (854 went up, 138 went down).

30 genes were overexpressed > 2 times in normal cells vs. both immortalized cells and cancer cells.

245 genes were overexpressed > 2 times in both immortalized and cancer cells vs. normal.

Time changes of the gene expression profiles in cancer cells.

To estimate the changes in gene expression pattern in cancer cells maintained for long periods of time we used one of the cancer cell lines we established. We cultured the cells for 7 months (about 120 population doublings) and used RNA isolated initially and at the end of the period for hybridization experiments. The results show changes in the expression profile of the cancer cells. From a total of 5124 genes and EST's, 175 genes changed their expression during the incubation period. From them 178 genes increased their expression more than 3 times, and 243 decreased their expression more than 3 times.

The general picture appearing from these results is that the transition from normal to immortalized phenotype involves the activation of many genes even if we compare embryo cells still retaining a capacity for cell division and the immortalized cells. Another big transition appears to exist between immortalized and the transformed phenotype. More genes are downregulated than upregulated, which confirms the highly specialized phenotype of the cancer cells.

The experiments addressing the genomic instability of cancers showed that overall about 8% of genes change their expression level during the 7 month period which is an indicator if the instability of the cancer cell line. This confirms that cancers are not stable as well as shows that the interpretation of gene expression data for cancers should be linked to particular time period and stage. Additionally this ques-

Table I

Antibodies against the following proteins were used to determine protein expression in normal, immortalized and transformed cells:

α E–Catenin	E-catenin	PR
β-catenin	ERα	pS2
BCL2	ERβ	PTEN
BRCA1	Fra1	RAD51
c Jun	HSP27	RAR α
cdk4	ICAM1	Rb
cFOS	Integrin b3	TGFa
cJun	MDM-2	TGFa
Connexin 45	Neu	tsg 101
Connexin43	p21	Tubulin
Cyclin A1	p27	Vimentin
CyclinB1	p27	Wnt1
CyclinD1	p53	Actin (total)
E Cadherin	PCNA	

tions the usefulness of relating data from cancer cell lines experiments to primary tumors – the incubation time increases the differences between the source and the line and this must be always taken into account.

Protein expression in normal immortalized and transformed MEF cells

To characterize further our model and to find useful transformation markers for it we determined protein expression by western blotting. The antibodies we used were selected on the basis of our gene expression experiments, published results and antibody availability (Table I). Every antibody was used to detect protein expression in two normal MEF pools, two immortalized cell lines and four transformed MEF cell lines. Total of 40 antibodies were used and six proteins were found to be expressed in very high levels in transformed cells but not in the immortalized and normal cells. The results are shown in fig. 1.

Conclusions

This study revealed changes in gene expression in the transition between normal, immortalized and transformed cells. It involves large numbers of genes and appear to be more complex than initially anticipated. The results from the gene expression experiments were used to characterize a system for transformation encompassing the transition from normal and immortalized to cancer phenotype. Six proteins highly expressed only in cancer cells were identified. These proteins could be used as a transformation markers for MEF. These markers will allow us to identify much more reliably transformed clones in comparison with the current morphological identification used in MEF transformation assays.

References

1. Kollmannsberger C, Hartmann IT, Kanz L and Bokemeyer C. Therapy-related malignancies following treatment of germ cell cancer. *Int J Cancer* **83**:860-3, 1999.
2. Murray EM, et al. Postradiation sarcomas: 20 cases and a literature review. *Int J Radiat Oncol Biol Phys* **45**:951-61, 1999.
3. Schichman S and Croche C. Oncogenes in Cancer Medicine. Edited by Pine IW, Williams & Wilkins, 1997.
4. Golub TR, Slonim DK, Tamayo P, et al. Molecular classification of cancer: class discovery and class prediction by gene expression monitoring. *Science* **286**:531-7, 1999.
5. Ross DT, Scherf U, Eisen MB, Perou CM, Rees C, Spellman P, Iyer V, Jeffrey SS, Van de Rijn M, Waltham M, Pergamenschikov A, Lee JC, Lashkari D, Shalon D, Myers TG, Weinstein JN, Botstein D, Brown PO. Systematic variation in gene expression patterns in human cancer cell lines. *Nat Genet* **24**:227-35, 2000.
6. Martin KJ, Kritzman BM, Price LM, Koh B, Kwan CP, Zhang X, Mackay A, O'Hare MJ, Kaelin CM, Mutter GL, Pardee AB, Sager R. Linking gene expression patterns to therapeutic groups in breast cancer. *Cancer Res* **60**:2232-8, 2000.
7. Ramaswamy S, Ross KN, Lander ES and Golub TR. A

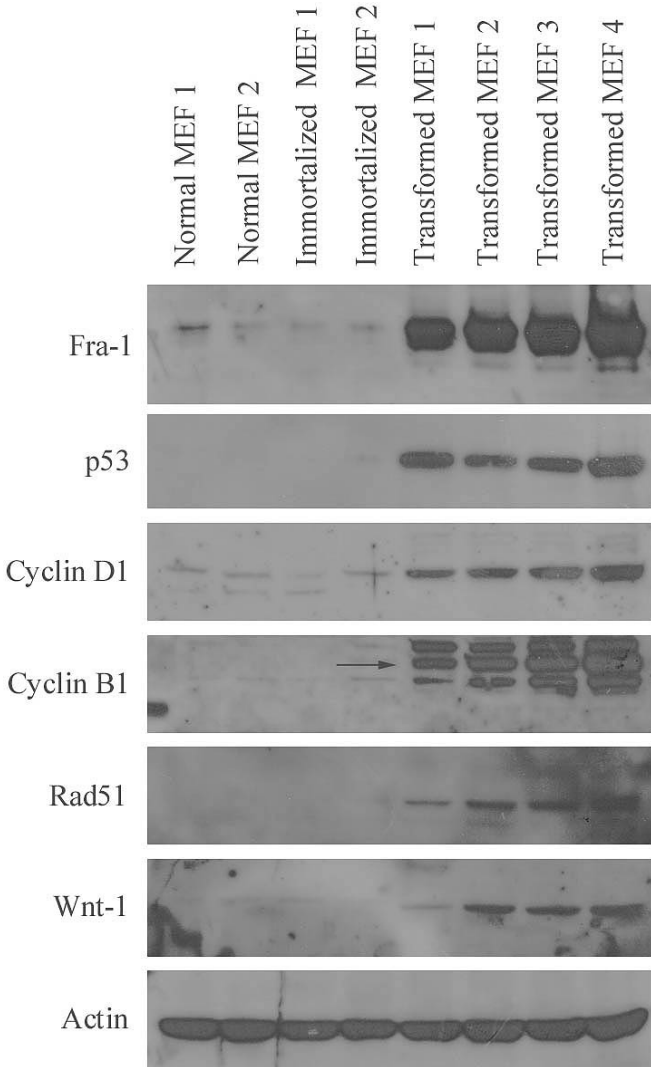

Fig. 1. Proteins overexpressed in transformed cells in comparison with normal and immortalized cells. The proteins were identified by western blotting.

molecular signature of metastasis in primary solid tumors. *Nat Genet* **33**:49-54, 2002.
8. Shridhar V, Sen A, Chien J, Staub J, Avula R, Kovats S, et al. Identification of underexpressed genes in early- and late-stage primary ovarian tumors by suppression subtraction hybridization. *Cancer Res* **62**:262-70, 2002.
9. Luo J, Duggan DJ, Chen Y, Sauvageot J, Ewing CM, Bittner ML, et al. Human prostate cancer and benign prostatic hyperplasia: molecular dissection by gene expression profiling. *Cancer Res* **61**:4683-8, 2001.

ATM Dependent γ-H2AX and RPA Assembly Constitutes an Early Component of DSB Repair in Human Cells

Adayabalam S. Balajee and Charles R. Geard

Human replication protein (RPA) functions in a wide variety of DNA transactions involving DNA replication, repair and recombination. RPA occurs in a heterotrimeric form composed of three sub-units with the molecular sizes of 70kd (RPA1), 34kd (RPA2) and 14kd (RPA3) respectively. RPA 2 is a phosphoprotein that is differentially phosphorylated throughout the cell cycle. RPA 2 phosphorylation occurs during the progression of cells from G1 to S-phase and the binding of RPA to ssDNA stimulates the phosphorylation. RPA2 becomes hyperphosphorylated in response to DNA damage induced by ionizing radiation (IR), ultraviolet radiation (UV) and DNA replication inhibitors such as hydroxyurea (HU) and aphidicolin (APC). RPA 2 phosphorylation by DNA damage is either attenuated or abolished in cells defective in DNA dependent protein kinase (DNA-PK) and ataxia telangiectasia mutated (ATM) genes (1, 2) indicating their involvement in RPA2 phosphorylation. RPA2, a crucial component of diverse DNA excision repair pathways, is recently implicated in DNA double strand break (DSB) repair. However, the precise role(s) of RPA in DSB repair and its functional relationship with other known DSB repair proteins remain to be characterized. Investigation on the intranuclear dynamics of RPA in relation to well-known DSB repair factors may enhance our understanding of RPA participation in DSB repair. With this objective in mind, we have investigated the functional relationship between RPA and the phosphorylated form of histone H2AX (γ-H2AX), which has been shown to recruit DSB repair factors to the sites of strand breaks.

Primary and SV-40 transformed fibroblasts derived from normal (MRC5 and GM637H) and AT (GM8391A and GM5849C) individuals were obtained from Coriell Cell Repository, Camden, New Jersey. All the cells were routinely maintained in 2X Eagle's minimal essential medium (E-MEM) supplemented with 15% fetal bovine serum (Gibco BRL) vitamins, essential amino acids, non-essential amino acids and antibiotics. The cultures were maintained at 37°C in a humidified 5% CO_2 atmosphere. Cells in exponential growth phase were irradiated with different doses of γ-rays (0.1-10 Gy) using a ^{137}Cs source delivering a dose rate of 0.98 Gy/min (Gamma cell 40, Atomic Energy of Canada, Canada). Immunolocalization of γ-H2AX and RPA in control and irradiated cells was performed using our standard protocol (3).

Several hundreds of phosphorylated H2AX (γ-H2AX) foci were detected in 85-90% of the irradiated human cells (GM637H) irrespective of the cell cycle stages. The γ-H2AX foci formation was detected in cells immediately after irradiation (10 min irradiation time; no recovery) and the intensity as well as the number of focal sites showed a gradual reduction with increasing post-irradiation times. The induction of γ-H2AX foci intensity in irradiated cells was found to be 3 fold more than that of the control cells. The γ-H2AX foci appeared fairly rapidly at the earliest time point analyzed (10 min irradiation time, 0 min recovery) and the fluorescence intensity reached the peak at 30 min after irradiation. In contrast to γ-H2AX, the homogenous distribution of RPA observed in unirradiated control cells showed a focal distribution after irradiation and focal sites ranging from 100-200 were observed in cells fixed either immediately or 2 hr after irradiation. The coincidence of RPA and γ-H2AX foci was detectable at 30 min after IR and the co-localization peaked at 2 hr after γ-rays indicating the assembly of both proteins at the DSB sites (Fig. 1). The co-localization of both these proteins was also observed on DNA chromatin fibers prepared from the irradiated cells. The co-localization of RPA and γ-H2AX, which was observed in more than 80% of the cells at 2hr after IR, was gradually diminished at 6hr (59%) and 8hr (22%) after irradiation. While RPA foci became much more intense at 4hr and 8hr after γ-rays, γ-H2AX foci became much fewer ranging from 40-50 in number. In order to validate the functional role of this complex in DSB repair, efficiency of RPA and γ-H2AX assembly was investigated in DSB repair defective cells derived from radiation sensitive AT patients. In contrast to normal human cells, induction of γ-H2AX foci formation was not markedly different from the unirradiated cells and the foci formation was greatly attenuated in SV-40 transformed (GM5849C) fibroblast cells. Consistent with this, western blotting analysis showed diminished γ-H2AX induction in AT cells as compared to normal human cells. Additionally, IR induced phosphorylation of RPA2 was hardly detectable in AT cells.

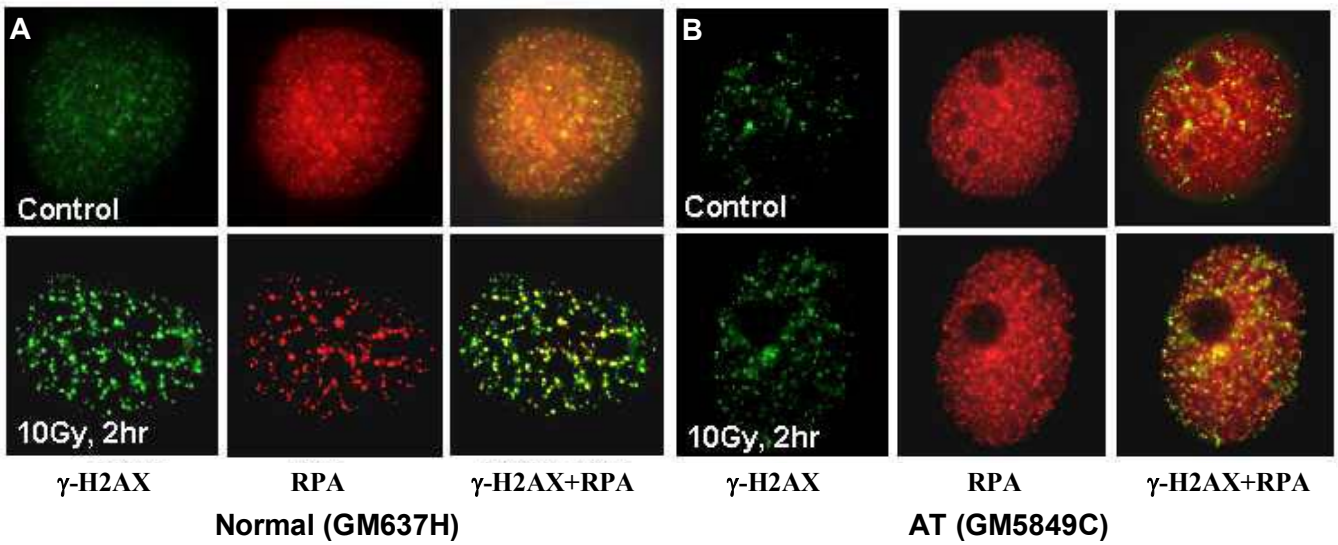

Fig. 1. Ionizing radiation triggers the functional assembly of γ-H2AX and RPA in a time dependent manner in normal cells (panel A) but not in ATM deficient cells (panel B). Control and irradiated cells were fixed in acetone: methanol and immunostained for γ-H2AX and RPA. γ-H2AX (green) was detected by using a rabbit polyclonal primary antibody and FITC conjugated secondary antibody. RPA (red) was detected by using a mouse monoclonal primary antibody and Texas red conjugated secondary antibody.

The homogenous RPA distribution remained essentially the same at different post-irradiation times and distinct RPA focal distribution triggered by γ-rays in normal cells was not noticed in AT cells (Fig.1). Transfection of AT cells with ATM cDNA fully restored the RPA and γ-H2AX assembly in AT cells. This finding clearly demonstrates the requirement of ATM gene in the formation of efficient γ-H2AX and RPA assembly in response to IR induced DNA damage.

The gradual coincidence of RPA with γ-H2AX containing focal sites in a time dependent fashion might indicate a key role for RPA in protecting the ends of the DNA and enhancing the DSB repair process. The attenuation of γ-H2AX phosphorylation and the lack of focal RPA redistribution observed in AT cells after IR suggest that ATM kinase may play a role in RPA and γ-H2AX complex formation. In corroboration, a role for ATM kinase in both H2AX and RPA phosphorylation has been demonstrated. RPA and H2AX complex assembly seems to be a vital component of DSB repair yet the molecular nature of their participation awaits further studies.

References

1. Shao RG, Cao CX, Zhang H, Kohn KW, Wold MS, and Pommier Y. Replication-mediated DNA damage by camptothecin induces phosphorylation of RPA by DNA-dependent protein kinase and dissociates RPA:DNA-PK complexes. *Embo J* **18**:1397-406, 1999.
2. Wang H, Guan J, Perrault AR, Wang Y, and Iliakis G. Replication protein A2 phosphorylation after DNA damage by the coordinated action of ataxia telangiectasia-mutated and DNA-dependent protein kinase. *Cancer Res* **61**:8554-63, 2001.
3. Balajee AS and Geard CR. Chromatin-bound PCNA complex formation triggered by DNA damage occurs independent of the ATM gene product in human cells. *Nucleic Acids Res* **29**:1341-51, 2001.

Transformation of hTERT-immortalized Human Bronchial Epithelial Cells by High Energy ^{56}Fe Ions

Chang Q. Piao and Tom K. Hei

The limited life span of normal human cells represents a substantial barrier to study the multiple steps involved in cancer progression. It has been proposed that maintenance of telomere stability is required for cells to escape from replicative senescence and to proliferate indefinitely. Human telomeres consist of repeats of the sequence TTAGGG at the ends of chromosomes. These sequences are synthesized by the ribonucleoprotein enzyme telomerase with its RNA tem-

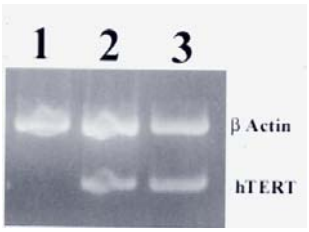

Fig. 1. hTERT expression detected by RT-PCR (above): 1. SAEC, 2. hSAE, 3. hSAE-Fe.

Fig. 2. Telomerase activity analyzed by TRAPEZE Telomerase Detection Kit (above right): 1. SAEC, 2. hSAE, 3. hSAE-Fe.

plate. Functional telomerase activity can be reconstituted by ectopic expression of catalytic subunit of telomerase (hTERT). The majority of normal somatic human cells do not express telomerase activity; however, their life span can be extended or immortalized by ectopic expression of hTERT. On the other hand, tumor cells are often immortal and most of them (80-90%) have telomerase activity. It has been demonstrated that cultured human cells can be transformed to a tumorigenic state by ectopic expression of hTERT together with an activated form of the ras oncogene, and SV-40 large or small T antigens (1-5). These observations suggest that telomerase plays an essential part in neoplastic transformation of human cells.

Previously studies from this laboratory have shown that human papillomavirus-immortalized human bronchial epithelial (BEP2D) cells can be malignantly transformed by a single, 30 cGy dose of high LET α-particles at a frequency estimated to be ~ $4X10^{-7}$ after successive cultivation for 3 to 4 months post-irradiation (6,7). Transformed cells progress through sequential stages including altered growth kinetics and anchorage independent growth, before becoming tumorigenic and producing progressively growing subcutaneous tumors upon inoculation into athymic nude mice. However, the model is not suitable to ascertain the early stage transformation events since both p53 and retinoblastoma genes are compromised in these cells. The use of the hTERT-immortalized cells represents a better alternative since these cells have functional p53 check point activities (Piao and Hei, unpublished data).

In the present studies, normal human small airway epithelial cells (SAEC) from Clonetics (Walkersville, MD) were transfected with hTERT by retrovirus-mediated gene transfer. The construct of pBabest2, in which the cDNA encoding hTERT was subcloned into the retroviral vector pBabe under the control of the promoter present in the Molonly murine leukemia virus LTR was been kindly provided by Dr. Homayoun Vaziri (8). The retroviral constructs were packaged using the highly efficient and helper free cell line Phoenix A (ATCC). Phoenix A cells were plated in 10 cm diameter dishes and transfected when reaching 80% confluence, with 4 μg/ml retroviral plasmid DNA in 10 ml medium using lipofectAMINE plus reagent (Gibco-BRL), according to instruction of the manufacture. Clones that were resistant to 400 μg/ml G418 were selected. The hTERT-expressing cells (hSAE) were irradiated with 60 cGy of ^{56}Fe ions at passage 5 after selected from G418 (hSAE-Fe). Both the h-HSAE and h-HASE-Fe cells had been cultured continuously over 100 population doublings (PD). Figure 1 shows the ectopic hTERT expression in hSAE and hSAE-Fe cells detected by RT-PCR. High telomerase activity was also observed in the hSAE and hSAE-Fe cells analyzed by

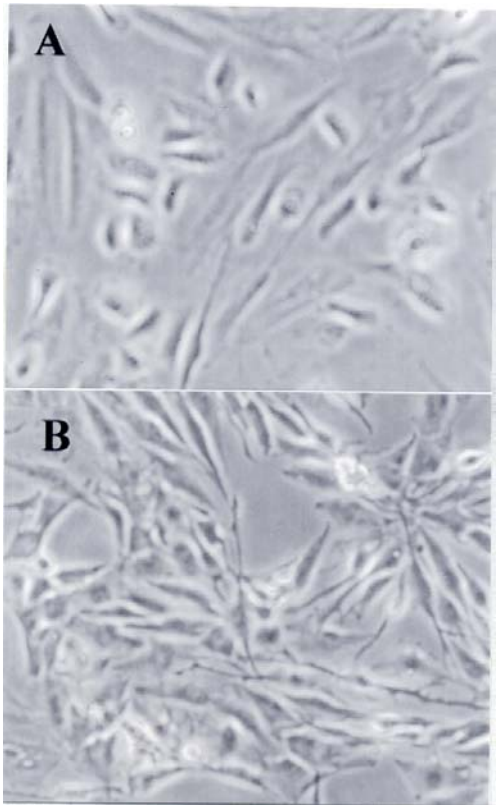

Fig. 3. Morphological alteration and loss of contact inhibition: A) hSAE, B) hSAE-Fe.

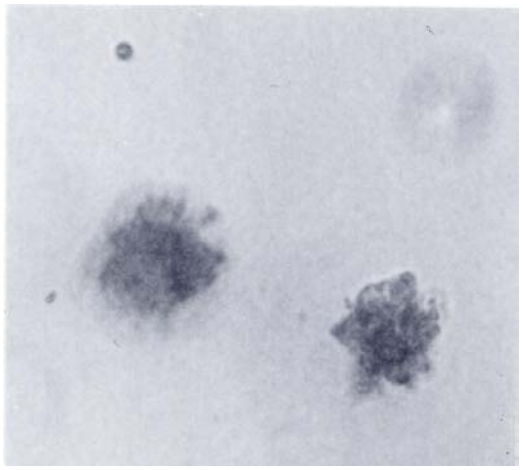

Fig. 4. Colony growth in soft agar of hSAE-Fe cells.

TRAPEZE Telomerase Detection Kit (Intergen) as shown in Fig. 2. After more than 100 PDs in culture, there were morphological changes detected in the irradiated cultures: these cells lost contact inhibition of growth when compared with the parental hSAE cells (Fig. 3). hSAE-Fe cells showed anchorage independent growth in soft agar test (Fig. 4) while hSAE cells remained anchorage dependent. Tumorigenicity in nude mice and studies on the molecular alterations in the hSAE-Fe cells are currently underway.

References

1. Hahn WC, Counter CM, Lundberg AS, Beijersbergen RL, Brooks MW and Weinberg RA. Creation of human tumor cells with defined genetic elements. *Nature (London)* **400**:464-8, 1999.
2. Yu J, Boyapati A and Rundell K. Critical role for SV40 small-t antigen in human cell transformation. *Virology* **290**:192-8, 2001.
3. Elenbaas B, Spirio L, Koerner F, Fleming MD, Zimonjic DB, Donaher JL, Popescu NC, Hahn WC and Weinberg RA. Human breast cancer cells generated by oncogenic transformation of primary mammary epithelial cells. *Genes Dev* **15**:50-65, 2001.
4. Hahn WC, Dessain SK, Brooks MW, King JE, Elenbaas B, Sabatini DM, DeCaprio JA and Weinberg RA. Enumeration of the simian virus 40 early region elements necessary for human cell transformation. *Mol. Cell. Biol.* **22**:2111-23, 2002.
5. Rich JN, Guo C, McLendon RE, Bigner DD, Wang XF and Counter CM. A genetically tractable model of human glioma formation. *Cancer Res.* **61**:3556-60, 2001.
6. Hei TK, Piao CQ, Willey JC, Thomas S and Hall EJ. Accelerated paper: Malignant transformation of human bronchial epithelial cells by radon-simulated alpha particles. *Carcinogenesis* **15**:431-7, 1994.
7. Hei TK, Piao CQ, Willey JC and Hall EK. Genomic instability and tumorigenic induction in immortalized human bronchial epithelial cells by heavy ions. *Adv Space Research* **22**:1699-1707, 1999.
8. Vaziri H and Benchimol S. Reconstitution of telomerase activity in normal human cells lead to elongation of telomeres and extended replicative life span. *Current Biol* **8**:279-81, 1998.

Apoptosis and Growth Inhibition Induced by γ-Rays in hTERT Over-expressing Human Fibroblast and MCF-10F Cells

Chang Q. Piao, Li Liu, Helen Yang and Tom K. Hei

It has been reported that normal human somatic cells have a limited proliferation in culture and do not express telomerase activity. Furthermore, over-expression of the core catalytic subunit of telomerase (hTERT) can induce immortalization of some normal human cells. On the other hand, cancer cells are often immortal and about 80-90% of them express high telomerase activity. Cell immortalization is often associated with both increased telomerase activity and resistance to apoptosis. Inhibiting telomerase can induce apoptosis in tumor cells. Radiation induces DNA damage, apoptosis, cell killing, and, is an important modality in cancer therapy. In this study, normal human dermal fibroblasts (NHDF) and spontaneously immortalized human mammary epithelial cell line (MCF-10F) cells were transfected with hTERT. hTERT transfected fibroblasts (Fbh) and hTERT transfected mammary cells (10Fh) were irradiated with γ-rays. The induction of apoptosis and growth inhibition were compared with their normal countparts.

Cells were cultured with DMEM medium plus 10% FBS in a 37° C incubator with 5% CO_2. Gene transfer of hTERT was achieved by retrovirus-mediated trasfection in NHDF cells, and Effectene Transfection Reagent (GIAGEN) with MCF-10F cells. Telomerase activity was detected by the TRAPEZE Telomerase Detection Kit (Intergen). Expression of hTERT was analyzed by RT-PCR. For growth inhibition analysis, the same number of irradiated and non-irradiated cells was plated in T25 flasks; cell number was counted after 24 hrs of incubation. Growth inhibition was calculated by the cell number of irradiated cells compared to the number of non-irradiated cells. To detect apoptosis, cells were plated in T25 flasks and chamber slides 24 hrs before irradiation, Fbh and Fb cells were irradiated with 2 doses, 10 and 15 Gy of γ-rays whereas 10Fh and 10F cells were irradiated with 3 and 6 Gy of γ-rays respectively. Apoptosis was detected after 24 hrs incubation by both DNA ladder and TUNEL analysis, Suicide-Track DNA Ladder Isolation kit (Oncogene) and In Situ Cell Death Detection Kit, AP (Roche) were used according to manufacture's instruction.

Fig. 1 shows ectopic hTERT expression in Fbh and 10Fh cells and no expression in Fb and 10F cells. Fig. 2 shows high telomerase activity expressed in hTERT transfected Fbh and 10Fh cells and no enzyme activity was detected in Fb and lower activity in 10F cells. In the cells irradiated with a 6 Gy dose of γ-rays, growth inhibition was 26% in Fb,

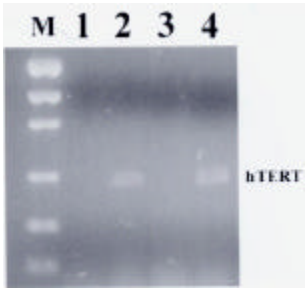

Fig. 1. hTERT expression (above): 1. 10F, 2. 10Fh, 3. Fb, 4. Fbh.

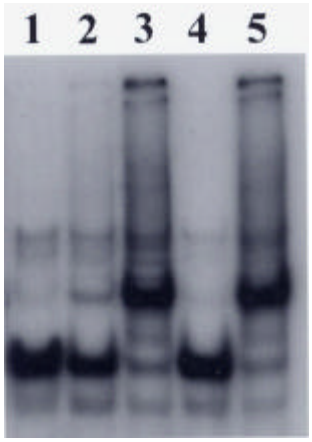

Fig. 2. Telomerase activity (above right): 1. 10Fh heated in 85? for 10 min. telomerase was inactive, 2. 10F, 3. 10Fh, 4. Fb, 5. Fbh.

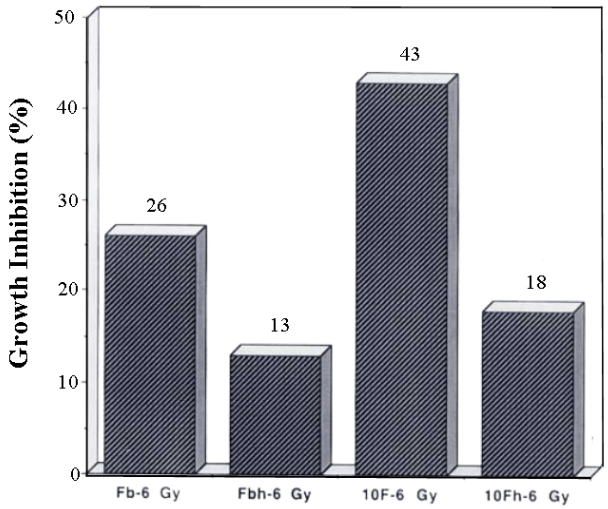

Fig. 3.

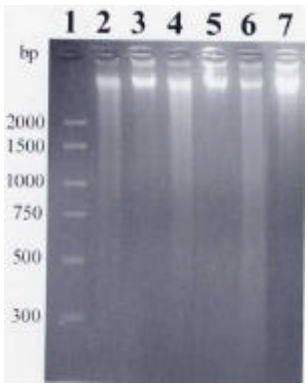

Fig. 4. Apoptosis detected by DNA ladder (above):
1. DNA marker
2. Fb
3. Fbh
4. Fb irradiated by 10 Gy
5. Fbh irradiated by 10 Gy
6. Fb irradiated by 15 Gy
7. Fbh irradiated by 15 Gy

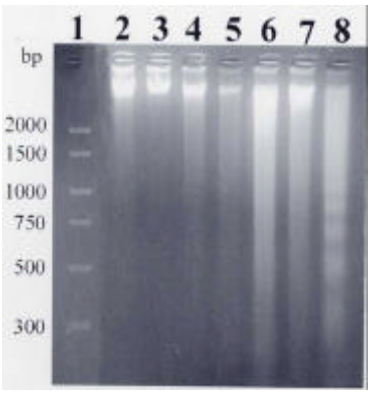

Fig. 5. Apoptosis detected by DNA ladder (above):
1. DNA marker
2. 10F
3. 10Fh
4. 10F irradiated by 3 Gy
5. 10Fh irradiated by 3 Gy
6. 10F irradiated by 6 Gy
7. 10Fh irradiated by 6 Gy
8. Positive control from kit

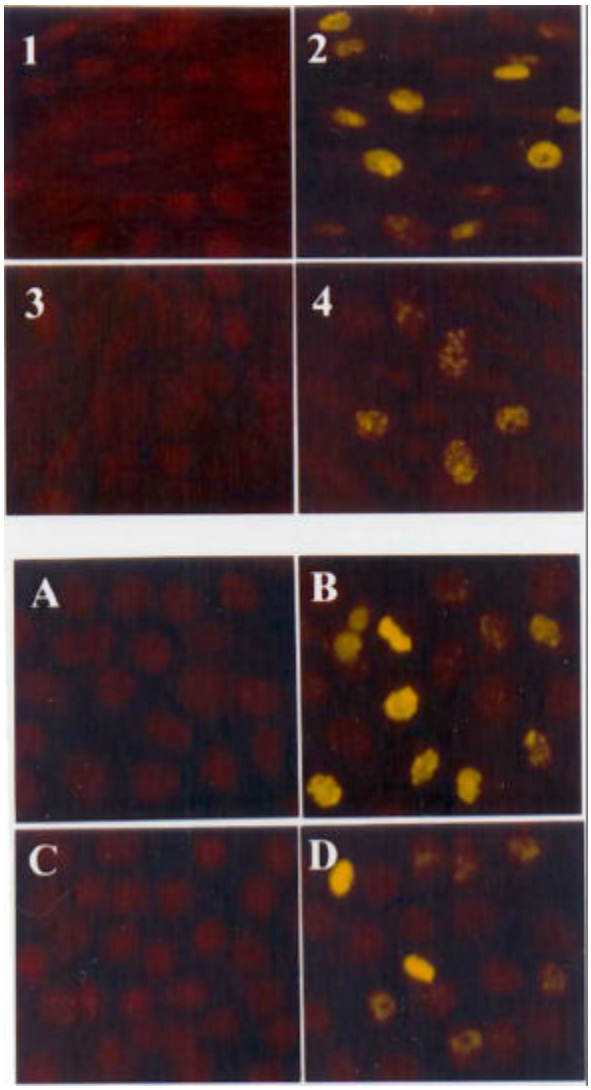

Fig. 6. Apoptosis detected by TUNEL: 1. Fb, 2. Fb irradiated by 15 Gy, 3. Fbh, 4. Fbh irradiated by 15 Gy, A. 10F, B. 10F irradiated by 6 Gy, C. 10Fh, D. 10Fh irradiated by 6 Gy.

13% in Fbh, 43% in 10F and 18% in 10Fh (Fig. 3), the numbers were from an average of three experiments. The results showed that the cells over-expressing hTERT are more resistant to radiation induced growth inhibition. Obvious apoptosis was observed in Fb cells irradiated by 15 Gy doses of ?-rays and in 10F cells irradiated by 6 Gy doses of ?-rays in both analyses by DNA ladder and TUNEL. Comparing with Fb and 10F cells, Fbh and 10Fh cells were relatively resistant to the same doses induced apoptosis (Fig. 4, 5, 6).

ur results show that:

1. Over-expressing hTERT in normal human fibroblast (NHDF) and spontaneously immortalized human mammary epithelial cells (MCF-F10) increase resistance to growth inhibition and apoptosis induced by ionizing radiation.

2. NHDF cells are more resistant to ?-rays induced growth inhibition, and apoptosis compared with MCF-10F cells.

Downregulation of the Betaig-h3 Gene is Causally Linked to Tumorigenic Phenotype in Asbestos Treated Immortalized Human BEP2D Cells

Yong L. Zhao, Chang Q. Piao and Tom K. Hei

Asbestos fibers represent a complex group of minerals that are associated with the development of malignant and non-malignant diseases (1). The persistent induction of c-fos, c-jun, and other stress-related DNA-binding proteins by asbestos signals chronic inflammation and are consistent with an increased level of reactive oxygen species reported in asbestos treated cultures (2,3). There is evidence that asbestos stimulates cellular proliferation in mesothelial cells which may facilitate clonal expansion of putative transformed cells resulting in a malignant phenotype (4). Although there are data in support of a possible role of tumor suppressor gene(s) in fiber carcinogenesis (5,6), there has been no clear association of either known oncogenes or tumor suppressor genes with the development of asbestos associated malignancies (7).

We have previously shown downregulation in the expression of DCC, p21cip1 and Betaig-h3 genes in asbestos-induced tumorigenic BEP2D cells (6,8). DCC is a known tumor suppressor gene and loss of its expression has been shown to occur in many human tumors (9). However, we have not been able to demonstrate that ectopic expression of wild type DCC gene can suppress the tumorigenic phenotype in asbestos-induced tumor cells (data not shown). The result suggests that the DCC gene does not play a causal role in asbestos-induced tumorigenic conversion of BEP2D cells. On the other hand, we have recently demonstrated that loss of one or two copies of chromosome 5, where Betaig-h3 is located, is a common cytogenetic alteration among fiber induced tumorigenic cells (10). Until now, there has been no published report on its role as a tumor suppressor in human cancers. In this study, the functional role of Betaig-h3 was investigated in asbestos-induced tumorigenic BEP2D cells. We provide evidence that loss of Betaig-h3 expression is causally linked to a tumorigenic process induced by asbestos treatment.

The Betaig-h3 gene is downregulated in asbestos-induced tumorigenic cell lines.

Tumorigenic cells were previously derived by treatment of exponentially growing BEP2D cells with a 4 mg/cm2 dose of chrysotile fibers for 7 days (11). Tumors >1 cm in diameter were resected from nude mice and used to establish independently generated cell lines (5). Fusion cell lines were generated by fusion of the highly malignant AsbTB2A cells with control BEP2D cells using polyethylene glycol as described (5,7). The resultant fusion cells were shown to be non-tumorigenic when inoculated into nude mice (6). By using cDNA microarrays, we identified a series of genes that were differentially expressed in asbestos-induced tumorigenic cell lines relative to parental BEP2D cells (6). Among these genes, Betaig-h3 expression was found to be markedly decreased in tumorigenic cells. As shown in Figure 1, the expression level of Betaig-h3 was further confirmed by Northern blot using mRNAs obtained from control BEP2D cells, non-tumorigenic trans-formed cells, early and late passage transformed cells, five tumorigenic cell lines (AsbTE, AsbTB, AsbTB2A, AsbTB2B and AsbTE2A) and a fusion cell line. Expression levels of the Betaig-h3 gene were not significantly different between the non-tumorigenic, early and late passage transformed cells relative to control BEP2D cells. However, the Betaig-h3 expression was downregulated about 7-8-fold in all five tumorigenic cell lines and restored to control level in the fusion cell line examined (Figure 1). Similar findings were also obtained with three other independently-generated, non-tumorigenic fusion cell lines (data not shown). The data indicate that decreased expression of may be related to the acquisition of a malignant phenotype in BEP2D cells induced by asbestos.

Ectopic expression of the Betaig-h3 gene in asbestos-induced tumorigenic cells inhibits their colony-forming efficiency in soft agar.

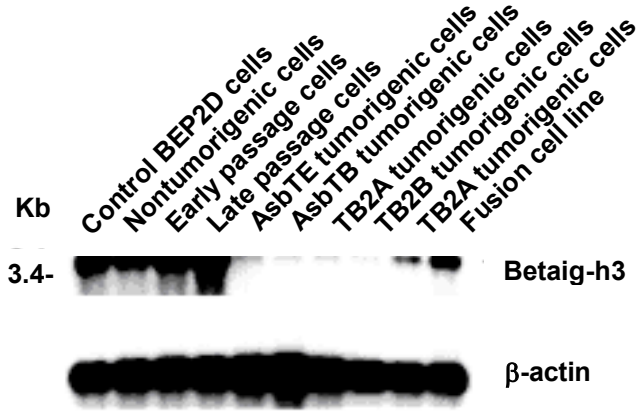

Fig. 1. Northern blotting analysis of Betaig-h3 gene in early and late passage transformed but non-tumorigenic cells, asbestos-induced tumorigenic cell lines and a fusion cell line relative to control BEP2D cells. Aliquots of 2.5 mg mRNAs were blotted and hybridized to 32P-labeled cDNA probes. After stripping, the membranes were rehybridized to human β-actin which is used as control.

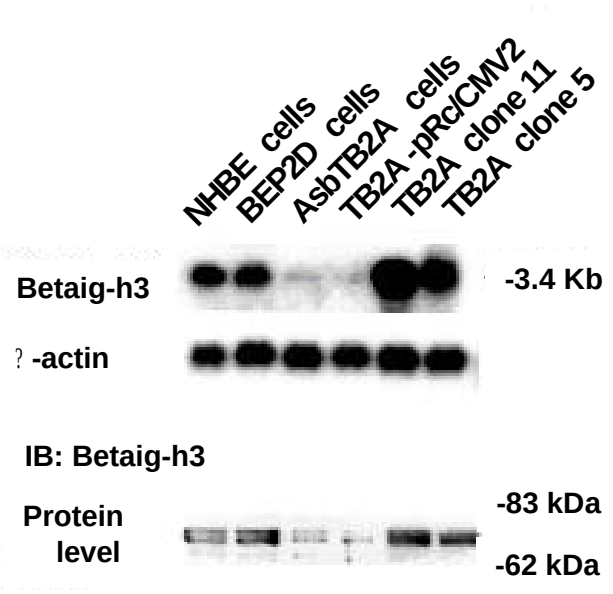

Fig. 2. TB2A-Betaig-h3 clone 5 mRNA and protein levels of Betaig-h3 gene in normal NHBE cells, BEP2D cells, asbestos-induced TB2A tumorigenic cells and Betaig-h3 transfected cells (clone 5 and clone 11).

To ascertain the tumor suppressive effect of the Betaig-h3 gene, we ectopically re-expressed the gene in a highly malignant cell line (AsbTB2A) using pRc/CMV2-Betaig-h3 expression vector. Two G418 resistant colonies (AsbTB2A-clone 5 and AsbTB2A-clone 11) that expressed different levels of the Betaig-h3 gene were chosen for further studies. From the Northern and Western blotting results (Figure 2), the parental TB2A cells and TB2A-pRc/CMV2 cells expressed a low, detectable, and similar level of the Betaig-h3 gene. After transfection, the expression of the Betaig-h3 gene in TB2A- clone 5 cells was restored to a level similar to that of control BEP2D cells, whereas in TB2A-clone 11 cells it was twofold higher than control. The mRNA and protein levels of the Betaig-h3 gene were similar between the primary NHBE cells and the immortalized, control BEP2D cells.

As shown in Table I, the colony-forming efficiency of Betaig-h3 transfected cells in soft agar (0.2-0.3%) was significantly decreased compared with parental TB2A cells (2.6%, P<0.01). The data indicate that ectopic expression of the Betaig-h3 gene in TB2A tumorigenic cells resulted in a significant lower ability for anchorage independent growth.

Tumorigenicity of asbestos-induced tumorigenic cells was significantly attenuated after the Betaig-h3 gene transfection.

To determine whether ectopic expression of the Betaig-h3 gene in asbestos-induced TB2A tumorigenic cells suppresses tumor formation in vivo, we injected 5-6 ? 10^6 of each of the following cell lines into nude mice, control BEP2D cells, AsbTB2A cells, TB2A-pRc/CMV2 and Betaig-h3 transfected cells (TB2A-clone 5 and TB2A-clone 11). The tumor volumes were measured weekly. As shown in Table 1, no tumor (0/10 mice) was detected in mice injected with the parental BEP2D cells after more than 20 weeks. However, 10/10 mice that were injected with either TB2A or TB2A-pRc/CMV2 tumorigenic cells developed progressively growing tumors at 4 weeks, with average volumes of 544.9 and 428.8 mm^3, respectively. In contrast, 5/10 mice injected with TB2A-clone 5 and 7/10 mice injected with TB2A-clone 11 cells formed small tumor nodules at 4 weeks, with an average volume of 59.1 mm^3 which was significantly smaller than that of the parental TB2A cells (P<0.01).

In this study, ectopic expression of the Betaig-h3 gene by transfecting pRc/CMV2-betaigh3 vector in tumorigenic cells significantly inhibits colony-forming efficiency in soft agar and tumor growth in nude mice relative to parental tumorigenic cells. The finding provides compelling evidence of a possible tumor suppressor role of the Betaig-h3 gene in asbestos-induced malignant conversion of human BEP2D cells. The data support the hypothesis that persistent activation of proto-oncogenes (such as c-fos) and inactivation of tumor suppressor genes (such as Betaig-h3 in this model) may cooperate in a multistep process to regulate critical events intrinsic to the pathogenesis of asbestos-associated human lung cancer (1).

Acknowledgements

The author thanks Dr. Paul C. Billings for kindly providing anti-Betaigh3 antibody. Work supported in part by grants from the National Institute of Health CA49062, ES07890 and Environmental Health Center grant P30 ES 09089.

Table I
Suppression of anchorage-independent growth and tumorigenicity in tumorigenic BEP2D cells by transfecting the *Betaig-h3* gene

Cell type	CFE in soft agar (%)[a]	Tumors/total mice		Tumor volume at 4 weeks (cm^3)[b]
BEP2D cells	0.02	0/10		?
TL1 tumor cells	2.6 ? 0.6	10/10		1.022 ? 0.331
TL1-pRc/CMV2	2.4 ? 0.3	10/10		0.971 ? 0.296
TL1-Betaig-h3 clone 18	0.2 ? 0.1[c]	5/10	} 12/20	0.087 ? 0.032[c]
TL1-Betaig-h3 clone 28	0.3 ? 0.1[c]	7/10		

[a] CFE: Colony-forming efficiency. [b] Tumor volume=(longest diameter × (shortest diameter)^2) × 0.5. [c] *P < 0.01*, compared with parental tumor cells.

References

4. Mossman BT, Kamp DW and Weitzman SA. Mechanisms of carcinogenesis and clinical features of asbestos-associated cancers. *Cancer Invest* **14**:464-78, 1996.
5. Robledo R and Mossman B. Cellular and molecular mechanisms of asbestos-induced fibrosis. *J Cell Physiol* **180**:158-66, 1999.
6. Xu A, Wu LJ, Santella RM and Hei TK. Role of oxyradicals in mutagenicity and DNA damage induced by crocidolite asbestos in mammalian cells. *Cancer Res* **59**:5922-6, 1999.
7. Heintz NH, Janssen YM and Mossman BT. Persistent induction of c-fos and c-jun expression by asbestos. *Proc Natl Acad Sci (USA)* **90**:3299-303, 1993.
8. Murthy SS and Testa JR. Asbestos, chromosomal deletions, and tumor suppressor gene alterations in human malignant mesothelioma. *J Cell Physiol* **180**:150-7, 1999.
9. Zhao YL, Piao CQ, Wu LJ, Suzuki M and Hei TK. Differentially expressed genes in asbestos-induced tumorigenic human bronchial epithelial cells: implication for mechanism. *Carcinogenesis* **21:**2005-10, 2000.
10. Ni Z, Liu YQ, Keshava N, Zhou G, Whong W and Ong T. Analysis of K-ras and p53 mutations in mesotheliomas from humans and rats exposed to asbestos. *Mutation Res* **468**:87-92, 2000.
11. Piao CQ, Zhao YL and Hei TK. Analysis of p16 and p21(Cip1) expression in tumorigenic human bronchial epithelial cells induced by asbestos. *Oncogene* **20**:7301-6, 2001.
12. Fearon ER, Pierceall WE. The deleted in colorectal cancer (DCC) gene: a candidate tumour suppressor gene encoding a cell surface protein with similarity to neural cell adhesion molecules. *Cancer Surv* **24**:3-17 (Review), 1995.
13. Suzuki M, Piao CQ, Zhao YL and Hei TK. Karyotype analysis of tumorigenic human bronchial epithelial cells transformed by chrysolite asbestos using chemically induced premature chromosome condensation technique. *Int J Mol Med* **8**:43-7, 2001.
14. Hei TK, Wu LJ and Piao CQ. Malignant transformation of immortalized human bronchial epithelial cells by asbestos fibers. *Environ Health Perspect* **105**(suppl 5):1085-8, 1997.

Expression of the Betaig-h3 Gene in Human Normal Tissues and Cancer Cells

Yong L. Zhao and Tom K. Hei

There is evidence that chromosome 5q31, where the Betaig-h3 gene has been regionally mapped, is often deleted in leukemias, myelodysplastic syndromes and many human cancers such as renal cell, esophageal and lung carcinoma (1-3), suggesting that deletion of the Betaig-h3 gene is a frequent event in human cancers. To check the expression of this gene in human normal tissues and tumor cells lines, multiple tissue blots various human tissues from Clontech and 14 tumor cell lines were used to ascertain the mRNA levels of the Betaig-h3 gene by Northern blot.

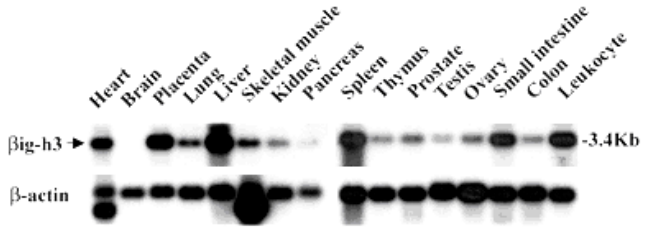

Fig. 1. Total mRNA levels of Betaig-h3 gene in normal human tissues. The multiple tissue blots was purchased from Clontech. High expression levels of Betaig-h3 were found in heart, placenta, liver, spleen, small intestine and leukocyte.

Betaig-h3 expression is ubiquitously expressed in normal human tissues.

We checked the expression of the Betaig-h3 gene in different normal human tissues. We found that the Betaig-h3 expression was ubiquitously expressed in normal tissues, with high expression levels in heart, placenta, liver, spleen, small intestine and peripheral blood leukocytes. Other tissues such as pancreas, kidney, thymus, testis and ovary expressed comparably lower levels of the gene, with the exception of brain which showed no Betaig-h3 expression (Fig. 1).

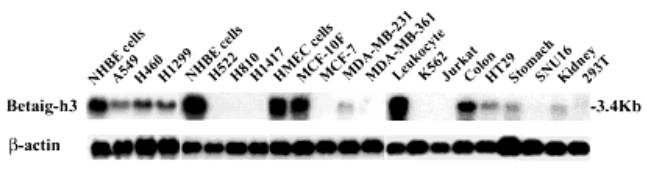

Fig. 2. Total mRNA levels of Betaig-h3 gene in various human tumor cell lines. Normal human bronchial epithelial (NHBE) cells, human mammary epithelial cells (HMEC), peripheral blood leukocyte, colon, stomach and kidney tissues were used as various controls.

The Betaig-h3 gene is decreased or absent in various human tumor cell lines.

Figure 2 shows mRNA levels of Betaig-h3 in 14 tumor cell lines. When compared with normal human cells or tissues, decreased or loss of Betaig-h3 expression was found in all tumor cell lines examined. Among the six lung tumor cell lines examined, five of them including A549, H460, H1299, H522 and H810 were derived from lung epithelial cells. Therefore, we chose normal human bronchial epithelial (NHBE) cells as control. We found a 3 5-fold lower expression level of this gene in three lung tumor cell lines (A549, H460 and H1299) and one colon cancer cell line (HT29), very low or undetectable levels in other tumor cell lines including lung cancer (H522, H810, H1417), leukemia (K562, Jurkat), stomach cancer (SNU16), breast cancer (MCF-7, MDA-MB- 231, MDA-MB-361) and kidney cancer (293T). MCF-10F, which is spontaneously immortalized, non-tumorigenic mammary epithelial cell line, had a similar level of Betaig-h3 expression as normal HMEC cells.

Previous data showed that reduced expression of the Betaig-h3 gene has been found in embryonal rhabdomyosarcoma cell lines and mesenchymal tumors (4,5). These data, together with our findings above, indicate that loss of Betaig-h3 expression contributes not only to asbestos or radiation-induced neoplastic transformation in BEP2D cell model, but also human tumors in general (6,7). Our present findings that expression of the Betaig-h3 gene is similar between MCF-10F and normal human mammary epithelial cells, suggest that down-regulation of the Betaig-h3 gene occurs at the late stage of transformation.

References

1. Brezinova J, Zemanova Z, Cermak J and Michalova K. Fluorescence in situ hybridization confirmation of 5q deletions in patients with hematological malignancies. *Cancer Genet Cytogenet* **117:**45-9, 2000.
2. Peralta RC, Casson AG,Wang RN, Keshavjee S, Redston M and Bapat B. Distinct regions of frequent loss of heterozygosity of chromosome 5p and 5q in human esophageal cancer. *Int J Cancer* **78:**600-5, 1998.
3. Wu X, Zhao Y, Kemp BL, Amos CI, Siciliano MJ and Spitz MR. Chromosome 5 aberrations and genetic predisposition to lung cancer. *Int J Cancer* **79**:490-3, 1998.
4. Genini M, Schwalbe P, Scholl FA and Schafer BW. Isolation of genes differentially expressed in human primary myoblasts and embryonal rhabdomyosarcoma. *Int J Cancer* **66**:571-7, 1996.
5. Schenker T and Trueb B. Down-regulated proteins of mesenchymal tumor cells. *Exp Cell Res* **239:**161-8, 1998.
6. Zhao YL, Piao CQ, and Hei TK. Overexpression of Betaig-h3 gene downregulates integrin alpha5beta1 and suppresses tumorigenicity in radiation-induced tumorigenic human bronchial epithelial cells. *British J Cancer* **86**:1923-8, 2002.
7. Zhao YL, Piao CQ and Hei TK. Downregulation of Betaig-h3 gene is causally linked to tumorigenic phenotype in asbestos treated immortalized human bronchial epithelial cells. *Oncogene* **21**:7471-7, 2002.

Role of Mitochondria in Arsenic Induced Genotoxicity in Mammalian Cells

Su-Xian Liu, Mercy Davidson and Tom K. Hei

Although arsenic is a well-established human carcinogen, its carcinogenic mechanism is not clear. Using the human hamster hybrid (A_L) cell assay that is proficient in the recovery of deletion mutants, we showed previously that arsenic is a potent gene and chromosomal mutagen and that reactive oxygen species mediate its genotoxic response (1, 2). If generation of reactive oxygen species is one of the major pathways for arsenic-mediated genotoxicity, then it could be expected to induce specific DNA lesions consistent with oxidative damages. One of the most common oxidative DNA lesions is 8-hydroxy-2'-deoxyguanosine (8-OHdG). Indeed, using a monoclonal antibody specific for 8-OHdG coupled with immunoperoxidase staining, we demonstrated the formation of the oxidative DNA damage product in A_L cells treated with a 4 μg/ml dose of sodium arsenite for 24 hr (3). 8-OHdG was found to localize mainly in the nucleus of both control and fiber treated cells. Although a faint, background staining was evident in the control cultures, treatment of A_L cells with arsenic resulted in a dose dependent increase in 8-OHdG levels. Quantification of staining intensity from 50-80 randomly selected cells treated with a 4 μg/ml dose of arsenite indicated a 2.1 fold increase in staining intensity above background. This increase was reduced to almost background level in the presence of antioxidants such as catalase and superoxide dismutase.

If hydroxyl radicals play an important role in mediating the genotoxicity of arsenic, the important issue remains as to the source of these oxyradicals. Mitochondria produce 80% of the cellular energy and are regarded as the power center of a cell. Consequently, it is not surprising that oxyradicals and other organic free radicals are constantly being produced in the mitochondria and that mitochondrial membrane dam-

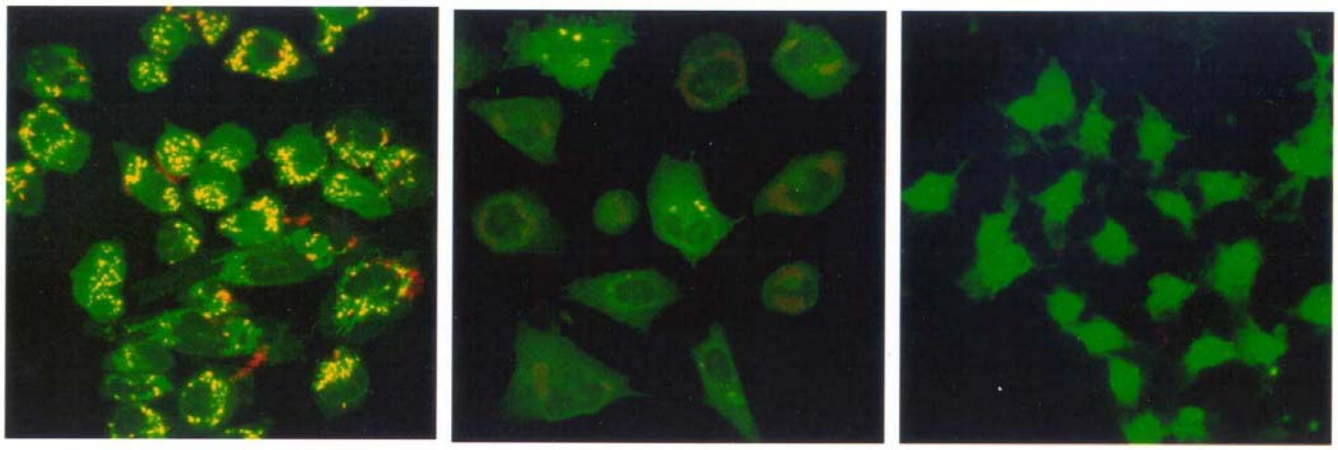

Fig. 1. Mitochondrial membrane potential as evidenced by JC-1 fluorescence in A_L cells. The panel on the left shows results for mitochondrial detection in untreated cells, while the middle and right panels show mitochondrial depletion after 4 days treatment with 4 and 6 μg/ml R6G respectively.

age has been shown to increase intracellular oxidant levels. To address the potential role of mitochondria in fiber mutagenesis, we have used two complementary approaches. We first determine if arsenite-treated cytoplasts (without nucleus) are capable of mediating mutagenicity at the *CD59* locus of the A_L cells when rescued by fusion with karyoplasts. The rationale is that if nucleus is the direct and immediate target in arsenite-induced mutagenesis, there should be few or no *CD59* mutations when nucleus is not present at the time of arsenite treatment. Alternatively, if the nucleus *is not* the direct and immediate target, we should be able to detect mutations in the progeny of fusion cells. Our results showed that treatment of enucleated cells with arsenic followed by rescue fusion with karyoplasts resulted in a mutant yield that was 3 fold higher than untreated cells.

In our second approach, we used Rhodamine 6G to inactivate mitochondrial function. Rhodamine 6G is a lipophilic dye that selectively accumulates within mitochondria. The exact mechanism by which it inhibits mitochondrial oxidative metabolism is not known. There is evidence that it blocks energy transfer in oxidative phosphorylation at two levels: affecting hydrogen ejection by redox complexes and inhibiting F1-ATP-ase activity.

Exponentially growing A_L cells were plated onto T-75 cm^2 tissue culture flasks. After 48 hr of incubation, cells were exposed to Rhodamine 6G at a concentration of 4 μg/ml for 4 days. Two days before treatment with arsenic, the cells were rinsed in Hank's buffer salt solution and cultured in Rhodamine 6G-free medium. To ascertain mitochondrial function after Rhodamine treatment, we used the membrane potential sensitive fluorescent probe, JC-1 (Molecular Probe) as shown in Figure 1. JC-1 is a cationic carbocyanine dye that presents itself as green fluorescent monomers at low concentrations, i.e. in cells with low mitochondrial function or membrane potential. In contrast, in cells with normal mitochondrial function, membrane potential driven accumulation of these dyes results in the formation of reddish yellow-fluorescent J-aggregates as shown in control A_L cells (Figure 1a). In Rhodamine-6G treated cells with depressed mitochondrial function (6 μg/ml for 4 days), the mitochondria appear green when stained with JC-1 dye for a comparable period of 30 min at 37°C (Figure 1c). In contrast, A_L cells treated with a lower dose of Rhodamine 6G (4 μg/ml for 4 days) showed only partial inactivation of mitochondria with patches of red stain among the mostly green background (Figure 1b).

Mitochondrial function/DNA depleted A_L cells, generated by pretreatment with Rhodamine-6G, were exposed to arsenite at a dose of 1.5 μg/ml for 18 hr. Following treatment, the cells were washed with buffered saline followed by rescue fusion with cytoplasts. Figure 2 shows the resultant mutant induction in arsenite treated A_L cells with or without functional mitochondria. While arsenite-treated, wild type A_L cells resulted in the usual mutant yield when fused with cytoplasts, the corresponding mutant yield for mitochondrial function-inactivated cells was similar to background level, i.e. resulted in few mutations. These data

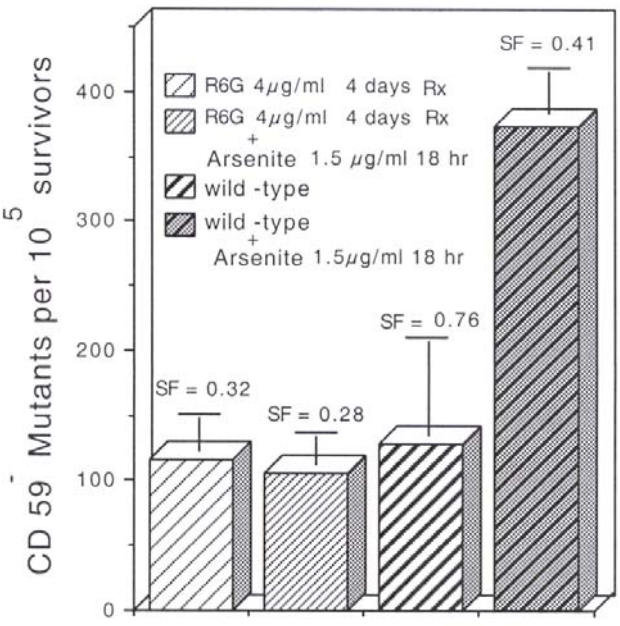

Fig. 2. Mutation frequency of CD59 after fusion of arsenite-treated A_L cells containing nonfunctional mitochondria (R6G 4 μg/ml 4 days Rx) with cytoplasts.

illustrate that nucleus is not the only target of the carcinogenic metal and that mitochondria may also play an important role in the genotoxic response of mammalian cells to arsenic as well.

References

1. Hei TK, Liu SX and Waldren C. Mutagenicity of arsenic in mammalian cells: role of reactive oxygen species. *Proc Natl Acad Sci (USA)* **95**:8103-7, 1998.
2. Liu SX, Athar M, Lippai I, Waldren C and Hei TK. Induction of oxyradicals by arsenic: implication for mechanism of genotoxicity. *Proc Natl Acad Sci (USA)* **98**: 1643-8, 2001.
3. Kessel M, Liu SX, Xu A, Santella R and Hei TK. Arsenic induces oxidative DNA damage in mammalian cells. *Mol and Cell Biochem* **234-235**:301-8, 2002.

Peroxynitrite Anions and Genotoxicity of Arsenic

Su-Xian Liu and Tom K. Hei

Arsenic is a well-established human carcinogen. We previously showed arsenite to be a potent gene and chromosomal mutagen using the human-hamster hybrid (A_L) cells and that it induces predominantly multilocus deletion. Furthermore, we have demonstrated the importance of reactive oxygen species (ROS) such as superoxide anion, hydrogen peroxide, and hydroxyl radicals in mediating arsenite-induced genotoxicity. Our recent studies have implicated the role of mitochondrial damage in the process as well (see the previous article). In this report, we examine the contribution of reactive nitrogen species, particularly peroxynitrite anions, in arsenite-induced mutagenicity using the A_L cell model.

For many years it has been generally recognized that nitric oxide (NO) is genotoxic and it can cause DNA damage and mutation. Increased NO production has been implicated in the co-localization of genotoxicity of transgenic SJL mice (1). In addition, an increased mutant fraction at the hypoxanthine guanine phosphoribosyl transferase (*hprt)* gene locus has been associated with NO exposure (2).

There is evidence that the cytotoxic effects of NO result either through a direct toxicity of the molecule or by a synergistic damage with other oxidants such as ROS. The reaction of NO and superoxide anions leads to the production of a range of NO metabolites that can have greater cytotoxic potential than NO and superoxide anions alone. The rapid reaction of NO with superoxide anions yields the potent oxidant peroxynitrite anions, which are implicated in many pathogenic responses. In mammalian cells, peroxynitrite anions are enzymatically generated from the reaction of superoxide anions and NO by nitric oxide synthase (3). This reaction can be inhibited by the specific inhibitor, N-methyl-L-arginine (L-NMMA).

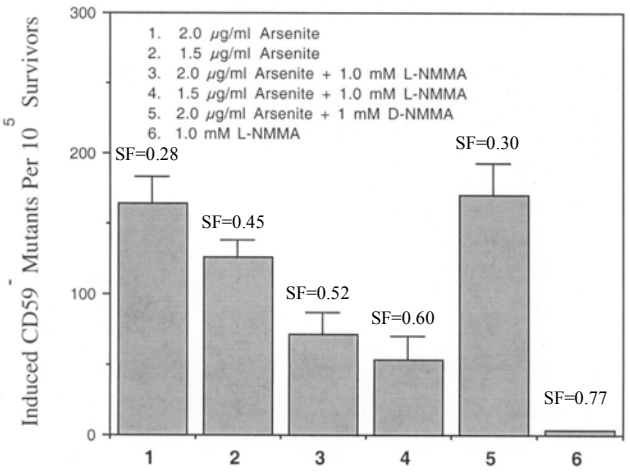

Fig. 1. Mutation frequency of CD59 by arsenic in the presence or absence of L-NMMA in mammalian cells.

To ascertain the functional role of peroxynitrite anions in arsenic-induced cytotoxicity and mutation frequencies, A_L cells were pretreated with 1mM L-NMMA for one hr. The inactive D-enantiomer, D-NMMA, at equivalent dose was used as a negative control. Sodium arsenite was then added to the cultures and the cells were incubated for another 24 hours. Both the L- and D-NMMA at the concentration used (1mM) were non-toxic and non-mutagenic to A_L cells.

Figure 1 shows the cytotoxicity as well as induced mutant yield at the *CD59* locus in A_L cells exposed to the various treatments. Addition of L-NMMA to the culture medium significantly enhanced the surviving fraction of arsenite-treated cells at both the 1.5 and 2.0 μg/ml doses. In contrast, addition of L-NMMA reduced the induced mutant yield at both doses of the arsenite examined, 60% and 50% suppression for 1.5 and 2.0 μg/ml doses, respectively. However, the inactive D-enantiomer, D-NMMA had essentially no effect on arsenic induced mutant yield (Figure 1).

Deregulated production of nitric oxide (NO) and other reactive nitrogen species have been implicated in the development of certain human disease, including cancer. We sought to assess the damaging potential of peroxynitrite anions in arsenite-treated mammalian cells in the present study. Our findings are consistent with the observations that mitochondria membrane damage (source of superoxide anions) and reactive nitrogen species contribute to the increase in intracellular oxidative stress in arsenic exposed cells.

References

1. Gal A, et al. Mutagenesis associated with nitric oxide production in transgenic SJL mice. *Proc Natl Acad Sci (USA)* **93**:15102-7, 1996.
2. Zhuang JC et al. Mutagenesis associated with nitric oxide production in macrophages. *Proc Natl Acad Sci (USA)* **95**:8286-91, 1998.
3. Prylor WA and Squadrito GL. The chemistry of peroxynitrite: a product from reaction of nitric oxide and superoxide. *Am J Physiol* **268**:699-722, 1995.

Susceptibility of Human Breast to Acetylcholinesterase Inhibitors

Gloria M. Calaf, Gertrudis Cabello[1] and Tom K. Hei

Exposure to environmental chemicals may be involved in the etiology of breast cancers. Many studies have found an association between cancer in humans and exposure to agriculture pesticide exposure. Parathion and malathion are organophosphorous pesticides, cholinesterase inhibitors responsible for the hydrolysis of body choline esters, including acetylcholine at cholinergic synapses (1). Their primary target of action in insects is the nervous system by inhibiting the release of the enzyme acetylcholinesterase at the synaptic junction. Atropine is a parasympatholytic alkaloid used as an antidote to acetylcholinesterase inhibitors. We have established an experimental breast cancer model, where epithelial cells in the rat mammary gland underwent a stepwise transformation into malignant cells by exposure to pesticides (2). The aim of this work was to examine whether parathion, malathion, estrogen and acetylcholine were able to induce changes at cellular and molecular levels in an immortalized human breast epithelial cell line, MCF-10F.

MCF-10F-treated cells showed phenotypic changes relative to control from the effect of parathion, malathion, estrogen and acetylcholine. Uncontrolled cell proliferation is the first step in cell carcinogenesis. Figure 1 shows the effects of parathion (100ng/ml), atropine (62.5

ng/ml), acetylcholine (10^{7}M) and combination with atropine on cell proliferation after 7 days. These studies showed that parathion as well as acetylcholine increased cell proliferation in comparison to controls, whereas atropine inhibited such action.

There is substantial experimental, epidemiological, and clinical evidence that breast cancer is influenced by the influence of hormones (3-5). Parallel to these results, MDM2, estrogen receptor α (ER α), estrogen receptor β (ER β), and mutant p53 protein expression was determined in control and transformed cells. Immunofluorescent signals of stained cells were analyzed following confocal microscopy and quantified by computation (6). MDM2, ER α protein expression were increased by the effect of 17 β-estradiol (E) (10^{-8}M). These studies showed that MDM2 and ER α protein expression was increased by the effect of estrogen, parathion, malathion and acetylcholine (Figure 2). p53, an important tumor suppressor gene in normal cells, was also studied. Results indicated that inactivation led to uncontrolled cell proliferation, as well as increase in protein expression from the effect of malathion and acetylcholine. These results indicate that acetylcholinesterase inhibitors alter cell proliferation and induce molecular changes indicative of breast carcinogenesis.

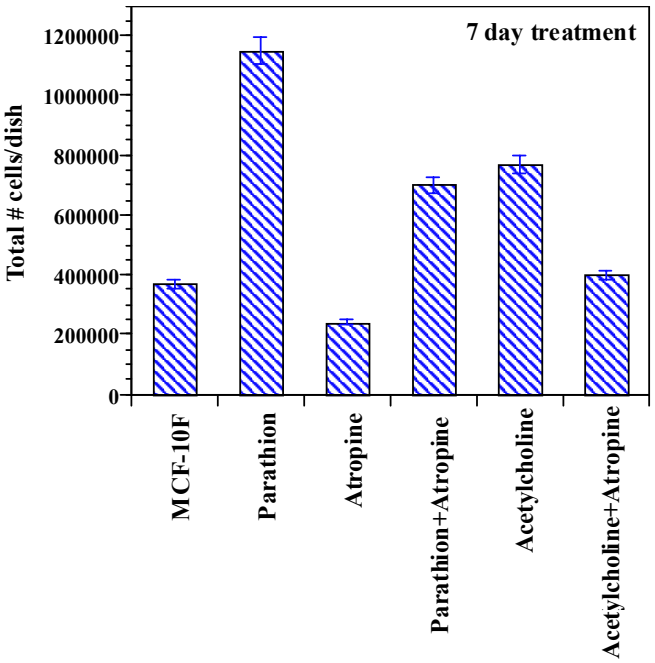

Fig. 1. Effect of several concentrations of parathion (100ng/ml), acetylcholine, atropine (62.5 ng/ml) and combination of either parathion or acetylcholine with atropine on total number of MCF-10F cells after 7 days in culture. Bars represent the average of total number of cells per dish (3 T25 dishes).

[1] *University of Tarapaca, Arica, Chile.*

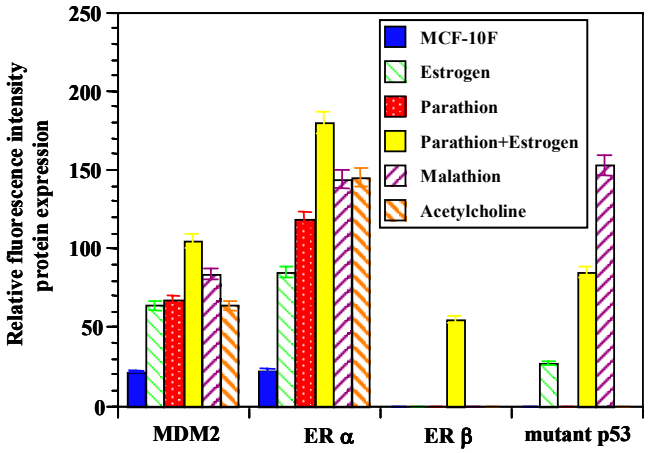

Fig. 2. Immunofluorescence imaging staining of MDM2, ER α, estrogen ER β, and mutant p53 protein expression protein expression of MCF-10F control, E, parathion, parathion plus E, malathion and acetylcholine. Protein expression of cells was determined by immunofluorescent staining and quantified using confocal microscopy and a computer program, which gives the area and the intensity of the staining as described in the text. The primary antibodies used were obtained from Biotechnology Inc., Santa Cruz, CA.

References

1. Taylor P. Anticholinesterase agents, in *The Pharmacological Basis of Therapeutics* (Goodman Gilman A, Rall TW, Nies AS, Taylor P, eds.), New York, NY, Pergamon Press Inc., 7, 131-47, 1990.
2. Cabello G, Valenzuela M, Rudolph I, Hrepic N and Calaf G. A rat mammary tumor model induced by the organophosphorous pesticides, parathion and malathion, possibly through acetylcholinesterase inhibition. *Environ. Health and Perspect* **109**:471-9, 2001.
3. Calaf G, Russo IH, Roi L, Russo J. Effect of estrogen on the length of S phase of human breast tissue. *Int Res Comm Syst Med Sci* **10**:307-8, 1982.
4. Henderson BE, Pike MC and Gray GE. The Epidemiology of Breast Cancer, in *Breast Cancer* (Hoogstraten B and McDevitt RW, eds.), CRC Press, Boca Raton, FL, 1-25, 1981.
5. Dickson RB, Breast Cancer. In *Molecular Biology in Cancer Medicine* (Razelle Kurzroch and Moshe Talpaz eds.), Martin Dunitz Ltd. 287-315, 1999.
6. Calaf G and Hei TK. Oncoprotein expressions in human breast epithelial cells transformed by high LET radiation. *Int J Radiation Biol* **77**:31-40, 2001.

Analysis of the Mammalian Cell Cycle by Flow Cytometry

Haiying Hang and Michael Fox[1]

At present, most researchers use flow cytometry to monitor the cell cycle of mammalian cells. It can measure DNA content of individual cells at a great speed, and thus conveniently reveal cell distribution over DNA content, which indicates the locations of cells in the cell cycle. DNA content distribution of a typical exponentially growing cell population is composed of two peaks of G1/G0 and G2/M phase and a valley of S phase (Figure 1). G2/M phase cells have twice the amount of DNA of G1/G0 phase cells, and S phase cells possess varying amounts of DNA between G1 and G2 cells. Some flow cytometric methods can distinguish four or even all the five cell cycle subpopulations: G0, G1, S, G2 and M (1-3). Furthermore, each subpopulation can be quantified (4). Obviously, flow cytometry with these unique features is irreplaceable for monitoring the cell cycle status and its regulation.

Cell cycle checkpoint genes are key elements in the cell cycle regulation. Checkpoint gene mutation can lead to defects in one or more cell cycle checkpoint controls, which then can result in cell death or cancer. Many cell cycle checkpoint genes are tumor suppressors such as p53, ATM, ATR and BRCA1 (5,6). In mammalian cells, the four well defined cell cycle checkpoint controls that can be analyzed by flow cytometry are G1 arrest, suppression of replication, and radiation-dose dependent as well as independent G2 arrests. Exposure to a genotoxic agent can activate some or all the four checkpoints. The methods to analyze the statuses of the four checkpoints are described in a chapter in a book titled *Cell Cycle Checkpoint Control Protocols* edited by Howard Lieberman (in preparation).

The unique features of the chapter include focusing on flow cytometrical analyses of individual checkpoint controls, and describing two procedures for analyzing S phase and radiation dose-independent G2/M checkpoint controls which are still commonly detected with other cumbersome methods.

Here only the analyses of S phase and radiation dose-independent G2/M checkpoint controls will be described.

Dose independent and transient G2 phase block ($G2_T$)

Normal cells have been found to stop entering mitosis within the first hour after irradiation. By 12 h after irradiation, these cells are released from G2 and begin to reenter mitosis (Fig. 1) (1,7). AT cells lack this brief block in G2 phase after irradiation; the number of AT cells in mitotic

[1] *Department of Environmental and Radiological Health Sciences, Colorado State University, Fort Collins, Co.*

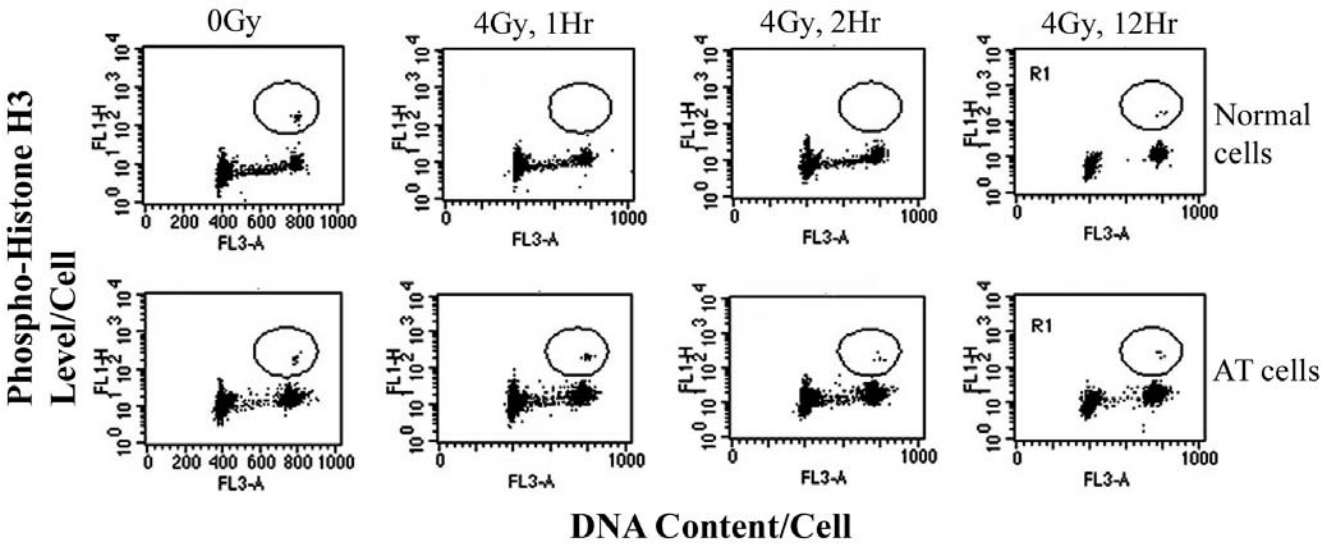

Fig. 1. Assessment of $G2_T$ checkpoint activity.

phase does not vary much following radiation exposure. Cells with mutated *BRCA1* are also deficient in $G2_T$. In contrast to radiation dose-dependent long-term checkpoint control ($G2_L$), the activity of $G2_T$ does not depend on dose of radiation.

The key of the assay is to probe the phosphorylated form of histone H3 in mitotic cells that contain a lot more phospho-histone H3 molecules than the cells in the other phases (8). The advantages of this method over conventional metaphase chromosome inspection with a microscope are more quantitative (count 10^4 cells in less than 2 min), and more informative (also simultaneous detection of cell distribution in G1/G0, S and G2 phases)

Cells with 4n DNA and high level of phospho-histone H3 (circled) are mitotic cells, and their detection by anti-phospho-histone H3 rabbit polyclonal antibody can be used to assess $G2_T$ checkpoint activity induced by radiation. Normal G2 cells stop moving into M phase within 1 hr after irradiation, and mutation on *ATM* gene as in AT cells destroys the ability. The circled cells can be quantified.

S phase checkpoint control

S phase checkpoint control by definition is the DNA synthesis suppression induced by genotoxic stress in the cells in S phase. Replicative DNA synthesis suppression can be detected by bivariate distributions of BrdU incorporation versus DNA content.

After UV light irradiation, both *Rad9*$^{-/-}$ and *Rad9*$^{+/+}$ ES cells reduce the incorporation of BrdU (measured by geometric mean of intensities of green fluorescence from BrdU-positive cells, gated area A) across S phase, indicating a lower replicative DNA synthesis (Figure 2). However, *Rad9*$^{-/-}$ cells were much less effected than *Rad9*$^{+/+}$ cells, indicating that *Rad9*$^{-/-}$ cells are defective in S phase checkpoint

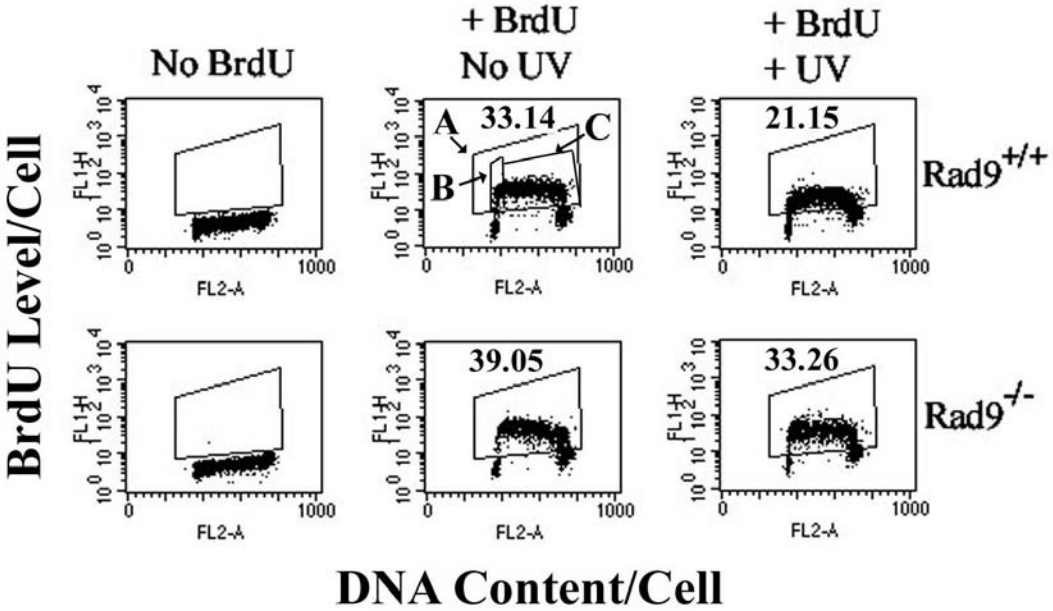

Fig. 2. Determination of S phase checkpoint activity by double detections of DNA content and BrdU uptake.

control. The degree of DNA synthesis after irradiation can be calculated as the ratio of the geometric mean of green fluorescence (FL1 in FACSCalibur) from irradiated BrdU-positive cells over that of unirradiated BrdU-positive cells ($R_{geo\text{-}mean}$); the ratios for *Rad9*$^{-/-}$ and normal cells are 85% (33.26/39.05) and 65% (21.15/33.14), respectively. Instead of including all the BrdU positive cells (area A), we can choose the cells in later stages of S phase (area C) to calculate the $R_{geo\text{-}mean}$ that gauges S phase checkpoint status of the Cells already in S phase when exposed to UV light (Figure 2).

The uptake rate of BrdU can be quantified (gated area A) and can be used to evaluate the cellular ability of suppressing replicative DNA synthesis induced by genotoxic stress (e.g. UV light). This ability of mouse ES cells is compromised by deleting both copies of *Rad9* gene. The number above each DNA profile represents BrdU-uptake rate calculated from BrdU-positive cells (surrounded area).

References

1. Xu B, Kim ST and Kastan MB. Involvement of Brca1 in S-phase and G(2)-phase checkpoints after ionizing irradiation. *Mol Cell Biol* **21:**3445-50, 2001.
2. Larsen JK, Munch-Petersen B, Christiansen J and Jorgensen K. Flow cytometric discrimination of mitotic cells: resolution of M, as well as G1, S, and G2 phase nuclei with mithramycin, propidium iodide, and ethidium bromide after fixation with formaldehyde. *Cytometry* **7**:54-63, 1986.
3. Pollack A, Moulis H, Greenstein DB, Block NL and Irvin GL 3rd. Cell kinetic effects of incorporated 3H-thymidine on proliferating human lymphocytes: flow cytometric analysis using the DNA/nuclear protein method. *Cytometry* **6**:428-36, 1985.
4. Ormerod MG. *Analysis of DNA-general methods, in Flow Cytometry: A Practical Approach* (second edition, Ormerod MG ed.) Oxford University Press, New York, NY, 1994.
5. Morgan SE and Kastan MB. p53 and ATM: cell cycle, cell death, and cancer. *Adv Cancer Res* **71**:1-25, 1977.
6. Zhou BB and Elledge SJ. The DNA damage response: putting checkpoints in perspective. *Nature* **408**:433-9, 2000.
7. Xu B, Kim ST, Lim DS and Kastan MB. Two molecularly distinct G(2)/M checkpoints are induced by ionizing irradiation. *Mol Cell Biol* **22**:1049-59, 2002.
8. Wei Y, Mizzen CA, Cook RG, Gorovsky MA and Allis CD. Phosphorylation of histone H3 at serine 10 is correlated with chromosome condensation during mitosis and meiosis in Tetrahymena. *Proc Natl Acad Sci (USA)* **95**:7480-4, 1998.

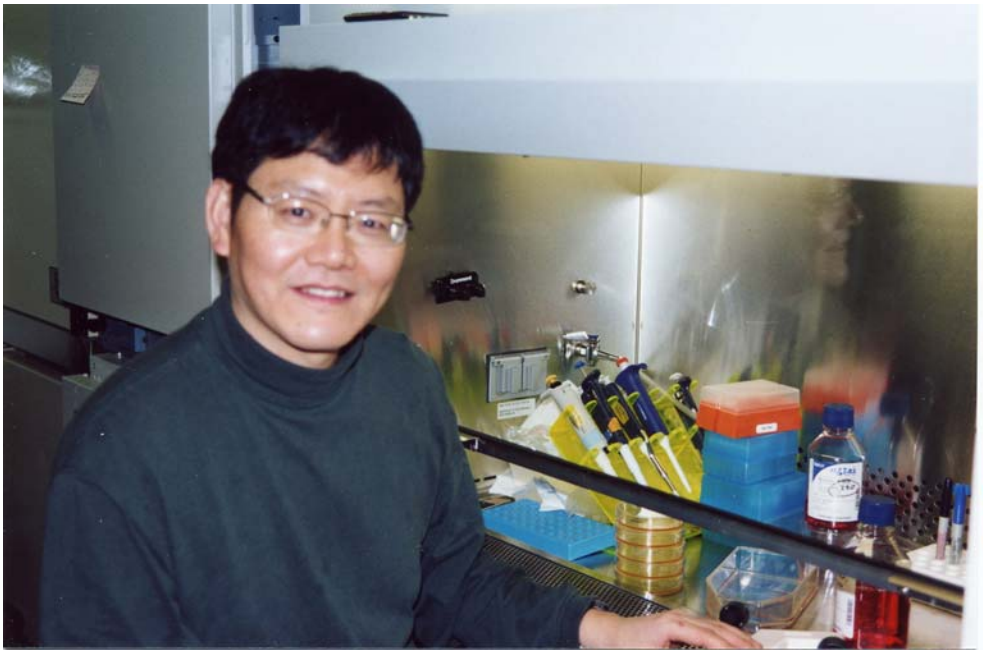

Dr. Haiying Hang preparing cell samples for flow cytometry.

Cytogenetic Analysis of Human Chromosomes from Individuals Previously Exposed to High-LET Radiation

Catherine R. Mitchell, M. Prakash Hande,[1] Tamara Azizova,[2] Charles R. Geard, Ludmilla Burak[2] and David J. Brenner

The aim of this study was to evaluate whether a "biomarker" for past radiation exposure is present in human chromosomes. Such a biomarker would increase the accuracy of epidemiological estimates of high-LET radiation exposed individuals such as nuclear workers, airline flight crew, astronauts and patients undergoing radiotherapy. As chromosomes are generally confined to well-defined spatial territories within the interphase nucleus, a single track of high-LET radiation passing through a cell causes dense areas of ionization and chromosome damage that is highly localized (1). This damage is in the form of DNA double strand breaks (dsbs) that tend to be closer together than with low-LET radiation which is less densely ionizing. As the dsbs are close together, when DNA repair takes place there may be errors (2) resulting in inversions within one chromosome (intra-chromosomal aberrations). The hypothesis is that high-LET produces more of these types of aberrations relative to other mutagens/clastogens such as X-rays or chemicals that produce less dense ionizations (3).

Fig. 1. A peripheral blood lymphocyte metaphase from a high Pu irradiated Mayak worker analyzed with mFISH. White arrows show the translocations. Complex inter-chromosomal aberrations can be observed involving chromosomes 11, 14, 13 and 7.

Until recently it has been difficult to visualize intra-chromosomal aberrations using established cytogenetic techniques. Single or two-three color whole chromosome painting techniques such as fluorescence in situ hybridization (FISH) do not allow the observation of aberrations occurring within one chromosome. It was also difficult to observe complex inter-chromosomal aberrations involving many chromosomes produced by exposure to ionizing radiation. However, the recent development of multicolor FISH (mFISH) and multicolor banding FISH (mBAND) techniques have allowed the visualization of all chromosomes in a metaphase (using mFISH) (4-6) and specific regions within one chromosome (using mBAND) (7-8).

The mFISH techniques employs a kit (Metasystems, Germany) which contains 24 different chromosome painting probes specific for each of the 24 different human chromosomes. Each probe is labeled with 1 of 5 fluorochromes or a unique combination of them. These probes are hybridized with chromosomes in metaphase preparations on slides. After hybridization, the chromosomes can be visualized. The fluorochromes in the paint are sequentially excited by filtered light using a fluorescent microscope. Returning to the ground state the fluorochromes emit light of a certain wavelength and the light is captured via a camera and the images fed to a computer. The software can detect differences in the emitted light and assigns the combinations of light to certain chromosomes. For mFISH, the software then assigns pseudocolors so that individual chromosomes can be observed by the human eye. The mBAND technique is similar to mFISH differing only in that the mBAND kit contains region-specific painting probes labeled with the fluorochromes. When visualized by the software the chromosomes can be manually scored for inter-chromosomal aberrations (mFISH) and intra-chromosomal aberrations (mBAND).

The types of aberrations that can be observed using mFISH include simple translocations which involve two chromosomes and complex translocations involving three or more chromosomes. An example is shown in Figure 1. Intra-chromosomal aberrations such as paracentric inversions (within one arm), pericentric inversions (between arms) and interstitial deletions can be used to visualized with mBAND and examples are illustrated in Figure 2.

We have used these techniques to investigate the presence of a stable high-LET biomarker in a population of

[1] *National University of Singapore.*
[2] *Southern Urals Biophysics Institute, Ozyorsk, Russia.*

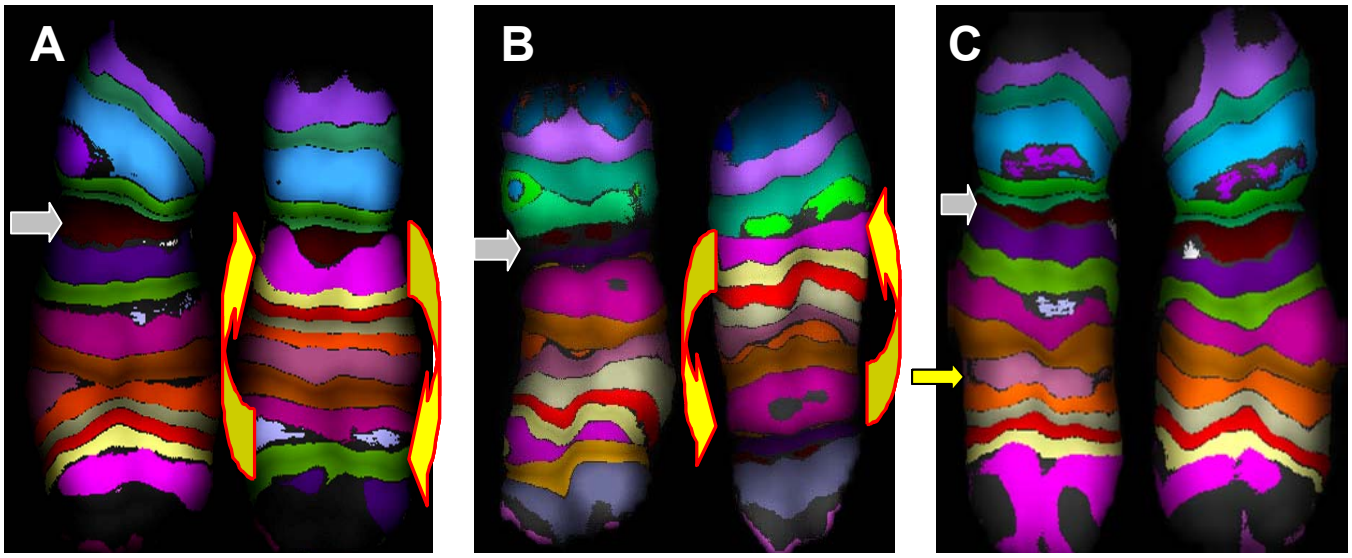

Fig. 2. mBAND analysis of human chromosomes from high Pu irradiated Mayak workers. The chromosome on the left is the normal chromosome. Grey arrows denote the centromere and yellow arrows denote the area of inversion or in C, the area which was deleted. A. Paracentric (intra-arm inversion) in chromosome 5. B. Pericentric (inter-arm inversion) in chromosome 2. C. Interstitial deletion in chromosome 5.

individuals who have had previous exposure to high-LET radiation. The chromosomes of healthy radiation workers from the Mayak Production Association near Ozyorsk, Russia who were occupationally exposed to Pu, γ-rays or both from 1949 onwards were studied (9). Blood samples were taken at the Southern Urals Biophysics Institute and metaphase spreads of peripheral blood lymphocytes were produced (10). The slides were then shipped to the USA and hybridized with mFISH and mBAND probes and scored for chromosome aberrations. Metaphase spreads from 31 individuals were analyzed (11 with high Pu exposure, 11 with high γ/no Pu exposure, 4 with mid-range Pu/mid-range γ exposure (11) and 5 controls). mFISH analysis was carried out to establish inter-chromosomal aberrations in all individuals and mBAND analysis to examine intra-chromosomal aberrations in chromosomes 1, 2 and 5 of all individuals. 120-150 metaphases were analyzed per individual.

The results for mFISH are shown in Figure 3. For simple inter-chromosomal aberrations (involving 2 chromosomes), individuals exposed to high doses of Pu have similar aberration frequency to those who had a high gamma exposure (5.8 ± 0.6 % vs. 4.7 ± 0.6 % respectively), while those with a moderate exposure to both and controls showed a dose-dependent response. For complex inter-chromosomal aberrations (involving 3 or more chromosomes), individuals exposed to high levels of Pu showed a much higher aberration

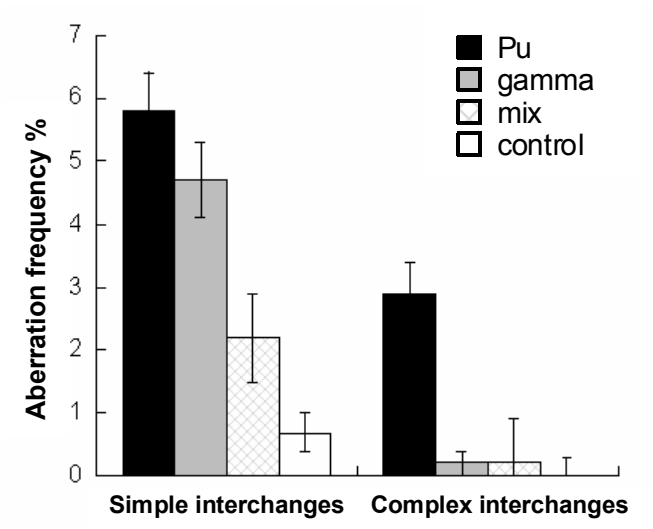

Fig. 3. The results of mFISH analysis on the Mayak worker cohort showing simple and complex aberration frequencies in the different groups. The large difference in frequency of complex aberrations between the high Pu and high gamma groups is a potential biomarker for past exposure to high-LET radiation.

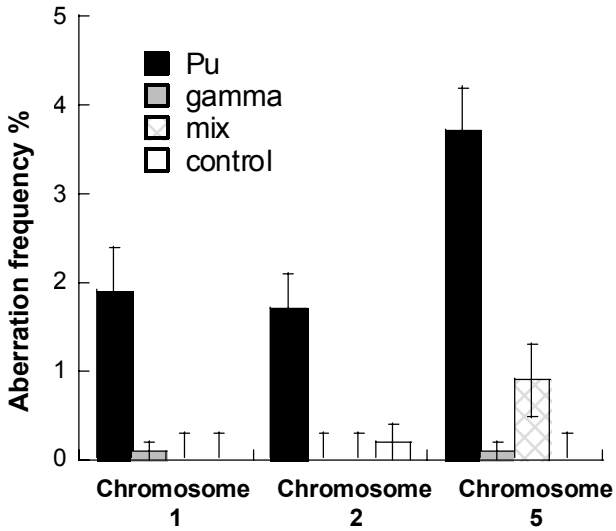

Fig. 4. The results of mBAND analysis of chromosome 1, 2 and 5 on the Mayak worker cohort showing frequencies of intra-chromosomal aberrations in the different groups. The large difference in frequency of intra-chromosomal aberrations between the high Pu and high gamma groups is a second potential biomarker for past exposure to high-LET radiation.

frequency compared with individuals with a high gamma exposure (2.9 ± 0.5 % vs. 0.2 ± 0.2% respectively). Individuals with moderate exposure to both and controls had negligible frequencies. This large difference in the frequency of complex aberrations between high Pu and high gamma exposure represents a potential biomarker for past exposure to high-LET radiation. The mBAND results (shown in Figure 4) show a large difference between the intra-chromosomal aberration frequencies for the high plutonium and the high gamma exposed individuals in all chromosomes studied (#1: 1.9 ± 0.5 % (n=7) vs. 0.1 ± 0.1% (n=5); #2: 1.7 ± 0.4% (n=7) vs. 0 [0 -0.3]% (n=6); #5: 3.7 ± 0.5 % vs. 0.1 ± 0.1 % respectively). The moderately exposed individuals and controls showed few or no intra-chromosomal aberrations. This is a second potential biomarker for past exposure to high-LET radiation.

This is the first study in which mFISH or mBAND have been used in a human population exposed to radiation in vivo. The biomarkers of past exposure to high-LET radiation that we have found are long-lived, sensitive and quantitative with a low background. They may be used in the future as a "biodosimeter" to estimate both the dose and type of previous radiation exposure in populations.

References

1. Prise KM, Pinto M, Newman HC and Michael BD. A review of studies of ionizing radiation-induced double-strand break clustering. *Radiat Res* **156**:572-6, 2001.
2. Savage JR, A brief survey of aberration origin theories, *Mutat Res* 404:139-47, 1998.
3. Brenner DJ and Sachs RK. Chromosomal "fingerprints" of prior exposure to densely ionizing radiation. *Radiat Res* **140**:134-42, 1994.
4. Speicher MR, Gwyn Ballard S and Ward DC. Karyotyping human chromosomes by combinatorial multi-fluor FISH. *Nat Genet* **12**:368-75, 1996.
5. Eils R, Uhrig S, Saracoglu K, Satzler K, Bolzer A, Petersen I, Chassery J, Ganser M and Speicher MR. An optimized, fully automated system for fast and accurate identification of chromosomal rearrangements by multiplex-FISH (M-FISH). *Cytogenet Cell Genet* **82**:160-71, 1998.
6. Greulich K M, Kreja L, Heinze B, Rhein A P, Weier H G, Bruckner M, Fuchs P and Molls M. Rapid detection of radiation-induced chromosomal aberrations in lymphocytes and hematopoietic progenitor cells by mFISH. *Mutat Res* **452**:73-81, 2000.
7. Chudoba I, Plesch A, Lorch T, Lemke J, Claussen U and Senger G. High resolution multicolor-banding: a new technique for refined FISH analysis of human chromosomes. *Cytogenet Cell Genet* **84**:156-60, 1999.
8. Johannes C, Chudoba I and Obe G. Analysis of X-ray-induced aberrations in human chromosome 5 using high-resolution multicolour banding FISH (mBAND). *Chromosome Res* **7**:625-33, 1999.
9. Anspaugh LR, Degteva MO and Vasilenko EK. Mayak Production Association: introduction. *Radiat Environ Biophys* **41**:19-22, 2002.
10. Burak LE, Kodama Y, Nakano M, Ohtaki K, Itoh M, Okladnikova ND, Vasilenko EK, Cologne JB and Nakamura N. FISH examination of lymphocytes from Mayak workers for assessment of translocation induction rate under chronic radiation exposures. *Int J Radiat Biol* **77**:901-8, 2001.
11. Romanov SA, Vasilenko EK, Khokhryakov VF and Jacob P. Studies on the Mayak nuclear workers: dosimetry. *Radiat Environ Biophys* **41**:23-8, 2002.

Dr. Catherine R. Mitchell, performing research involving mFISH and mBAND analysis.

Paralogs of HRAD9 and Mrad9 Checkpoint Control Genes are Expressed Primarily in Testicular Tissue

Kevin M. Hopkins, Xiaojian Wang, Ayana Morales, Haiying Hang, and Howard B. Lieberman

The fission yeast *Schizosaccharomyces pombe rad9* gene promotes radioresistance and regulates cell cycle checkpoint control. Human (*HRAD9*) and mouse (*Mrad9*) orthologs of this gene have been isolated and demonstrate similar biological functions (Lieberman et al., 1996; Hang et al., 2002). In this report, we describe the isolation of human and mouse paralogs of *HRAD9* and *Mrad9*, which we call *HRAD9B* and *Mrad9B*, respectively. Figure 1 illustrates a comparison of the proteins encoded by *HRAD9* and *Mrad9* with their corresponding paralogs. As indicated, amino acid homology extends throughout the length of the proteins, and is not confined to a limited number of regions. *HRAD9* and *HRAD9B* encoded proteins are 55% similar and 35% identical. *Mrad9* and *Mrad9B* gene products are 50% similar and 35% identical. Seventy-six percent of similarly located amino acids in HRAD9B and Mrad9B have related physiochemical properties and 63% are identical. Interestingly, BLAST searches did not reveal yeast orthologs of HRAD9B or Mrad9B.

Northern blot analysis was used to determine whether *HRAD9B* is expressed in a tissue specific manner. As shown in Figure 2, three strong bands are detected in testis, perhaps representing alternatively spliced RNA, but little or no corresponding message was found in numerous other tissues examined. *Mrad9B* RNA was also predominantly located in testis. This is in contrast to *HRAD9* and *Mrad9*, which are expressed more universally in different tissues.

These results suggest a key role for *HRAD9B* and *Mrad9B* specifically in mammalian testis. Studies are un-

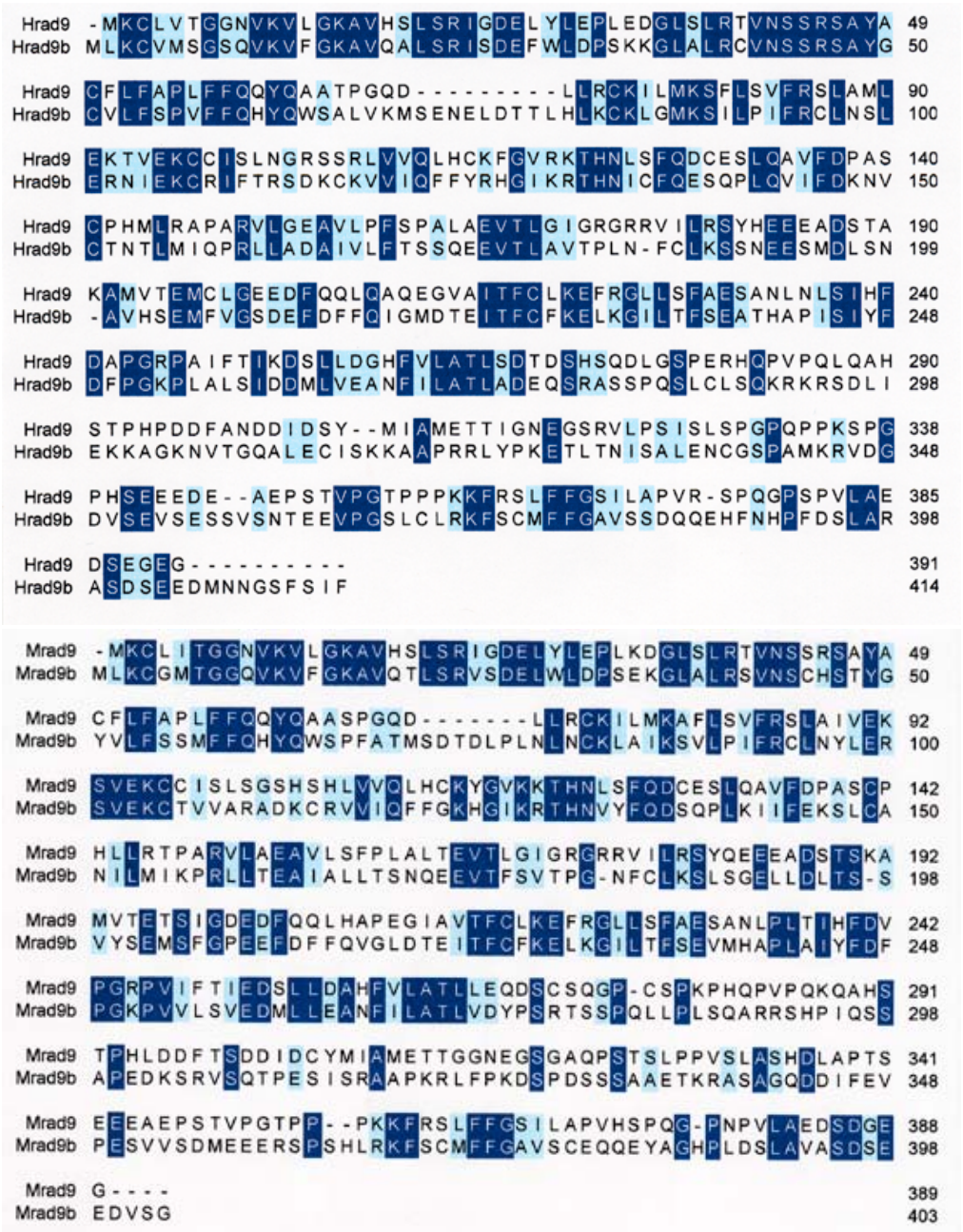

Fig. 1. Comparison of HRAD9 and Mrad9 proteins with their respective paralogs. Top: HRAD9 versus HRAD9B; Bottom: Mrad9 vs. Mrad9B. Dark blue, identical amino acids; Light blue, amino acids with similar physiochemcial properties.

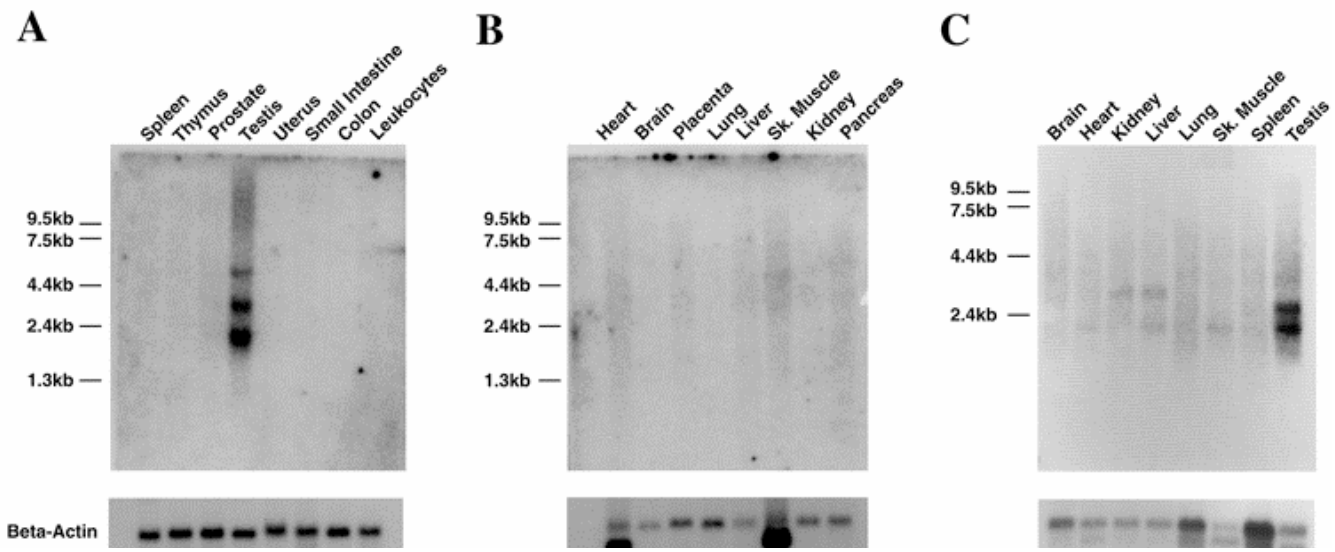

Fig. 2. Northern blotting indicates that *HRAD9B* and *Mrad9B* RNA are most abundant in testis (panel C).

derway to characterize these genes in more detail with respect to their biological function, relationship to *HRAD9*/*Mrad9*, and role in radioresistance and carcinogenesis.

References

1. Hang H, Rauth SJ, Hopkins KM, Davey SK and Lieberman HB. Molecular cloning and tissue-specific expression of Mrad9, a murine orthologue of the Schizosaccharomyces pombe rad9+ checkpoint control gene. *J Cell Physiol* **177**:232-40, 1998.
2. Lieberman HB, Hopkins KM, Nass M, Demetrick D and Davey S. A human homologue of the Schizosaccharomyces pombe rad9+ checkpoint control gene. *Proc Natl Acad Sci (USA)* **93**:13890-5, 1996.

Identification of PAC1 as a Transcriptional Target of p53 in Signaling Apoptosis

Yuxin Yin and Cynthia Y. Liu

Our research interest is in the understanding of the molecular basis of p53-mediated apoptosis. p53 is the most frequently mutated gene in human cancers (1). p53 plays a fundamental role in multiple cell processes, including gene transcription regulation, cell cycle checkpoint control, cell death induction, DNA repair, and genetic stability (2-4). p53 acts as a sequence-specific DNA binding protein and activates transcription through binding to specific DNA consensus sequences (5). p53 is a negative regulator of cell cycle progression and functions as a checkpoint protein in controlling the transition from G1 to S phase of the cell cycle. p53 is required for the cell cycle response to DNA damage by radiation (6).

In recent years, much progress has been made towards understanding the role of p53 in programmed cell death. p53 functions as a cell death mediator (7). p53 is required for irradiation-induced apoptosis in mouse thymocytes and the status of p53 is associated with cellular sensitivity to drug-mediated cell killing in chemotherapy (8, 9). p53 is also required for cellular apoptotic response to oxidative stress (10). However, the mechanism by which p53 mediates cell death is unclear. It is known that p53 transactivation plays an essential role in induction of apoptosis (11, 12), suggesting that p53 downstream genes may be involved in this process. Some transcriptional targets of the p53 protein have been identified and they are involved in regulation of cell growth, DNA repair or cell death processes (13). Among them, Bax is a direct transcriptional target of p53 and it is a cell death mediator that forms a heteradimer with Bcl-2 (14, 15). Because p53 is involved in multiple cellular processes, it is likely that there are other genes that are regulated by p53 and play roles in the cellular response to genotoxic stress and tumorigenesis.

Mitogen activated protein kinases (MAPKs) are key elements in mediating signal transduction from the cell surface to the nucleus (16, 17). MAP kinases can be grouped

into three families: ERK, JNK and p38 (18). Upon activation, MAPKs, including ERK1 and ERK2, translocate into the nucleus where they phosphorylate transduction targets, including transcription factors (19). The MAP kinase cascade is one of the most predominant pathways for cell growth and proliferation (17). The activity of MAP kinases is regulated by dual phosphorylation of their tyrosine and threonine residues. MAPKs are activated upon dual phosphorylation by MAP kinase kinase (MEK), which in turn is activated by the Ras/Raf pathway (20). In contrast, MAPKs are inactivated upon dephosphorylation of tyrosine and threonine residues by MAPK phosphatases, including MKP-1, MAK-2 and PAC1 (21). PAC1 is an early response gene encoding a dual threonine/tyrosine phosphatase that specifically dephosphorylates and inactivates ERK1 and ERK2 (22, 23). The mechanism whereby PAC1 is regulated and its role during tumorigenesis are unknown.

Using DNA microarray technique, we have previously identified more than sixty genes upregulated by p53 (24). PAC1 is among those p53 responsive genes. PAC1 functions to inactivate ERK1 and ERK2 kinase activity through dephosphorylation of ERK1/2 (22). Therefore, it is important to dissect the molecular link between a powerful tumor suppressor gene p53 and an essential cell signaling pathway, the MAK kinase cascade. To confirm the data from the microarray readout, we performed Northern analysis of PAC1 expression in a p53 inducible system, using EB-1 cells. The EB cell line was derived from a human colon cancer with mutant p53. EB-1 is a stable clone containing a wild-type p53 transgene under the control of the metallothionein promoter and expressing wild-type p53 upon administration of zinc chloride ($ZnCl_2$) (25). These cells undergo apoptosis following serum deprivation in the presence of p53 (25). As expected, p21, a p53-target gene (26,27), is absent in EB-1 without wild-type p53 (wt p53) (Fig. 1A, middle panel, lane 1) but increased following wt p53 expression induced by ($ZnCl_2$) (middle panel, lanes 2, 3). As shown in Fig. 1A, PAC1 transcript is low in EB-1 without p53 (upper panel, lane 1). Interestingly, PAC1 is not increased in EB-1 cells with 100 μM $ZnCl_2$ (lane 1 vs. lane 2), which induces the expression of p21 (middle panel, lane 2), and causes cell cycle arrest (data not shown). However, PAC1 expression is greatly increased in the EB-1 cells treated with both 100 μM $ZnCl_2$ and serum deprivation (upper panel, lane 3), which activates p53 and induces apoptosis (25). As expected, PAC1 is not induced by serum starvation in the absence of p53 (lane 4). These results suggest that PAC1 transcription can be regulated by p53 and induction of PAC1 is dependent of p53 status and is influenced by stress conditions.

In order to understand the molecular basis for regulation of PAC1 by p53, we set up an approach to clone the regulatory region of the human PAC1 gene. We used a 600-bp fragment flanking the 5'UTR and partial coding sequence of the PAC1 gene as a probe to screen a human genomic library in the pWE15 cosmid (Stratagene) for the promoter of the PAC1 gene. Screening procedure was performed according to the manufacturer's protocol. The resulting positive clones were subjected to secondary screening. We obtained two identical clones that contain 2.1 kb regulatory region of the

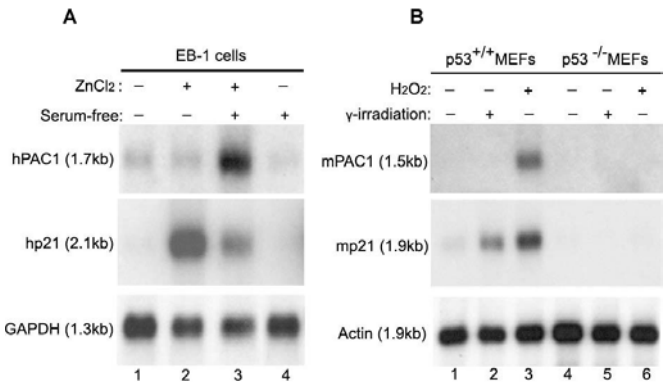

Fig. 1. Northern analysis of PAC1 expression induced by p53. (A) EB-1 cells were cultured under the following conditions: MEM with 10% fetal bovine serum (lane 1); 100 μM zinc chloride with 0.1% fetal bovine serum (serum starvation, SS) for 6 hours (lane 2), 100 μM zinc chloride ($ZnCl_2$) and 10% fetal bovine serum for 6 hours (lane 3). (B) Exponentially growing MEF cells were exposed to 6 grays of γ-radiation or 88 μM H_2O_2. The cells from groups **A** and **B** were harvested after 3 hours and 2 μg mRNA of each group was fractionated on 1.2% formaldehyde agarose gel and transferred to a nylon transfer membrane for Northern blotting using a [α-^{32}P]dCTP-labeled PAC1 or p21 cDNA probes, respectively, following standard procedures. After exposure of films for PAC1 or p21 band visualization, the blot was stripped and re-hybridized with GAPDH or β-actin cDNA probes as loading controls.

human PAC1 gene. Our sequence analysis of the promoter region reveals no known p53 con-sensus binding site as 5'-PuPuPuC(A/T)(T/A)GPyPyPy-3' (28). However, there is a palindromic site from -202 to -191 in the PAC1 promoter. To determine whether the PAC1 promoter is regulated by p53, the PAC1 promoter was am-plified from -726 to -15, which contains the palindromic sequence. This 711-bp promoter was ligated into a luciferase reporter vector pGL3-basic (Promega) adjacent to a luciferase reporter gene, resulting in the reporter of pGL3/PAC1-0.7. To examine luciferase activity, the PAC1 luciferase reporter and other reporters were transfected into H1299 cells along with a pCMV vector as a control, or with a wild-type p53 expression vector (pCMV/wtp53) (29). Also, a mutant p53 plasmid containing a double point mutation in the transactivation domain was used as a control in our lu-ciferase assays. We also included promoter reporters for some known p53-target genes, including p21, MDM2 and Bax as controls.

Luciferase assays were conducted using a Dual-Light chemiluminescent reporter gene assay system for the combined detection of luciferase and β-galactosidase (TROPIX, INC), according to the manufacturer's protocol. As shown in Fig. 2, there is a basal activity of the PAC1 promoter in the absence of p53. The activity of the pGL3/PAC1-0.7 is greatly induced by wild-type p53, but not by a mutant p53 plasmid (pC53-248), which contains a point mutation at codon 248. As expected, the promoter reporters of three known p53-target genes, p21, *MDM2* and *bax*, are also activated by p53. The fold induction of the PAC1 promoter activity is similar to that of the p21 promoter activity by wild-type p53. However, induction of the PAC1 promoter activity

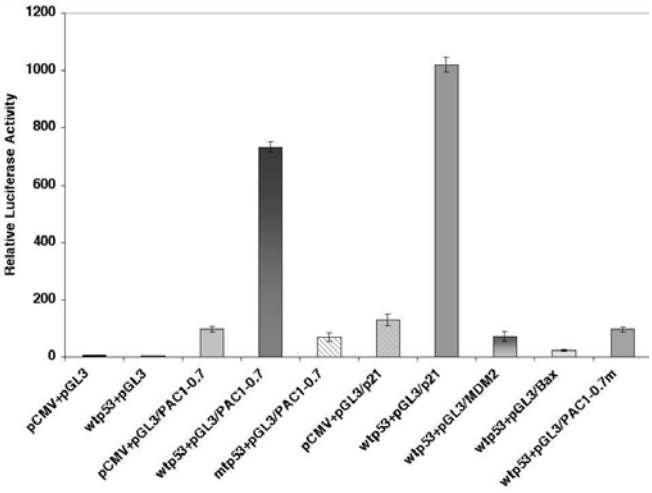

Fig. 2. Transactivation of the PAC1 promoter by p53. Luciferase assays were carried out for induction of promoter activities of PAC1, p21, MDM2, and Bax by wild-type p53. H1299 cells were transiently transfected with respective plasmids described below using LipofectAMINE in OPTI-MEM medium (GIBCO, BRL). Cell extracts were assayed for luciferase activity on a Berthold Autolumat LB953 Rack Luminometer. The luciferase activity readout is expressed as means ± S.D. of triplicate cultures and transfections. The transfection groups are as follows (from the left to right in the figure): (1) empty pCMV vector; (2) pCMV/wtp53 plus pGL3-Basic; (3) pCMV vector plus pGL3/PAC1-0.7; (4) pCMV/wtp53 plus pGL3/PAC1-0.7; (5) pC53-248 plus pGL3/PAC1-0.7; (6) pCMV plus p21 promoter luciferase reporter pGL3/p21; (7) pCMV/wtp53 plus pGL3/p21; (8) pCMV/wtp53 plus MDM2 promoter luciferase reporter pGL3/MDM2; (9) pCMV/wtp53 plus Bax promoter luciferase reporter pGL3/Bax, (10) pCMV/wtp53 plus a mutated PAC1 reporter pGL3/PAC1-0.7m.

by p53 is much higher than that of both *MDM2* and *Bax* luciferase promoters. These results suggest that the PAC1 promoter is highly responsive to p53 function. To test whether the palindromic sequence is important to p53 transactivity, we constructed a series of luciferase reporters with or without the palindromic region. We observed that luciferase activity was reduced greatly in all of the luciferase reporters omitting the palindromic sequence in the presence of p53 (data not shown). These results suggest that p53 regulates the PAC1 promoter activity likely through a region containing this palindromic site. To further test this possibility, we performed a PCR-based site-directed mutagenesis to create a mutant form of pGL3/PAC1-0.7, pGL3/PAC1-0.7m, which lacks a 6-bp core sequence (CCCCAC) of the palindrome.

The induction of luciferase activity of this mutant reporter by p53 was reduced to the basal level (Fig. 2). These results demonstrate that the palindromic site is crucial for induction of the PAC1 promoter activity by p53.

Because PAC1 is primarily regulated by p53, it is possible that the expression of PAC1 may be altered in some cancer cells due to p53 mutations and dysfunction. To test this possibility, we examined the levels of PAC1 message in a group of cancer cell lines derived from various types of cancer. We observed that the levels of PAC1 mRNA vary, but they are low in most of these cancer cells. PAC1 is high in Ov2008 and ZR-75-1, which contain wild-type p53. However, the expression of PAC1 is low or absent in most of cancer cell lines with mutant p53, suggesting a correlation between p53 status and PAC1 expression.

We have previously demonstrated that p53 is required for the cellular apoptotic response to oxidative stress (10). Our preliminary results indicate that PAC1 is up-regulated by p53 in response to serum starvation and oxidative stress, suggesting that PAC1 may be involved in signaling cellular response to environmental stresses. In order to determine the role of PAC1 in the apoptotic process, we constructed a human PAC1 expression vector by cloning a 1.1 kb human PAC1 cDNA containing the full coding sequence in frame into a mammalian expression vector driven by a human cytomegalovirus (pcDNA3/hygro, Invitrogen). The resulting PAC1 expression vector, pcDNA3/PAC1, or an empty vector pcDNA3, was transfected into EB, a colon cancer cell line, and MDA-MB435, a breast cancer cell line, which were then selected with hygromycin B for isolating stable clones of EB/PAC1 and MB435/PAC1. We found that EB/PAC1-c5, which contains a high level of ectopic PAC1, undergo typical apoptosis under the condition of serum starvation. Also, we observed that MB435/PAC1 cells, particularly, MB435/PAC1-c6, are highly susceptible to cell killing by H_2O_2 treatment.

Our results demonstrate that PAC1 functions as a cell death mediator in cellular response to nutritional stress and oxidative stress. To determine whether overexpression of PAC1 influences anchorage-independent growth, we compared MB435 cells and MB435 cells overexpressing PAC1 for their ability to form colonies in soft agar. We found that the colony numbers from MB435/PAC1-c6 cells in soft agar are significantly less than those from the MB435/pcDNA3 control group. These data indicate that PAC1 may function as a repressor of cancer cell growth. Because PAC1 induces apoptosis in MB435 cells, it is conceivable that PAC1 inhibits colony formation through induction of cell death. In the next year, we will explore the potential role of PAC1 in tumor suppression using the nude mouse model.

References

1. Hollstein M, Sidransky D, Vogelstein B and Harris CC. p53 mutations in human cancers. *Science* **253**:49-53, 1991.
2. Levine AJ. p53, the cellular gatekeeper for growth and division. *Cell* **88**:323-31, 1997.
3. Kastan MB, Canman CE and Leonard CJ. p53, cell cycle control and apoptosis:implications for cancer. *Cancer Metastasis Rev* **14**:3-15, 1995.
4. Yin Y, Tainsky MA, Bischoff FZ, Strong LC and Wahl GM. Wild-type p53 restores cell cycle control and inhibits gene amplification in cells with mutant p53 alleles. *Cell* **70**:937-48, 1992.
5. Kern SE, Kinzler KW, Bruskin A, Jarosz D, Friedman P, Prives C, and Vogelstein B. Identification of p53 as a sequence-specific DNA-binding protein. *Science* **252**:1708-11, 1991.

6. Kastan MB, Zhan Q, el Deiry WS, Carrier F, Jacks T, Walsh WV, Plunkett BS, Vogelstein B and Fornace AJ Jr. A mammalian cell cycle checkpoint pathway utilizing p53 and GADD45 is defective in ataxia-telangiectasia. *Cell* **71**:587-97, 1992.
7. Yonish Rouach E, Resnitzky D, Lotem J, Sachs L, Kimchi A and Oren M. Wild-type p53 induces apoptosis of myeloid leukaemic cells that is inhibited by interleukin-6. *Nature* **352**:345-7, 1991.
8. Lowe SW, Schmitt EM, Smith SW, Osborne BA and Jacks T. p53 is required for radiation-induced apoptosis in mouse thymocytes. Nature **362**:847-9, 1993.
9. Lowe SW. Cancer therapy and p53. *Curr-Opin-Oncol* **7**:547-53, 1995.
10. Yin Y, Terauchi T, Solomon GG, Aizawa S, Rangarajan PN, Yazaki Y, Kadowaki T and Barrett JC. Involvement of p85 in p53-dependent apoptotic response to oxidative stress. *Nature* **391**:707-10, 1998.
11. Sabbatini P, Lin J, Levine AJ and White E. Essential role for p53-mediated transcription in E1A-induced apoptosis. *Genes Dev* **9**:2184-92, 1995.
12. Yonish Rouach E, Deguin V, Zaitchouk T, Breugnot C, Mishal Z, Jenkins JR and May E. Transcriptional activation plays a role in the induction of apoptosis by transiently transfected wild-type p53. *Oncogene* **11**:2197-205, 1995.
13. El-Deiry WS. Regulation of p53 downstream genes. *Semin Cancer Biol* **8**:345-57, 1998.
14. Miyashita T and Reed JC. Tumor suppressor p53 is a direct transcriptional activator of the human bax gene. *Cell* **80**:293-9, 1995.
15. Yin XM, Oltvai ZN and Korsmeyer SJ. Heterodimerization with Bax is required for Bcl-2 to repress cell death. *Curr Top Microbiol Immunol* **194**:331-8, 1995.
16. Guan KL. The mitogen activated protein kinase signal transduction pathway:from the cell surface to the nucleus. *Cell Signal* **6**:581-9, 1994.
17. Nishida E and Gotoh Y. The MAP kinase cascade is essential for diverse signal transduction pathways. *Trends Biochem Sci* **18**:128-31, 1993.
18. Lange-Carter CA, Pleiman CM, Gardner AM, Blumer KJ and Johnson GL. A divergence in the MAP kinase regulatory network defined by MEK kinase and Raf. *Science* **260**:315-9, 1993.
19. Minden A, Lin A, McMahon M, Lange-Carter C, Derijard B, Davis RJ, Johnson GL and Karin M. Differential activation of ERK and JNK mitogen-activated protein kinases by Raf-1 and MEKK. *Science* **266**:1719-23, 1994.
20. Buscher D, Hipskind RA, Krautwald S, Reimann T and Baccarini M. Ras-dependent and -independent pathways target the mitogen-activated protein kinase network in macrophages. *Mol Cell Biol* **15**:466-75, 1995.
21. Sun H, Charles CH, Lau LF and Tonks NK. MKP-1 (3CH134), an immediate early gene product, is a dual specificity phosphatase that dephosphorylates MAP kinase in vivo. *Cell* **75**:487-93, 1993.
22. Rohan PJ, Davis P, Moskaluk CA, Kearns M, Krutzsch H, Siebenlist U and Kelly K. PAC-1:a mitogen-induced nuclear protein tyrosine phosphatase. *Science* **259**:1763-6, 1993.
23. Ward Y, Gupta S, Jensen P, Wartmann M, Davis RJ and Kelly K. Control of MAP kinase activation by the mitogen-induced threonine/tyrosine phosphatase PAC1. *Nature* **367**:651-4, 1994.
24. Zhao R, Gish K, Murphy M, Yin Y, Notterman D, Hoffman WH, Tom E, Mack DH and Levine AJ. Analysis of p53-regulated gene expression patterns using oligonucleotide arrays. *Genes & Dev* **14**:981-93, 2000.
25. Shaw P, Bovey R, Tardy S, Sahli R, Sordat B and Costa J. Induction of apoptosis by wild-type p53 in a human colon tumor-derived cell line. *Proc Natl Acad Sci (USA)* **89**:4495-9, 1992.
26. Xiong Y, Hannon GJ, Zhang H, Casso D, Kobayashi R and Beach D. p21 is a universal inhibitor of cyclin kinases. *Nature* **366**:701-4, 1993.
27. El Deiry WS, Tokino T, Velculescu VE, Levy DB, Parsons R, Trent JM, Lin D, Mercer WE, Kinzler KW and Vogelstein B. WAF1, a potential mediator of p53 tumor suppression. *Cell* **75**:817-25, 1993.
28. El Deiry WS, Kern SE, Pietenpol JA, Kinzler KW and Vogelstein B. Definition of a consensus binding site for p53. *Nat-Genet* **1**:45-9, 1992.
29. Baker SJ, Markowitz S, Fearon ER, Willson JK and Vogelstein B. Suppression of human colorectal carcinoma cell growth by wild-type p53. *Science* **249**:912-5, 1990. CRR

Mouse Rad1 Knockout

Haiying Hang

Accumulated evidence indicates that cell cycle checkpoint proteins Rad1, Rad9 and Hus1 can form a complex (1-4), believed to resemble a PCNA-like DNA sliding clamp, a heterotrimer structure (5-7). Mouse *Rad9*$^{-/-}$ and *Hus1*$^{-/-}$ cell lines have been established and both demonstrate genome instability and extreme sensitivity to genotoxic stress (unpublished data on *Rad9*$^{-/-}$ ES cells, HBL *et al*., CRR, Columbia University; Weiss *et al.*, 2000). However, this trimer

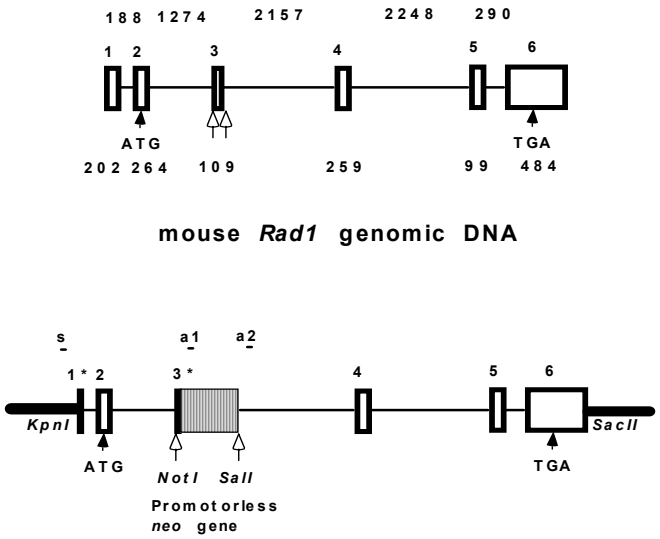

Fig. 1. Construct for targeting Mouse *Rad1*.

Above: Mouse *Rad1* genomic DNA has been cloned from mouse 129 ES cells and sequenced. It contains 6 exons. The start codon ATG resides within the second exon, and the stop codon TGA is located in the last exon. Below: A mouse *Rad1* targeting construct. The DNA fragment between the middle of exon 1 (1*) and the end of the last exon is inserted in between *Kpn*I and *Sac*II sites in pBluescript SK(+) (shown as the two thick lines on the two sides). The construct contains a promoterless and ATG-free *neo* gene (1095 bp) which replaces the most portion of exon 3 and excision region of exon 3 /intron 3. Care has been taken to ensure *neo* is in frame with the start codon ATG of *mRad1*. When *mRad1* in ES cells is successfully targeted, PCR using primer pairs s/a2 will yield 2.8 kb, instead of 1.75 kb, DNA fragment, and another PCR using primer pairs s/a1 will produce 1.6 kb, instead of none, DNA fragment.

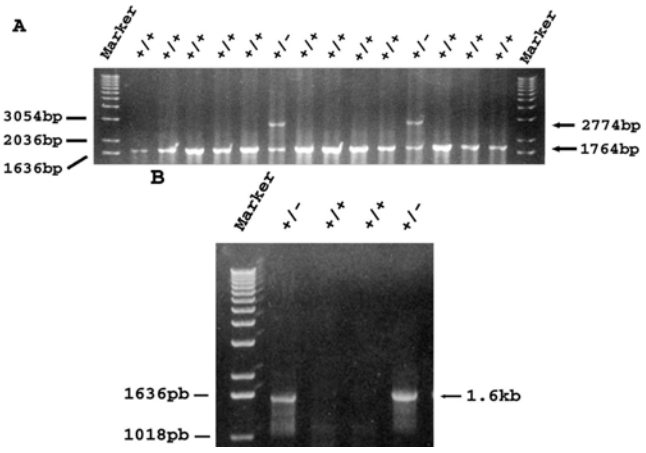

Fig. 2. Screening for ES cell clones containing a disrupted *mRad1*.

ES cells were transfected with *neo/mRad1* targeting construct DNA linearized with *kpn*I, and grew into colonies in G418 containing medium. Four clones out of 35 tested colonies have *mRad1*$^{-/+}$ genotype. A. Primer s contains a sequence that is located upstream of the 5' end of *mRad1* genomic DNA but not included in *mRad1* targeting construct. Primer a2 contains a sequence within the third intron. PCR using s/a2 primers indicates here that one copy of *mRad1* gene in 2 clones are disrupted (both 2774 and 1766 bp DNA products appeared) and no *mRad1* disruption happened in the other 12 clones (only yielded 1766 bp DNA product). B. To confirm the above result, PCR using s/a1 primer pair was also performed. Primer a1 contains a stretch of *neo* sequence. If one copy of *mRad1* is disrupted, the PCR should produce a 1.6 kb DNA fragment. Indeed, the PCR on the two positive clones in panel A did yield the expected 1.6 kb band, but only produced background bands when using negative clone DNA as template.

model does not exclude the possibility that each of the three proteins play its distinct roles in cells without one or two of the other two proteins. Experimental data consistent with this idea include: 1) *mRad9*$^{-/-}$ cells are defective in G2/M checkpoint control while *mHus1*$^{-/-}$ cells manifest normal G2/M checkpoint control when challenged with ionizing radiation (unpublished data on *mRad9*$^{-/-}$ cells, HBL *et al*.; unpublished data on *mHus1*$^{-/-}$ cells, HH, CRR, Columbia University; and communication on *mHus1*$^{-/-}$ cells with Dr. Robert Weiss, Harvard University); 2) Hus1 can directly interact with another Hus1 molecule (3); 3) a newly identified Hus1 homologue protein, Hus1b, strongly interacts with Rad1 but not Rad9 or Hus1(8); 4) a Rad9b (homologous to Rad9) has also been identified recently (HBL); and 5) no *Rad1b* exists in human genome. Therefore, it is important to compare defects of *mHus1*$^{-/-}$, *mRad9*$^{-/-}$ and *mRad1*$^{-/-}$ cells to fully understand how these proteins play roles in cell cycle checkpoint controls and radiation resistance. *MRad1* knockout has not been reported, and is one of my research focuses.

I cloned *mRad1* genomic DNA, built a *mRad1*-targeting construct (Figure 1), and successfully disrupted one copy of *mRad1* from ES cells (Figure 2).

I am currently targeting the other copy of *mRad1* to create *mRad1*$^{-/-}$ ES cells. One of the strategies is to increase the concentration of G418 (the toxic substrate of neo protein) to force the disrupted *mRad1-neo* to replace the intact *mRad1* in *mRad1*$^{-/+}$ ES cells. The second strategy is to transfect *mRad1*$^{-/+}$ ES cells with a *hygro*-containing *mRad1*-targeting construct, and screen for hygromycin-resistant clones in which the intact *mRad1*copy have been disrupted. The above two experiments are under way.

mRad1$^{-/+}$ ES cell clones are currently being used to make *mRad1*$^{-/+}$ mouse in the Columbia University Cancer Center knockout mouse facility.

References

1. Volkmer E and Karnitz LM. Human homologs of Schizosaccharomyces pombe rad1, hus1, and rad9 form a DNA damage-responsive protein complex. *J Biol Chem* **274**: 567-70, 1999.
2. St. Onge RP, Udell CM, Casselman R and Davey S. The human G2 checkpoint control protein hRAD9 is a nuclear phosphoprotein that forms complexes with hRAD1 and hHUS1. *Mol Biol Cell* **10**:1985-95, 1999.
3. Hang H and Lieberman HB. Physical interactions among human checkpoint control proteins HUS1p, RAD1p, and RAD9p, and implications for the regulation of cell cycle progression. *Genomics* **65**:24-33, 2000.

4. Lindsey-Boltz LA, Bermudez VP, Hurwitz J and Sancar A. Purification and characterization of human DNA damage checkpoint Rad complexes. *Proc Natl Acad Sci (USA)* **98**:11236-41, 2001.
5. Cai RL, Yan-Neale Y, Cueto MA, Xu H and Cohen D. HDAC1, a histone deacetylase, forms a complex with Hus1 and Rad9, two G2/M checkpoint Rad proteins. *J Biol Chem* **275**:27909-16, 2000.
6. Venclovas C and Thelen MP. Structure-based predictions of Rad1, Rad9, Hus1 and Rad17 participation in sliding clamp and clamp-loading complexes. *Nucleic Acids Res* **28**:2481-93, 2000.
7. Burtelow MA, Roos-Mattjus PM, Rauen M, Babendure JR and Karnitz LM. Reconstitution and molecular analysis of the hRad9-hHus1-hRad1 (9-1-1) DNA damage responsive checkpoint complex. *J Biol Chem* **276**:25903-9, 2001.
8. Hang H, Zhang Y, Dunbrack RL Jr, Wang C and Lieberman HB. Identification and characterization of a paralog of human cell cycle checkpoint gene HUS1. *Genomics* **79**:487-92, 2002.

Disruption of the Betaig-h3 Gene in Mouse Embryonic Stem Cells by Gene Targeting

Yong L. Zhao and Tom K. Hei

Although the Betaig-h3 gene has been demonstrated to be involved in tumorigenic processes by using in vitro systems (1,2), generation of Betaig-h3-null mice will provide an invaluable tool to ascertain the links between deletion of this gene and specific cellular changes including apoptosis, gene instability, and cancer formation. For this purpose, we made a targeting construct overlapping intron 2 to intron 3 genomic locus resulting in the deletion of exon 2. Linearized targeting vector DNA (70 μg) was electroporated into 1×10^7 ES cells generated from the 129SvEv mouse at 960 V, 0.22Kv in 0.4 cm gap cuvette. Immediately after electroporation, cells were plated onto six 100 mm dishes. G418 (200 μg/ml) selection is applied 24 h after plating without subculture and allowed to proceed for 9-12 days.

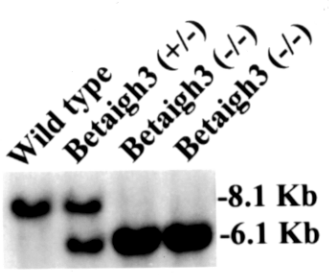

Fig. 1. Southern blot analysis of heterozygous and homozygous targeting clone cells.

Heterozygous clones for the Betaig-h3 gene were identified by Southern blot. Homozygous mutant (Betaigh3-/-) ES cells were generated by culturing the heterozygous ES cells in an elevated level (6 mg/ml) of G418 and also identified by Southern blot hybridization. Figure 1 shows a southern blot analysis of Betaigh3(+/-) and Betaigh3(-/-) ES clone cells using BamHI digestion and southern probe. The 8.1 Kb fragment represent the WT allele and the 6.1 Kb represents the targeted allele. A total of 17 heterozygous clones and 20 homozygous clones were identified. Three different Betaigh3(+/-) ES clones are used to generate the chimeric animals by injection into wild-type C57BL/6J blastocyte stage embryos. Chimeric mice have successfully been generated. Germ line transmission of the mutated allele will be generated using these chimeric mice.

References

1. Zhao YL, Piao CQ and Hei TK. Overexpression of Betaig-h3 gene downregulates integrin alpha5beta1 and suppresses tumorigenicity in radiation-induced tumorigenic human bronchial epithelial cells. *British Journal of Cancer* **86**:1923-28, 2002.
2. Zhao YL, Piao CQ and Hei TK. Downregulation of Betaig-h3 gene is causally linked to tumorigenic phenotype in asbestos treated immortalized human bronchial epithelial cells. *Oncogene* **21**:7471-7, 2002.

Identification of Differentially Expressed Sequences in Radiation Induced Breast Epithelial Cells by Subtractive Suppression Hybridization

Debasish Roy, Gloria M. Calaf and Tom K. Hei

Differential gene expression is associated with a large spectrum of biological and pathological processes. The progression of breast cancer is also associated with a number of differentially expressed genes as a result of point mutations, chromosomal rearrangements, genomic amplifications and deletions (1). The biological heterogeneity of breast cancers may arise from many possible molecular changes accumulated during the neoplastic process, with variable efficiency at each step. Mutations in the malignant growth process involve many genes and signaling pathways controlling cell proliferation, death, and differentiation (2,3). Breast cancer progression follows a complex multi-step process from constant exposure to different mutagenic factors which leads to DNA damage and genomic instability. As a result, cells have evolved an elaborate defense mechanism against these factors by utilizing differential expression of cell cycle checkpoint control genes.

DNA based approach for the identification and discovery of differentially expressed novel genes has not been very successful in case of complex disease like breast cancer due to multiple gene-gene and gene-environment interactions. However, there are alternative strategies in the field of gene discovery, such as RNA (gene expression) or proteomics-based approaches. There are a number of RNA-based technologies currently available to identify and isolate differentially expressed transcripts. These include differential display polymerase chain reaction (DDPCR), serial analysis of gene expression (SAGE), representative differential analysis (RDA), subtractive suppression hybridization (SSH) and cDNA microarray. One advantage of the SSH technique is the equalization of high- and low abundance messages, which allows for the identification of differentially expressed low abundance mRNAs. There is also a reported lower incidence of false positives for SSH as compared with DDPCR, especially when used for the identification of genes in tissues with many differentially expressed transcripts. After the isolation of sequences by SSH, their differential expression was verified by using rapid and high-throughput method of cDNA microarray (4).

The recently established radiation-induced breast carcinogenesis model based on MCF-10F cell lines irradiated with α-particles was used in these studies (5). The spontaneously immortalized human breast epithelial cell line MCF-10F was used as a control whereas Tumor-2 (passage 30), one of the three primary tumor cell lines derived from the previous tumorigenic cell line was used as an experimental cell lines for this study. Total RNA was extracted by TRIZOL reagent (Life Technologies, Inc., NY) and purified following usual procedures (6). Various cDNAs were synthesized and amplified from this purified total RNA with the help of SMART PCR cDNA synthesis kit (Clontech, Palo Alto, CA). The cDNAs were purified by the QIAquick Purification Kit (QIAGEN, Valencia, CA). The analysis was performed according to the PCR-Select cDNA Subtraction Kit (Clontech, Palo Alto, CA). Two SSH experiments were performed in parallel using different testers (i.e., containing the transcript of interest) and cDNA made from MCF-10F RNA used as driver. Briefly, each set of cDNA was submitted to a RsaI digestion to generate shorter, blunt-ended cDNA fragments. The tester cDNA was then subdivided into two portions and each was ligated with a different cDNA adaptor. Each adaptor had a different PCR primer annealing site. A first hybridization between an excess of driver and each sample of tester lead to equalization and enrichment of differentially expressed sequences. During the second hybridization, the two primary hybridizations were mixed together to generate templates for PCR amplification from differentially expressed sequences. The entire population of molecules was then subjected to two rounds of PCR to amplify these sequences. PCR products were then cloned by AdvanTAge PCR Cloning Kit (Clontech, Palo Alto, CA) and white colonies were selected and screened from LB agar plates containing antibiotic, X-Gal and IPTG (7). Plasmid DNAs were isolated and purified from all the subtracted clones and their DNA inserts were eluted by digesting with EcoRI.

Results from initial subtractive analysis identified about 32 positive clones (Figure 1). For further confirmation, these clones were digested with restriction enzyme EcoRI (Figure

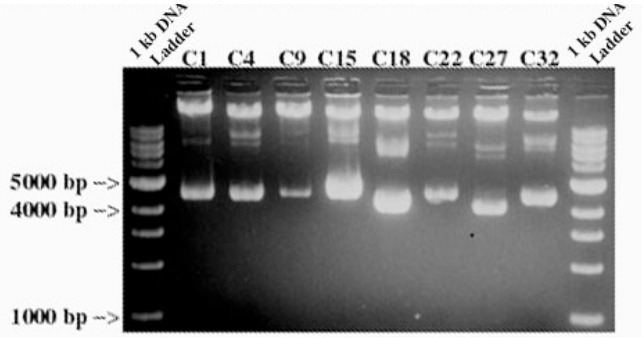

Fig. 1. Gel electrophoresis of some of the subtractive clones in the range of 4000-5000 bp in length (pTV-Adv vector 3.9 kb + ~ 400-1500 bp of inserts).

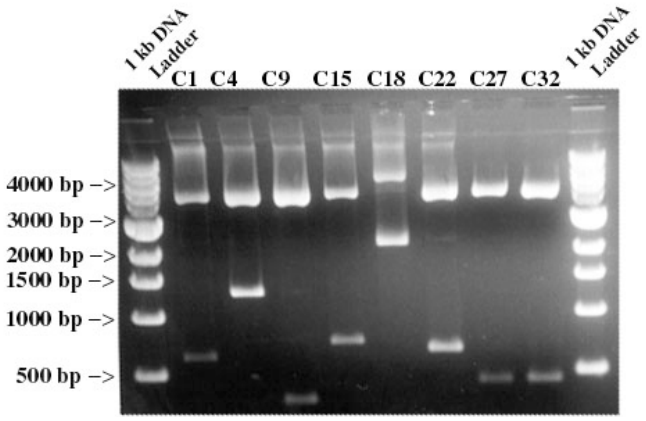

Fig. 2. Restriction digestion of subtractive clones by EcoRI show different inserts in the range of 400-1500 bp in length where pT-Adv vector is ~ 4000 bp in length.

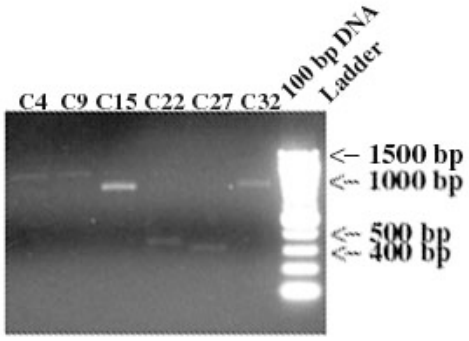

Fig. 3. Gel electrophoresis of few of the subtractive differentially expressed inserts in the range of ~ 400-1500 bp in length.

2). It was observed that out of 32 clones 30 clones contained an the insert with a size range between 400bp to 1500bp in length (Figure 3). Inserts obtained from these 30 clones were blotted onto nylon membrane for differential screening. Complete sequencing of these clones is in progress.

References

3. Lengauer C, Kinzler KW and Vogelstein B. Genetic instabilities in human cancers. *Nature (Lond)* **396**:643-9, 1998.
4. Smith HS, Lu Y, Deng G, Martinez O, Krams S, Ljung BM, Thor A and Lagios M. Molecular aspects of early stages of breast cancer progression. *J Cell Biochem* **17**G:144-52, 1993.
5. Dorosevich AE, Golubev OA, Abrosimov S and Bekhtereva IA. The role of cell communication in the pathogenesis of breast cancer. *Vopr Onkol* **44**:398-402, 1998.
6. Xie D, Jauch A, Miller CW, Bartram CR and Koeffler HP. Discovery of over-expressed genes and genetic alterations in breast cancer cells using a combination of suppression subtractive hybridization, multiplex FISH and comparative genomic hybridization. *Int J Oncol* **21**:499-507, 2002.
7. Calaf G and Hei TK. Establishment of a radiation- and estrogen-induced breast cancer model. *Carcinogenesis* **21**:769-76, 2000.
8. Sambrook J, Fritsch EF and Maniatis T. *Molecular Cloning - A Laboratory Manual*, Cold Spring Harbor Laboratory Press 1989.
9. Diatchenko L, Lau YFC, Campbell AP, Chenchik A, Moqadam F, Huang B, Lukyanov S, LuKyanov K, Gurskaya N, Sverdlov ED and Siebert PD. Suppression subtractive hybridization: A method for generating differentially regulated or tissue-specific cDNA probes and libraries. *Proc Natl Acad Sci (USA)* **93**:6025-30, 1996.

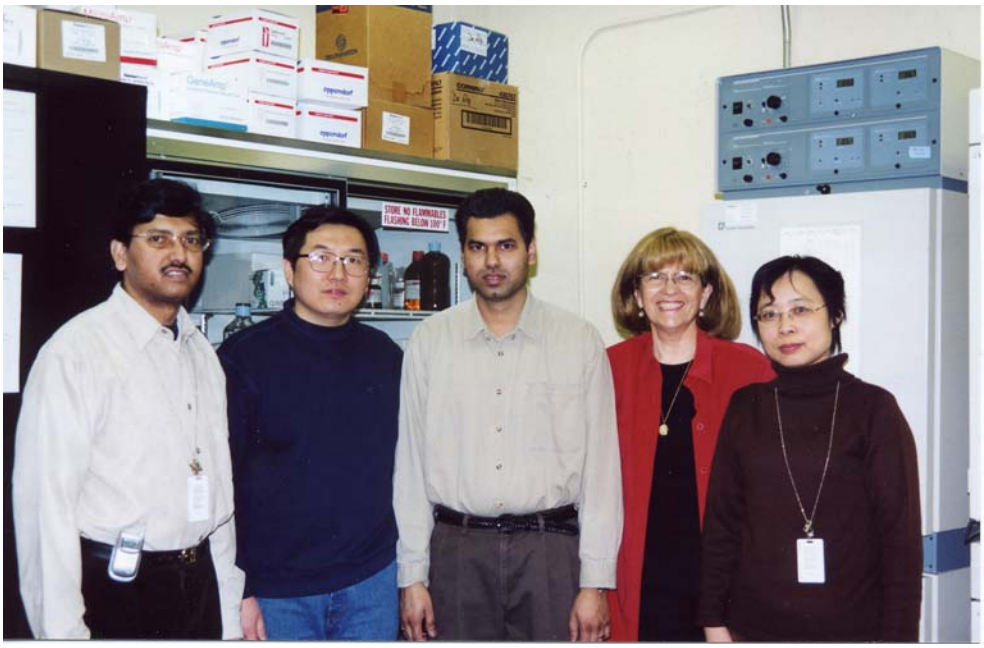

Dr. Debasish Roy, Dr. Hongning Zhou, Dr. Ravi Persaud, Dr. Gloria Calaf and Dr. Peng He.

ATM Heterozygous Mice are More Sensitive to Radiation Induced Cataracts than are Their Wildtype Counterparts

Basil V. Worgul,[1] Lubomir Smilenov, David J. Brenner, Anna K. Junk,[1] Wei Zhou[1] and Eric J. Hall

It is important to know whether the human population includes genetically predisposed radiosensitive subsets. In vitro studies have shown that cells from individuals homozygous for ataxia telangiectasia (A-T) are much more radiosensitive than cells from unaffected individuals. While cells heterozygous for the *ATM* gene (*ATM*+/-) may be slightly more radiosensitive in vitro it remained to be determined if the greater susceptibility of *ATM*+/- cells translates into an increased sensitivity for late effects in vivo, although there is a suggestion that radiotherapy patients, heterozygous for the *ATM* gene, may be more at risk of developing late normal tissue damage. We chose cataractogenesis in the lens as a means to assay for the effects of *ATM* deficiency in a late-responding tissue.

Descendents of breeding Atm knockouts kindly provided by Dr. Philip Leder (Harvard University) were used throughout the study. The genetic background of the mice is a cross of the 129SvEv and Black Swiss strains. The *ATM* gene was disrupted by inserting a neo cassette within an exon at a site corresponding to nucleotide number 5460 of the human *ATM*. There was no presence of full length or truncated protein in the *ATM* knockout mice. The *ATM* deficient mice display many characteristics associated with A-T, such as retarded growth, defective lymphocytic differentiation, neurological dysfunction and hypersensitivity to ionizing radiation. Heterozygotes on the other hand appear healthy. It is on the heterozygotes that we focused our attention since 1 to 3% of the human population are *ATM* heterozygotes and are clinically indistinguishable from the general population.

Mice were genotyped as wildtype Atm, heterozygous or knockout and one eye exposed to 0.5, 1.0, 2.0 or 4 Gy, with

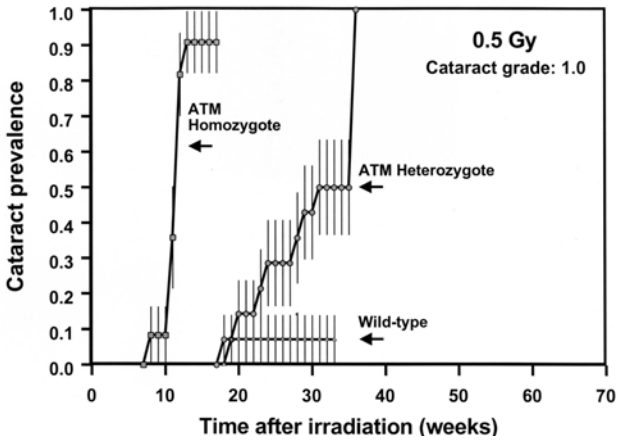

Fig. 1. Cataract prevalence (grade 1) as a function of time after exposure to 0.5 Gy in wild-type mice or in animals homozygous or heterozygous for the *ATM* gene. Note, that at this dose, the lowest used in this study, wild-type animals are essentially unaffected, while half of the AT heterozygotes develop a grade 1.0 cataract. The vertical bars are standard errors, calculated using Greenwood's formula.

[1] *Dept. of Ophthalmology, Eye Radiation & Environmental Health Laboratory, Columbia University.*

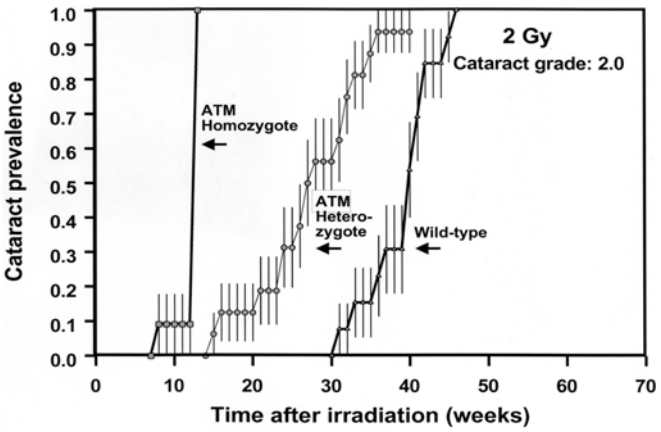

Fig. 2. Prevalence of cataracts of grade 2 (vision impairing) as a function of time following exposure to 2 Gy in wild-type mice and in animals homozygous or heterozygous for the *ATM* gene. The heterozygous animals develop grade 2 cataracts (vision impairing) about 10 weeks earlier than wild type animals. The vertical bars are standard errors, calculated using Greenwood's formula.

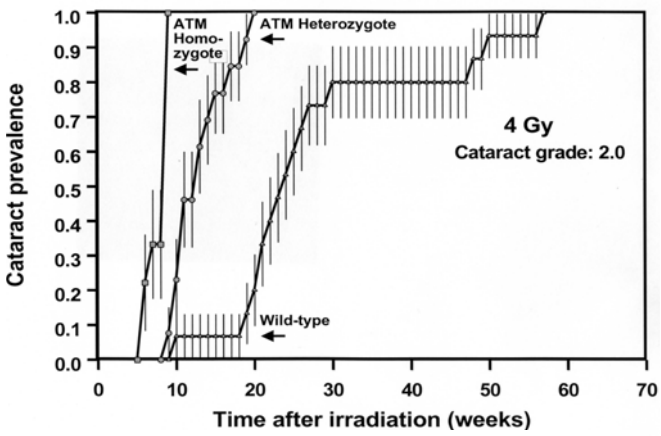

Fig. 3. Prevalence of cataracts of grade 2 (vision impairing) as a function of time after exposure to 4 Gy in wild-type mice and in animals homozygous or heterozygous for the *ATM* gene. The heterozygous animals develop grade 2 (vision impairing) cataracts about 10 weeks earlier than wild-type animals. The vertical bars are standard errors, calculated using Greenwood's formula.

the other eye serving as a control. The animals were followed weekly for cataract development by conventional slitlamp biomicroscopy. Cataract development in the animals of all three groups was strongly dependent on dose. The lenses of homozygous mice were the first to opacify at any given dose. Most important in the present context is that cataracts appeared earlier in the heterozygous versus wild-type animals, as shown in Figures 1-3.

The data strongly suggest that *ATM* heterozygotes in the human population may also be radiosensitive. This may influence the choice of individuals destined to be exposed to higher than normal doses of radiation, such as for example the astronauts, and may also suggest that radiotherapy patients who are *ATM* heterozygotes could be predisposed to increased late normal tissue damage. CRR

WEB-RAD-TRAIN

Web-Based Educational Program for Diagnostic and Interventional Radiologists: Radiobiology, Radiation Protection, and Risks vs. Benefits

http://www.web-rad-train.org

Carl D. Elliston, David J. Brenner and Eric J. Hall

The WEB-RAD-TRAIN is a web-based training course in radiation biology, radiation protection, and risk/benefit analysis, conceived and targeted primarily for radiologists, specifically radiologists in training who elect to study the biological foundations of radiology. This web-based teaching site is starting its second year in operation and currently presents eight topics. Within each topic there is a review of the pertinent material and links to books, articles, and other web sites for more in-depth coverage of the background information.

The centerpiece of this web-based training course is a series of review questions. Each topic contains five questions, typically framed in terms of an incident or situation in a radiology department. Once the student selects an answer, correct or incorrect, an explanation popup window appears to review the information needed or missed, succinctly, so that the correct answer is justified and the incorrect answers are eliminated.

Ultimately the WEB-RAD-TRAIN will present twelve topics, covering all aspects of radiation biology. The twelve Review Topics in the order in which they will be presented are:

I. Interactions of Radiation with Matter
II. DNA Damage / Chromosomal Aberrations / Cellular Response
III. Tissue Response to Radiation, Including Local Injury (Direct Effects)
IV. Factors Affecting Radiation Response
V. Whole-Body Radiation Effects
VI. Effects on the Developing Embryo and Fetus
VII. Hereditary Effects & Fertility
VIII. Radiation Carcinogenesis
IX. Radiation Cataractogenesis
X. Radiation Exposure to the Human Population
XI. Patient/Personnel Exposure; Risk-Benefit in Radiology
XII. Radiation Protection

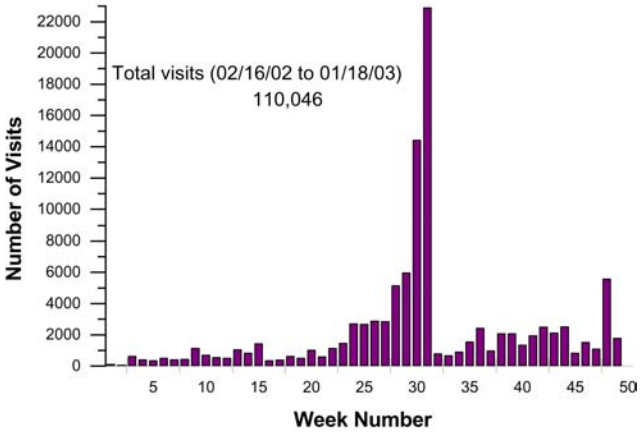

Fig. 1. The weekly number of files accessed on the WEB-RAD-TRAIN since its inception. Usage peaked just before the Board exams. (Courtesy of Richard Miller of the Radiological Society of North America).

An important aspect of the WEB-RAD-TRAIN is the acquisition of feedback from users. To achieve this, after a user has accessed the material for the first of the twelve topics, in order to access the remaining eleven topics, he/she is required to register and fill out a survey regarding the web site's structure and utility. We have documented the number of individuals who have thus far visited the site as a function of age, occupation, and education (M.D., Ph.D., etc.). In addition we have monitored the weekly number of visits to the site (Fig. 1). To date there have been over 100,000 visits to the WEB-RAD-TRAIN. Ride the WEB-RAD-TRAIN by visiting our web site: http://www.web-rad-train.org

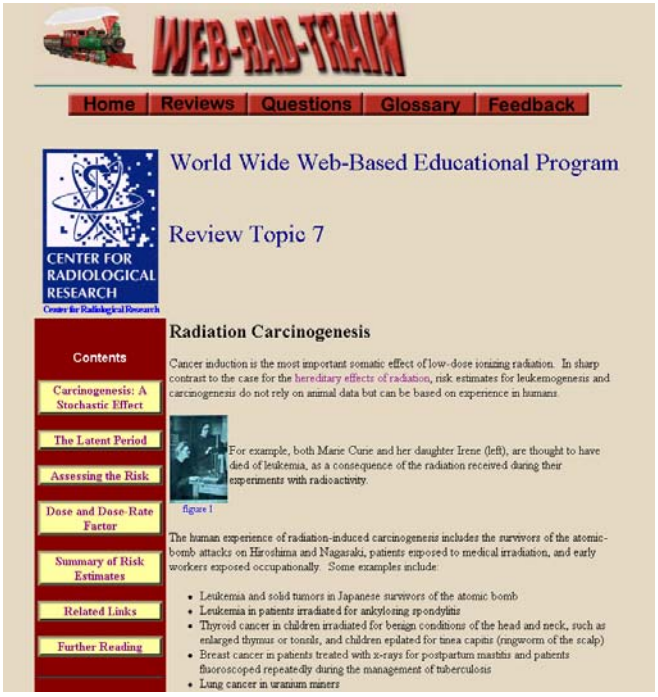

Screening Mammography: How Important is the Radiation-Risk Side of the Benefit-Risk Equation?

David J. Brenner, Satin G. Sawant,[1] Prakash Hande,[2] Richard C. Miller,[3] Carl D. Elliston, Gerhard Randers-Pehrson and Stephen A. Marino

There has been much recent debate about the benefits of routine screening mammography. However there has been rather less discussion regarding possible radiation-related risks associated with these examinations, specifically the risk of radiation-induced breast cancer, although some risk-benefit analyses have been reported.

Glandular examination doses for screening mammography are small, typically around 3 mGy of 26-30 kVp low-energy x-rays. A particular issue here, however, is that these very low-energy x-rays are expected to be more hazardous, per unit dose, than higher-energy x or gamma rays (i.e., those on which radiation risk estimates are based, such as from the Japanese A-bombs). The underlying biophysical reason for the expected increase in biological effectiveness for these lower-energy x-rays is that they set in motion slower secondary electrons, with correspondingly higher LET.

An increase in the relative biological effectiveness (RBE) of low-energy *vs.* high-energy photons is of relevance in assessing the risk side of the benefit-risk equation for mammography, in that the radiation-related risks are calculated based on studies of populations (A-bomb survivors and women who received multiple fluoroscopies) exposed to higher-energy photons.

We have measured *in-vitro* oncogenic transformation frequencies in $C_3H10T½$ cells, induced by monoenergetic x-rays in the 15 to 25 keV range, produced at the Brookhaven National Synchrotron Light Source (NSLS). Transformation data for 15.2 keV monoenergetic x-rays are shown in Fig. 1. Using linear-quadratic fits (see Fig. 1) to the low-dose data, we estimate a low-dose RBE (ratio of alpha terms) of 1.96±0.78 for 15.2-keV x-rays *vs.* 662-keV ^{137}Cs gamma rays. While these experiments are still in progress, in no case have we estimated a low dose RBE (defined, as above, as the ratio of alpha terms) of greater than 1.5 relative to 250-kVp x-rays (0.2 mm Cu, 1 mm Al external filtration), or greater than 2.5 relative to ^{137}Cs gamma rays.

These fairly modest RBE estimates are consistent with the earlier experimental data, as well as theoretical estimates (1) of 1.3 (*vs.* 250-kVp x-rays) and 2.0 (*vs.* gamma rays at Hiroshima and Nagasaki), for the low-dose RBE of 23-kVp filtered x-rays. The reason for the comparatively small predicted enhancements in effectiveness at mammographic x-ray energies is that the differences in energy deposition patterns between the higher and the lower-energy photons are relatively subtle.

We stress, however, that even if the risks per unit dose of mammographic x-rays are just twice as large as those from the radiations at Hiroshima and Nagasaki, this would be of some significance. For example, Fig. 2 shows the age-dependent risk-benefit ratio, as estimated in NCRP Report 85 (1986) for 5 annual mammograms, each producing a glandular dose of 2 mGy. Here the "benefit" is assumed to be a 10% decrease in mortality, and the excess relative risk of radiation-related breast cancer was appropriately derived from studies of the Japanese A-bomb survivors. Now if it is assumed that mammographic x-rays are twice as hazardous, per unit dose, than the radiations at Hiroshima and Nagasaki, the benefit-risk ratio would also be decreased, by this same factor of 2.

As illustrated in Fig. 2, such a reduction in the benefit-risk ratio would be reflected in the age at which commencement of annual breast screening is recommended. For example, the American Cancer Society recommendation to begin annual screening at age 40 corresponds to the age when the estimated benefit-risk ratio reaches an acceptable value (numerically equal to 7 in Fig. 2). If the benefit-risk ratio were halved, because the radiation risk was twice that previously estimated, then the age above which this same benefit-risk ratio is reached would be increased (see Fig. 2), in this case from age 40 to 47. Similarly, if annual screening were recommended from age 50 (NIH consensus panel, 1997),

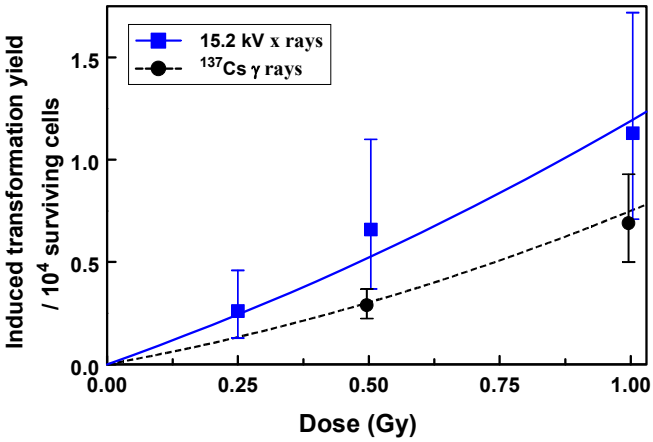

Fig. 1. Measured induced oncogenic transformation frequencies per 10^4 surviving $C_3H10T½$ cells, as a function of the dose of 15.2-kV monoenergetic x-rays and 662-keV ^{137}Cs gamma rays. Estimated 68% confidence limits are shown. For clarity, only low-dose data points are shown. Curves represent fits to the full data set using the model $TF_{15keV}=\alpha_{15keV}D+\beta D^2$ and $TF_{662keV}=\alpha_{662keV}D+\beta D^2$, where α_{15keV}= 0.90±0.15 Gy^{-1}, and α_{662keV}= 0.46±0.11 Gy^{-1}.

[1] *Current Address: Amgen Inc., Thousand Oaks, CA.*
[2] *Department of Physiology, National University of Singapore.*
[3] *Radiological Society of North America, Oak Brook, IL.*

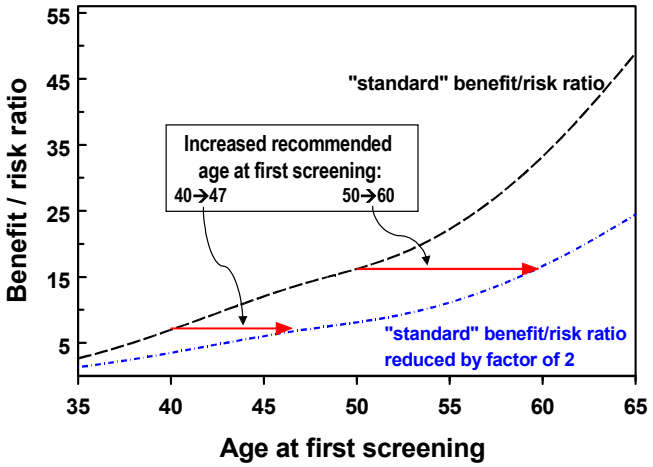

Fig. 2. *Dash curve:* Estimated benefit-risk ratio for yearly mammographic screening examinations for 5 years, assuming a total glandular dose of 2 mGy per exam (NCRP Report 85, 1986). The benefit is assumed to be a 10% reduction in breast cancer mortality, and the excess relative risk for radiation-induced breast cancer was assumed to be 2.2×10^{-4}/mGy.

Dot-dash curve: Corresponding benefit-risk ratio in which the estimated radiation risk is doubled, to account for an increased risk per unit dose of about 2 for low-energy mammographic x-rays

Arrows indicate the increase in age at which a given benefit-risk ratio would be achieved, assuming the radiation risk were doubled; these suggest that recommended starting ages for routine mammography might reasonably be increased, if the radiation risk from mammographic x-rays was larger than that previously assumed.

doubling the radiation risk, while keeping fixed the benefit-risk ratio for commencement of screening, would imply an increase in the recommended age to begin screening, from age 50 to about 60 (Fig. 2). Similar quantitative conclusions are obtained if other estimates of the age-dependent benefit-risk ratio for mammographic screening are re-analyzed by doubling the radiation risk.

In summary, there is evidence that low-energy x-rays as used in mammography have an increased biological risk relative to higher-energy photons. However the RBE values are not large, probably less than a factor two. Thus it is extremely unlikely that the radiation risk alone could prove to be a "show stopper" regarding screening mammography because, for older women, the benefit is still likely to considerably outweigh the radiation risk. For women below 50, however, this increase in the estimated radiation risk might suggest a somewhat later age than currently suggested, by about 5 to 10 years, at which to recommend commencement of routine breast screening.

References

1. Brenner DJ, Amols HI. Enhanced risk from low-energy screen--film mammography X rays. *Br J Radiol* **62**:910-4, 1989.

The Impact of IMRT on the Incidence of Radiation-Induced Second Cancers

Eric J. Hall and Cheng-Shie Wuu[1]

Intensity Modulated Radiotherapy (IMRT) represents the latest effort to tailor dose distribution to conform more closely to the tumor outline and so to minimize the volume of normal tissue receiving the higher doses. It typically employs a larger number of fields, and the use of multi-leaf collimators allow field sizes to be shaped and changed over time. This complex plan replaces the relatively simple four-field box technique used in the past. The hope is that tumor control will be increased because doses can be escalated, and normal tissue morbidity decreased. The expected gains remain an expectation but have not yet been proven in practice. Meanwhile, there is some concern that IMRT may have a down-side in terms of an increase in the incidence of radiation induced cancers. This may result from two sources.

First, delivery of a specified dose to the isocenter from a modulated field, delivered by IMRT, will require the accelerator to be energized for longer by a factor of 2 to 3 (hence more monitor units are needed) compared with delivering the same dose from an unmodulated field. The total body dose due to leakage radiation will therefore be at least doubled. This may result in a doubling of the incidence of second cancers from 0.25% to 0.5% (assuming a risk estimate for fatal cancer of 1%/Sv in elderly patients).

Second, there is likely to be an increased incidence of radiation induced cancers for IMRT compared with conventional techniques due to the different dose distribution. IMRT exposes a larger volume of normal tissue to lower doses which might be expected to result in more radiation-induced tumors. The impact of this change is difficult to assess since it depends on the shape of the dose response relationship for radiation induced carcinomas in the dose range from 10 to 70 Gy. At doses of a few Gy, good esti-

[1] *Dept. of Radiation Oncology, Columbia University.*

mates are available from the Japanese survivors, but data for higher doses are uncertain. The best estimate is that IMRT will result in a 0.5% increase in second cancers due to this cause.

In summary, the increased monitor units and the modified dose distribution may result in an extra 0.75% of surviving patients developing a radiation induced malignancy. This approximately doubles the rate seen in patients treated by conventional techniques. This is the price which must be offset against the gains expected from improved tumor control.

Radiation Risks Associated with CT Screening of Smokers for Lung Cancer

David J. Brenner

There is increasing interest in the possibility of using low-dose computed tomography (CT) scans for annual screening of smokers and former smokers for early-stage lung cancer. Several pilot studies have already taken place, showing an increased capability for detecting small malignant nodules, and a National Lung Screening Trial is now underway.

Whilst the potential benefits of lung cancer screening have been much debated, less attention has been paid to the potential risks, specifically radiation-induced lung cancer, associated with the radiation from these CT scans. In part this is because the screening technique involves "low dose," rather than standard, CT lung scans, and in part this is because excess relative risks (ERR) of radiation-induced cancer generally decrease markedly with increasing age. There are, however, several indications that the radiation risk to the lung associated with this screening technique may not be insignificant: Cancer risks from radiation are generally multiplicative of the background cancer risk, which is, by definition, high for lung cancer in the target population here. In addition, while radiation-related cancer risks do generally decrease markedly with increasing age at exposure, the ERR for radiation-induced lung cancer does not follow this pattern, and does not decrease significantly through adulthood.

These considerations suggest that risk of radiation-induced lung cancer associated with the radiation from repeated CT scans of the lung may not be negligible. We report here on estimates of these risks, and use these to define the minimum benefits from annual CT screening which will be necessary to outweigh these potential radiation risks.

These estimated radiation dose- (D), gender- (G), and smoking-status- (S) dependent low-dose / low-dose-rate excess relative risks (ERR) of lung cancer in a US population were used to calculate the excess lung cancer risk, R_{CT}, associated with a single individual CT lung scan at a given age (A):

$R_{CT}(A, G, S) = ERR(D, G, S) \times D_{CT} \times B(A+10, G, S) \times P_{10}(A)$, where D_{CT} is the lung dose for a single CT scan (see below), $B(A, S, G)$ is the lifetime lung-cancer risk for an individual alive at aged A (US tumor registries data with adjustments for smoking status), and $P_{10}(A)$ is the probability of living at least 10 years from age A. This approach essentially assumes a latency period of 10 years after each radiation exposure before any risk is manifest. 95% credibility intervals associated with these risk estimates were also estimated, combining estimates of the various individual sources of uncertainty (such as in the risk transfer from Japanese to U.S. populations, and in dose-fractionation effects) that contribute to the overall credibility limits.

Low dose CT lung scans use an exposure setting in the range from 30 to 100 mAs, with the National Lung Screening Trial recommending 60 mAs. We have used a direct measurement by Nishizawa et al (1) scaled to a 60 mAs setting, yielding a dose to the lung of 5.2 ± 0.9 Sv.

Fig. 1 shows the estimated lifetime radiation-related lung-cancer risks, R_{CT}, summed for a series of annual low-dose CT scans starting at age A and ending at age 75. For example, a 50 year old female current smoker who plans annual low-dose screening CT lung scans starting in 2002, would accrue an estimated excess lung cancer risk, associated with the total radiation exposure, of about 0.72% [95% C.I. 0.24 – 1.9%]; this is in addition to her otherwise expected lung cancer risk of about 11.5%. The corresponding estimated radiation-related excess lung cancer risk for 50 year old male smoker currently planning annual low-dose CT screens is 0.24% [95% C.I. 0.06 – 0.66%], in addition to his expected lung cancer risk of about 16%.

Fig. 2 shows the predicted numbers of radiation-related lung cancers in the population, assuming that 50% of the current smoking and former-smoking US population above a given age receive annual low-dose lung CT scans, starting in 2002, until age 75. Thus, for example, if the entire ever-smoking current population US population aged between 50 and 75 (about 39,000,000 individuals) were offered annual CT screens up to age 75, with a 50% compliance rate the estimated number of lung cancers associated with the radiation from these scans would be about 14,000 [95% C.I.: 4,400 – 36,400].

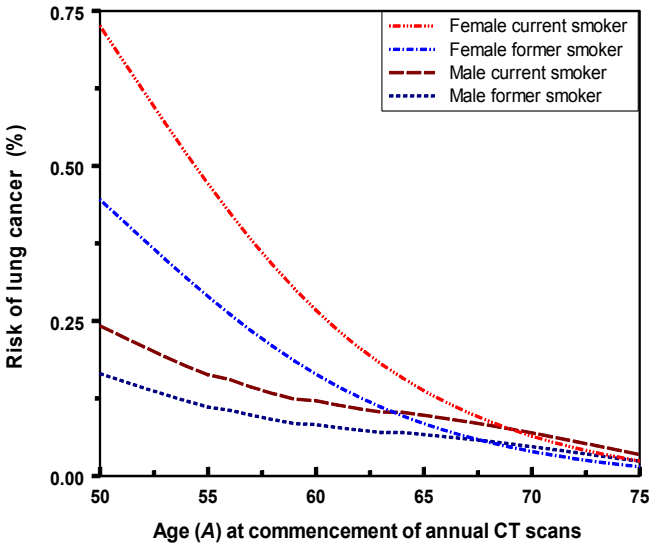

Fig. 1. Estimated risks of lung cancer associated with the radiation from annual low-dose CT lung scans. Annual scans are assumed to commence in 2002 at age *A* and continue till age 75. Estimated 95% credibility limits are approximately a factor of 3 in either direction. Risks were estimated using a lung dose of 5.2 mSv; risks for other doses can be proportionately scaled according to the dose.

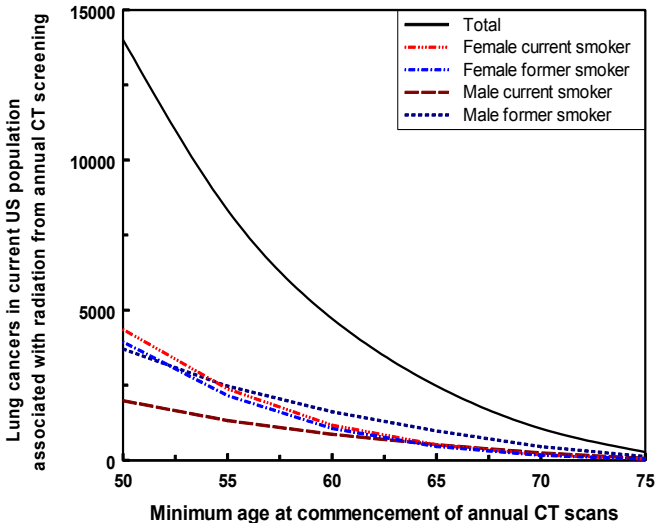

Fig. 2. Predicted numbers of lung cancers in the current US population associated with the radiation from annual low-dose CT lung scans. Assumed is that 50% of the current smoking and former-smoking population received annual low-dose CT scans at the given age until age 75. These results can be linearly scaled for different doses, different compliance rates and, approximately in North American and Western European populations, different population numbers in the four smoking categories here.

While baseline screening would result in fairly small radiation risks, yearly screening from aged 50 would add about 0.5% to the ~14% lung cancer risk faced by a 50 year old ever smoker. The estimated radiation-associated risks can, of course, only be assessed in the context of the potential benefits of CT lung cancer screening. Of the 50% of the current 50 to 75 year old ever-smoking US population who are assumed here to undergo annual CT lung scans, about 1,300,000 would be expected to develop lung cancer, independent of the radiation. An additional 14,000 radiation-associated lung cancer cases thus represents about a 1.1% [95% C.I.: 0.4% - 2.8%] increase. At this time, the magnitude of the potential mortality benefit from screening adult ever smokers with CT is not yet established, but a mortality benefit of considerably greater than 3% in the screened population would potentially be necessary to appropriately outweigh these estimated radiation risks.

References

1. Nishizawa K, Iwai K, Matsumoto T, Sakashita K, Iinuma TA, Tateno Y, Miyamoto T, Shimura A and Takagi H. Estimation of the Exposure and a Risk-Benefit Analysis for a CT System Designed for a Lung Cancer Mass Screening Unit. *Radiat Protec Dosim* **67**:101-8, 1996. CRR

What Protocols are Appropriate for Clinical Trials of Hypofractionated Prostate Radiotherapy?

David J. Brenner, Jack F. Fowler,[1] Mark A. Ritter[1] and Rick J. Chappell[1]

Motivated by radiobiological concepts originating *in vitro*, recent analyses of clinical results have suggested that the fractionation sensitivity of prostate tumors is remarkably high; corresponding point estimates of the α/β ratio for prostate cancer are around 1.5 Gy, much lower than the typical value of 10 Gy for most other tumors. This low α/β value is comparable to the nominal α/β value of 3 Gy for surrounding late-responding tissues, suggesting that logistically-convenient hypofractionated schemes could be designed for prostate cancer with no loss in tumor control or increase in

[1] *University of Wisconsin, Madison, WI.*

late effects. An even more advantageous scenario arises if the α/β ratio for prostate tumors was actually significantly *less* than that for late rectal complications; in fact there is credible evidence that α/β for late rectal complications might actually be somewhat higher – in the 4-5 Gy range, due to contributions from "consequential" late effects which originate from tissue with high α/β values. If the α/β value for prostate is really less than for late-responding rectal damage, hypofractionated regimens could be designed with fewer but larger dose fractions (and, of course, a lower total dose), to maintain equivalent late sequellae whilst yielding improved tumor control. One would also expect less acute sequellae and less "consequential" late effects, provided that overall time is not shortened too drastically.

The low α/β ratio for prostate relative to that for the surrounding late-responding normal tissue gives the potential for therapeutic gain, and we analyze here possible protocols for prostate cancer to test this suggestion. Using standard linear-quadratic (LQ) modeling, a set of high-gain/low-risk hypofractionated protocols can be designed in which a series of dose steps is given, each step of which keeps the late complications constant in rectal tissues. This is done by adjusting the dose per fraction and total dose to maintain a constant level of late effects. The effect on tumor control is then investigated.

If the α/β value for prostate is less than that for the surrounding late-responding normal tissue, the clinical gains can be rather large. For example, 10 fractions, each of 4.4 Gy, are predicted to give about the same tumor control as 75 Gy in 2 Gy fractions, *but with the same late complications as 66 Gy in 2 Gy fractions*; in this case, the estimated bNED for tumors has increased from 51.6% (with 33F × 2 Gy) to 77.1% (with 10F × 4.44 Gy), so the therapeutic ratio has been increased substantially. This possible increase in bNED would require a clinical trial with two arms of 72 patients in each, to have a 90% power of demonstrating the difference. In this particular protocol, one-third of the number of fractions would have to be delivered, no increase in late complications would be expected, and the early sequellae rate would be expected to decrease. An overall time not shorter than 5 weeks appears advisable, at least initially, for the hypofractionation schedules considered, because of a possible risk of acute or consequential late reactions in the rectum. Sensitivity tests suggest that, even if the prostate tumor α/β ratio turns out to be the same (or even slightly larger than) the surrounding late-responding normal tissue, these hypofractionated regimens would be very unlikely to result in significantly increased late effects.

The hypofractionated regimens that we suggest be tested for prostate-cancer radiotherapy have high potential therapeutic gain as well as economic and logistic advantages. They appear to have little potential risk and considerable potential for therapeutic gain, as long as excessively short overall times (<5 weeks) and very small fraction numbers (<5) are avoided. CRR

Dietary Supplements and Radiation Therapy: Effects of Lycopene and Vitamin E on Prostate Cancer Cells

Jill Rossinow,[1] Adayabalam S. Balajee, Richard M. Gewanter,[2] Ronald D. Ennis,[2] Peter B. Schiff,[2] Aaron E. Katz[3] and Charles R. Geard

Lycopene and alpha-tocopherol (Vitamin E) are both among the potent dietary antioxidants being investigated for their potentially protective role against the formation of free radical-induced mutagenesis involved in the development of cancer. In particular, lycopene – a biological carotenoid found in high concentration in tomatoes, watermelon, apricots, guava, rosehips and pink grapefruit – has been shown to be an extremely efficient quencher of singlet oxygen radicals, with a quenching rate of more than double that of beta-carotene.

Studies investigating the correlation between lycopene intake and prostate cancer have shown that increased dietary intake of tomato-based products increases serum levels of lycopene, and that healthy men with elevated serum lycopene have a decreased risk of developing prostate cancer, particularly aggressive, extraprostatic tumors.

These findings have led to brand name vitamin manufacturers promoting products that are supplemented with lycopene and other antioxidants, including Vitamin E, selenium and zinc, in an effort to advance prostate health in their consumers.

However, in men already diagnosed with prostate cancer who are being treated with radiation therapy, the effect of dietary antioxidants is unclear. Because the effectiveness of radiotherapy is believed to depend upon radiation-induced free radical formation and the subsequent oxidative damage caused to cancer cell DNA, dietary antioxidants taken during radiation therapy may decrease this therapy's potency and ability to kill malignant cells.

Studies investigating the effect of lycopene on cells have

[1] *Albert Einstein College of Medicine, New York, NY.*
[2] *Department of Radiation Oncology.*
[3] *Department of Urology.*

been somewhat variable, showing it to have both anti-oxidant and pro-oxidant properties. In contrast with the variable effects observed with lycopene in vitro, Vitamin E demonstrates more consistent trends, appearing to be harmful to cancer cells, but protective of normal cells.

In this study, a clonogenic survival assay and micronucleus assay were performed on DU-145, PC3, and LNCaP prostate cancer cell lines in vitro to determine the effect that lycopene and Vitamin E may have on survival and DNA damage in gamma-irradiated prostate cancer cells.

DU-145 cells were grown in DMEM, and PC-3 and LNCaP cells were grown in RPMI, all containing 1% streptomycin-penicillin and 15% FBS. Cells were seeded into 4 cm petri dishes, and were incubated at 37˚C for 24 hours. Dishes were then treated with lycopene at 4.0 μM and 7.2 μM, Vitamin E at 50 μM, and a combination of Vitamin E (50 μM) and lycopene (4.0 μM for PC3 cells; 7.2 μM for DU-145 and LNCaP cells). Controls were done for untreated media, 0.4 % THF (corresponding to lycopene of 4.0 μM), 0.7% THF (corresponding to lycopene of 7.2 μM) and 0.05% ethanol (corresponding to Vitamin E of 50 μM). Once treated, cells were incubated for three hours before irradiation with 137Cs gamma rays (1.1 Gy/min) at doses of 0, 0.5, 1, 2, 4, 6 and 8 Gy. DU-145 cells were then incubated for 9 days, LNCaP cells for 18 days, and PC3 cells for 21 days at 37˚C, allowing colonies to become large enough to be counted without magnification. Colonies were then fixed with 70% ethanol, stained with crystal violet, and counted. All dishes were done in triplicate for each cell line.

For the micronucleus assay cytochalasin B at a concentration of 3 μg/ml of PBS was added to dishes immediately after irradiation. DU-145 cells were harvested after 30 hours of incubation with cytochalasin B, and PC3 and LNCaP cells after 80 hours of incubation, to allow for the difference in cell cycle timing between cell lines. To prepare the binucleated cells, cells were trypsinized, treated with cold (4˚C) hypotonic (0.075 M) KCl, and centrifuged at 800 rpm for 8 minutes, without disturbing the pellet. Leaving only 2.5 ml of supernatant, 7.5 ml of 3:1 methanol: acetic acid fixative and 4 drops of formaldehyde (a preservative) were then added to each tube, drop by drop, and tubes were again centrifuged at 800 rpm for 8 minutes. Tubes were treated with two more cycles of 3:1 methanol: acetic acid fixative and centrifugation at 1000 rpm for 8 minutes, breaking up the pellet. The fixed cell solution was then placed on slides and allowed to air dry before staining with Acridine Orange (0.03 mg/ml in PBS) and scoring via fluorescent microscopy.

Lycopene clearly protects prostate cancer cells against gamma radiation-induced DNA damage in the form of decreased micronuclei formation, resulting in a significant increase in survival in both androgen-sensitive and androgen-insensitive cell lines. In contrast, vitamin E dramatically enhances gamma radiation-induced apoptosis in prostate cancer cells, leading to a significant reduction in survival in both androgen-sensitive and androgen-insensitive cell lines. The impact of these antioxidants on survival was maintained in both non-irradiated cells, and irradiated cells across a broad spectrum of radiation doses which included doses typically used in radiation therapy.

The inclusion of the micronucleus assay was essential to this study for several reasons. First, the micronucleus assay successfully provided both a mechanism, as well as corroboration, for the results of the survival assay in both Vitamin E- and lycopene-treated cells. While the survival assay clearly showed Vitamin E to significantly decrease survival in all three treated prostate cancer cell lines, this was explained and supported by a dramatic increase in the percentage of apoptotic cells, as well as a modest increase in the percentage of micronucleated cells. Additionally, while lycopene was shown to increase survival in DU-145 and LNCaP cells, this was supported by a significant decrease in the percentage of micronucleated cells seen.

This study's findings, that Vitamin E inhibits growth and induces apoptosis in gamma-irradiated prostate cancer cells, are a consistent addition to the published literature. However, in contrast to previous studies demonstrating lycopene to inhibit growth and survival in cancer cells, the protective effect seen with lycopene in gamma-irradiated prostate cancer cells is unique to this study.

The absolute impact that lycopene and Vitamin E had on survival and DNA damage varied, both among the different cell lines, and with respect to one another. In general, Vitamin E appeared to have a greater impact on decreasing survival than lycopene did on increasing survival. Vitamin E not only decreased survival in all three cell lines (as compared to lycopene increasing survival in only the DU-145 and LNCaP cells), but Vitamin E's effects were greater in each cell line than lycopene.

The findings of this study, that lycopene protects prostate cancer cells in vitro against gamma radiation-induced DNA damage leading to an increase in cell survival at clinically-relevant radiation doses, raises a query at this time about the use of dietary lycopene supplements in men with prostate cancer undergoing radiation therapy. Although it cannot be claimed from these findings that the protective role observed in lycopene-treated cells in vitro would necessarily translate into a survival advantage for prostate cancer cells treated with radiation therapy in human subjects, the deficiency of literature in this area reflects the lack of knowledge regarding the role of dietary antioxidants in this population of patients. In addition, the different effects observed in other studies between purified and oxidized lycopene may have clinical implications, making it important to verify which form of lycopene is present in tomato-based products and vitamin supplements available to consumers.

Conversely, the findings of this study that Vitamin E decreases survival in irradiated prostate cancer cells in vitro by the induction of apoptosis may hold clinical promise in the future for Vitamin E supplementation during radiation therapy. Particularly when considered in the context of the findings of others that such an effect is not seen in normal cells. Additional studies are certainly warranted at this time to more definitively clarify the impact that antioxidant supplementation may have on the effectiveness of radiation therapy for prostate cancer, and to determine whether oncologists should recommend Vitamin E and lycopene supplementation during radiation therapy. CRR

The Radiological Research Accelerator Facility

AN NIH-SUPPORTED RESOURCE CENTER – WWW.RARAF.ORG

Director: David J. Brenner, Ph.D., D.Sc.
Manager: Stephen A. Marino, M.S.
Chief Physicist: Gerhard Randers-Pehrson, Ph.D.

Research Using RARAF

The "bystander" effect, in which only some cells are irradiated and a response is obtained that is greater than would be expected for the fraction irradiated remains of great interest. Several experiments examining this effect were continued, observing a variety of endpoints to determine the size of the effect and the mechanism by which it is transmitted. There is evidence for both direct cell-cell communication through cell membranes and indirect, longer-range communication through some release by the cells into the cell medium. In some experiments, the unirradiated cells can be identified due to a different staining and scored directly. In other experiments, unirradiated cells are physically separated from the irradiated cells. Both the microbeam and the track segment facilities continue to be utilized in various investigations of this phenomenon. The single-particle microbeam facility provides precise control of the number and location of particles but is somewhat limited in the number of cells that can be irradiated. The track segment facility provides broad beam irradiation that has a random pattern of charged particles but allows large numbers of cells to be irradiated.

In Table I are listed the experiments performed at RARAF from May 1, 2001 through April 30, 2002 and the number of days each was run in this period. Fourteen different experiments were run during this 12-month period, about the same as the average for 1996-2001. Eight experiments were undertaken by members of the CRR, supported by grants from the National Institutes of Health (NIH) and the Department of Energy (DOE). Six experiments were performed by outside users, supported by grants and awards from the NIH, NASA, the Department of Defense (DoD), the University of Toronto and the Ministry of Education, Science, Sports and Culture of Japan. Brief descriptions of these experiments follow.

Investigations involving the oncogenic neoplastic transformation of mouse C3H 10T½ cells (Exp. 73) were continued by Eric Hall and Stephen Mitchell (who has replaced Satin Sawant) of the CRR. Using the microbeam facility, 10% of the cells were irradiated through the nucleus with 2 to 12 helium ions. Cells were plated at densities of approximately 200 and 2000 per dish to try to observe the relative contribution of cell-cell communication to the bystander

Table I

Experiments Run at RARAF May 1, 2001 - April 30, 2002

Exp. No.	Experimenter	Institution	Exp. Type	Title of Experiment	Days Run
73	S. Mitchell, E.J. Hall	CRR	Biology	Neoplastic transformation of C3H10T½ cells by specific numbers of α particles	1.0
76	A. Xu, T.K. Hei	CRR	Biology	Mutation at the S1 locus of human-hamster hybrid (A_L) cells by specific numbers of alpha particles	2.0
89	R.H. Mauer, et al.	Johns Hopkins Univ.	Physics	Calibration of a portable real-time neutron spectrometry system	3.5
94	B. Ponnaiya, C.R. Geard	CRR	Biology	Single cell responses in hit and bystander cells: single-cell RT-PCR and protein immunofluorescence	12.0
96	J. Zimbrick, J. Katanic	Purdue Univ.	Chemistry	Response of tooth enamel to neutrons	2.5
101	K. Komatsu (Zhou)	Hiroshima Univ.	Biology	Bystander effect of *Ataxia Telangiectasia* cells	1.0
103	G. Jenkins, C.R. Geard	CRR	Biology	Damage induction and characterization in known hit versus non-hit human cells	18.0
106	B. Ponnaiya, C.R. Geard	CRR	Biology	Track segment alpha particles, cell cocultures and the bystander effect	8.0
108	H. Zhou, T.K. Hei	CRR	Biology	Modulation of adaptive response in alpha-particle-induced bystander effects	10.5
109	A. Balajee, C.R. Geard	CRR	Biology	DNA damage induction in microbeam-irradiated cells assessed by the comet assay	7.0
110	H. Zhou, D. Roy T. K. Hei	CRR	Biology	Identification of molecular signals of alpha particle-induced bystander mutagenesis	25.0
111	R. Bristow, S. Al Rashid	University of Toronto	Biology	Visualization of the localization of repair proteins after microbeam irradiation	2.0
112	Y. Horowitz, M. Zaider	Ben Gurion Univ., Memorial Sloan Kettering	Physics	HCP and neutron irradiation of LiF:Mg, TI TLD chips to determine 5a/5 intensities and characterization of 5a peak as a Q/RBE nanodosimeter	6.5
113	A. Miller	AFRRI	Biology	Role of alpha particle radiation in depleted uranium-induced cellular effects	0.5

Note: Names in parentheses are CRR members who collaborated with outside experimenters.

effect. Cell survival was about the same for both cell densities for two particles, but for 12 particles the lower density has a survival of 90% while the higher density has a survival of only 75%. This would imply little or no bystander effect at low density (only the 10% of cells hit die) but a large effect at high density where 2.5 times as many cells as were hit don't survive.

Studies of the mutation of hamster hybrid (A_L) cells by specific numbers of helium ions (Exp.76) were extended by An Xu and Tom Hei of the CRR to protons. These irradiations were only preliminary because protons that have a range less than that of the collimator thickness have such a low momentum that they are scattered more easily than the helium ions that are normally used. This increases the effective diameter of the beam at the cell position so that it may be larger than the diameter of the cell nuclei. These experiments will resume as soon as the focused microbeam, which will produce a beam 2.5 μm in diameter for both helium ions and protons, is operational.

Richard Mauer, David Roth and James Kinnison of Johns Hopkins University continued development of a neutron spectrometer for the energy range 0.5 to 100 MeV (Exp. 89). The spectrometer will be used on the International Space Station and the manned mission to Mars. Emphasis is now on determining the efficiencies of the detectors at different neutron energies and investigating the rise times of the pulses generated by gamma rays and neutrons to perform gamma-ray discrimination. In addition, a CCD camera was irradiated with 2.2 MeV neutrons to determine its resolution as a function of neutron fluence. The camera is being considered for a probe that will be sent to Pluto and the asteroid belts beyond. Because solar panels will not be able to produce enough energy that far from the sun, a Radioactive Thermal Generator will be used, producing a spectrum of neutrons with a mean energy of approximately 2.2 MeV. The long-term exposure to neutrons raised questions of the survival and the resolution of the camera.

Brian Ponnaiya and Charles Geard of the CRR continued two studies investigating the bystander effect. In one study (Exp. 94), single cells are observed for gene expression using reverse transcription polymerase chain reaction (RT-PCR) in conjunction with immunofluorescence techniques. This procedure permits observation of individual responses to radiation instead of just the average response of a large number of cells. Irradiated and unirradiated cells can be identified by a differential staining administered prior to irradiation. Individual cells are selected using a micromanipulator on the off-line microscope system of the microbeam facility. Copies of DNA segments are created by reverse transcription (RT) from mRNA produced by each cell. The DNA is then amplified by polymerase chain reaction (PCR) until enough material is available for gel electrophoresis to measure the amount of mRNA. Immunofluorescent staining is used to determine the amount of the protein associated with a particular mRNA for corroboration. Based on previous results indicating the induction of p21/WAF1 in irradiated and bystander normal human fibroblasts, microbeam experiments were conducted to standardize protocols for the analyses of other early response genes. The other investigation involves use of the track segment facility for broad-beam charged particle irradiations of human fibroblasts and epithelial cells immortalized with telomerase (Exp. 106). Special cell dishes are made from stainless steel rings with thin Mylar windows epoxied on both sides. Cells are plated on both inner Mylar surfaces and the dish volume is filled with medium. This eliminates all possibility of cell-cell contact between cells on opposite sides. Cells on one surface are irradiated with ^{4}He ions; cells on the opposite surface are unirradiated because the particles are stopped before reaching them. Cells are observed *in situ* after irradiation with doses from 0.1 to 10 Gy of 125-keV/μm ^{4}He ions. Plateau phase cells are scored for cell cycle delay and micronucleus production while log phase cells are scored for chromosomal aberrations. It was observed that irradiated fibroblasts can induce micronuclei in bystander fibroblasts, but bystander epithelial cells are refractory to irradiated epithelial cells. Furthermore, epithelial cells are capable of responding to irradiated fibroblasts, which results in the induction of micronuclei in the bystander epithelial cells. Chromosomal analyses of irradiated fibroblast populations and bystander cells at the first cell division post irradiation demonstrated the induction of gross chromosome aberrations in the irradiated population and chromatid aberrations (of the simple type –breaks and gaps) in the bystander population. Elevated yields of similar types of chromatid type aberrations were also observed in both irradiated and bystander fibroblast populations up to 20 population doublings post irradiation.

Studies of the response of tooth enamel to neutrons (Exp. 96) were continued by John Zimbrick and Janine Katanic of Purdue University. Damage to the enamel by X and gamma rays is permanent and can be observed by electron spin measurements, making teeth useful as biological dosimeters. Previous studies by others of the response of tooth enamel to neutrons had large uncertainties. Enamel irradiated at RARAF by 14 MeV neutrons with and without 3 mm of plastic for secondary charged particle equilibrium showed no observable effects. It was hoped that teeth extracted from atomic bomb survivors for medical reasons might be used to help determine the neutron doses received.

Kenshi Komatsu of Hiroshima University in Japan, in collaboration with H. Zhou of the CRR, continued a study of the bystander effect on *Ataxia Telangiectasia* (AT) cells (Exp. 101) using the microbeam facility. There is considerable evidence indicating that p53 may play a crucial role in the bystander effect. Atm , a kinase for the phosphorylation of several proteins including p53, seems to be the sensor of DNA damage or center of signal transduction. AT cells lack Atm and therefore could provide useful information on the role of p53 in the bystander effect. In current experiments, cell survival was measured for radiation sensitive AT cells and normal Hx cells. In addition, the bystander effect for HPRT mutation in Hx cells was determined by irradiating 10% of the cell nuclei with 20 alpha particles.

Hongning Zhou and Tom Hei of the CRR continued to use the single-particle microbeam facility for two experiments investigating the bystander effect. One study is examining adaptive response in bystander effects in human-

hamster hybrid (A_L) cells (Exp. 108). After low-dose X-ray irradiation, 10% of the cells are traversed by 1 or 20 helium ions. There is a decrease in the bystander effect for mutation when neighbor cells are traversed by one particle and a somewhat smaller decrease for traversal by 20 particles. . In addition, they found that the bystander cells showed an increase in sensitivity to a subsequent, challenging dose of X-rays. The mutation spectra are being analyzed and should provide some evidence for understanding the mechanism of bystander mutagenesis and adaptive response. With Debasish Roy of the CRR, they are trying to identify the molecular signals of cell-cell communication in bystander mutagenesis (Exp. 110). Hybrid A_L cells, human fibroblasts, and normal human bronchial epithelial cells were irradiated using the microbeam facility. A fraction of the cells was irradiated with a single alpha particle. The irradiated (stained) cells are separated from the unirradiated cells by a cell sorter and accumulated from experiments over four consecutive days. The cells were then analyzed using microarrays. Preliminary data show some gene expression change in the bystander cells.

Investigations of damage induction in human fibroblasts and *Ataxia Telangiectasia* cells (Exp. 109) were extended by Adayabalam Balajee and Charles Geard of the CRR to include a search for foci of damage and repair proteins. Cells irradiated through the nucleus using the microbeam facility are stained and examined to observe these proteins, which should cluster around the helium ion track.

Robert Bristow and Shahnaz Al Rashid of Princess Margaret Hospital, Toronto initiated efforts to visualize the localization of repair proteins around particle tracks (Exp. 111). The microbeam facility was used to irradiate human fibroblast strains with one helium ion per nucleus. At times they observed a discrete sub-nuclear focus with H2AX, but never with rad50, although there was co-localization with one of the rad50 foci and the discrete H2AX. The ser15-p53 foci were diffuse, but observed in both irradiated and unirradiated cells.

Yigal Horowitz of BenGurion University of the Negev in Israel and Marco Zaider of the Memorial Sloan-Kettering Cancer Center in New York are investigating the use of thermoluminescent dosimeter (TLD) chips as nanodosimeters to determine the quality factor of radiations (Exp. 112). Radiation damage to the crystal structure of the LiF:Mg,Ti crystal structure can be removed by heating, with different kinds of damage repaired at different temperatures. As the damage is removed, excess energy is emitted in the form of light (glow peaks). It has been found that the ratio of peak 5a to peak 5 is 7-8% for gamma rays but 25-30% for alpha particle irradiation. The dependence of damage to the crystals on ionization density is similar to that for DNA double strand breaks and the physical structure giving rise to peak 5a is about 2 nm, similar to the diameter of DNA. These features make the TLD system applicable as a nanodosimeter. TLDs were irradiated with 0.22 and 14 MeV neutrons and with charged particles having six different LETs in the range of 10-180 keV/μm to observe the dependence of the ratios of the glow peaks on radiation quality.

The Department of Defense is interested in the biological effects of depleted uranium (DU), especially since its significant use in the Gulf War. The primary focus has been the chemical effects of DU on human cells. Alexandra Miller of the Armed Forces Radiobiological Research Institute has begun a study of neoplastic transformation of immortalized human osteoblast cells by helium ions (Exp. 113). Graded doses of ions were delivered using the track segment facility to try to determine the contribution to cell transformation of the alpha particles emitted by the DU.

Accelerator Utilization and Operation

Accelerator usage is summarized in Table II. Use of the accelerator for radiobiology and associated dosimetry decreased by about 10% over last year but was still ~35% higher than the average for 1996-2001. This year less than 80% of the accelerator use for all experiments was for microbeam irradiations because of increased use of the track segment facility and the increase in physics and chemistry usage. Because of the relatively low number of cells that can be irradiated in a day, microbeam experiments often require considerable beam time to obtain sufficient biological material, especially for low probability events such as transformation and mutation.

Utilization of the accelerator by radiological physics and chemistry increased this past year, back to the level in 1999-2000. Two ongoing projects, one for physics and the other for chemistry, resumed this year and two more physics experiments have begun, one very recently.

Development of Facilities

Development of the single-particle microbeam facility is described here briefly:

- Testing of the single electrostatic quadrupole quadruplet continued, using the existing microbeam facility. A beam approximately 2.5 μm in diameter had been obtained in November 2000, just before the rods that make up the lens were severely damaged due to an accidental application of a voltage that caused sparking. New rods have been constructed, the new lens is in place and initial tests are encouraging.
- There has been interest, especially by the DOE, in the effects of radiations with LETs of 10 keV/μm or less. The present gas detector used to count the ions that have passed through the cells has unity gain and the small signal from the protons is lost in the electronic noise. Efforts to reduce the noise level were unsuccessful, so a new detector with gas gain was built. The signal from the protons is now far removed from the noise and proton irradiations with the mi-

Table II

Accelerator Use, May 2001 - April 2002
Percent Usage of Available Days

Radiobiology and associated dosimetry	32.8%
Radiological physics and chemistry	4.9%
On-line facility development and testing	28.8%
Off-line facility development	12.4%
Safety system	2.4%
Accelerator-related repairs/maintenance	18.3%
Other repairs and maintenance	0.4%

crobeam facility can commence as soon as the lens system is operational.

- After successful testing of the laser ion source obtained from the University of Arkansas, a system has been designed for use in the Van de Graaff accelerator. This system will use a spherical electrostatic analyzer lens to focus the beam rather than the cylindrical lens used in the Arkansas design. This lens focuses in both the horizontal and vertical directions to better inject the beam into the accelerator. A mock-up of the lens has been machined in plastic to assure that the lens can be constructed in our shop. A new high-power Nd:YAG laser has been purchased to replace the obsolete one obtained from The University of Arkansas. The laser has been installed and tested.
- A feedback system has been developed for the voice coil stage. The position of the stage is monitored using linear variable differential transformers (LVDTs). Circuitry to drive the voice coils based n the error signal from the sensors has been designed and is being tested. This stage should provide both more accurate and faster positioning than the present stage, which is moved by stepping motors.
- Construction of the new microbeam facility on the floor over the exit of the Van de Graaff continued. New on-line and off-line microscopes, a CCD camera with a built-in image intensifier and a bench for the off-line microscope were purchased. The on-line microscope will have to be modified so that it can be moved in and out of place over the irradiation port. A new industrial computer system with two flat panel monitors and an image analysis board have also been purchased. One monitor will display the operating program and the other the image from the image analysis board. Work is being done on integrating the camera, image analysis system and irradiation control program.

Personnel

The Director of RARAF is Dr. David Brenner. The Van de Graaff accelerator facility is operated by Mr. Stephen Marino and Dr. Gerhard Randers-Pehrson.

Dr. Alan Bigelow, a postdoctoral fellow, is continuing the development of the laser ion source and the voice coil positioning stage for the microbeam facility.

Dr. Alexander Dymnikov, an expert on ion beam transport, left RARAF in June 2002. We will consult with him on the design of the electrostatic lenses for the microbeam facility.

Mr. Mutian Zhang, the accelerator technician, left RARAF in April 2002 for another position at Columbia University.

Dr. Furu Zhan, a postdoctoral fellow from China, arrived in June 2002. He is assisting in performing the microbeam irradiations and developing the facility.

Mr. Kurt Michel, an undergraduate student from Pace University, is a part-time intern assisting with the development of the voice coil positioning stage for the microbeam facility.

Biologists from the Center for Radiological Research not supported by the RARAF grant are stationed at the facility in order to perform experiments:

- Dr. Charles Geard, the Associate Director of the CRR, continues to spend most of each working day at RARAF. In addition to his own research, he is collaborating with several outside users on experiments using the single-particle microbeam facility.
- Dr. Brian Ponnaiya is an Associate Research Scientist performing experiments using the track segment and microbeam irradiation facilities.
- Ms. Gloria Jenkins, a biology technician, performs experiments on the microbeam facility for Dr. Geard.
- Dr. Steven Mitchell, a postdoctoral fellow who arrived in February 2002 is replacing Dr. Satin Sawant in research involving neoplastic transformation of C3H10T1/2 cells.
- Dr. Oleg Belyakov, another postdoctoral fellow, arrived in April 2002. He is performing experiments on the track segment and microbeam facilities using model tissue culture systems.
- Ms. Allison Groome, an undergraduate student from Pace University, is an intern assisting Drs. Geard and Ponnaiya on a part-time basis.

Recent Publications of Work Performed at RARAF (2001-2002)

1. Bigelow AW, Randers-Pehrson G and Brenner DJ. Laser ion source development for the Columbia University microbeam. *Rev Sci Instrum* **73**:770-2, 2002.
2. Brenner DJ and Elliston CD. The potential impact of the bystander effect on radiation risks in a Mars Mission. *Radiat Res*. **156**:1594-7, 2002.
3. Brenner DJ and Hall EJ. Microbeams: A potent mix of physics and biology. *Rad Protec Dosim* **99**:283-6, 2002.
4. Hall EJ. Genomic instability, bystander effect, cytoplasmic irradiation and other phenomena that may achieve fame without fortune. *Physica Medica* **17**(Supp. 1):21-5, 2001.
5. Hei TK, Zhao YL, Roy D, Piao CQ, Calaf G and Hall EJ. Molecular alterations in tumorigenic human bronchial and breast epithelial cells induced by high LET radiation. *Adv Space Res* **27**:411-9, 2001.
6. Piao CQ and Hei TK. Gene amplification and microsatellite instability induced by tumorigenic human bronchial cells by alpha particles and heavy ions. *Radiat Res*. **155**:263-7, 2001.
7. Ponomarev AL, Cucinotta FA, Sachs RK, Brenner DJ and Peterson LE. Extrapolation of the DNA fragment-size distributions in a high-dose PFGE assay to low doses. *Radiat Res* **156**:594-7, 2001.
8. Roy D, Calaf G and Hei TK. Profiling of differentially expressed genes induced by high LET radiation in breast epithelial cells. *Mol Carcin*. **31**:192-203, 2001.
9. Sawant SG, Zheng W, Hopkins KM, Randers-Pehrson G. Lieberman HB and Hall EJ. The radiation-induced bystander effect for clonogenic survival. *Radiat Res* **157**:361-4, 2002.
10. Zhao YL, Piao CQ, Hall EJ and Hei TK. Mechanism of radiation induced transformation of human bronchial epithelial cells. *Radiat Res* **155**:230-4, 2001.
11. Zhou H, Randers-Pehrson G, Suzuki M, Waldren CA and Hei TK. Genotoxic damage in non-irradiated cells: contribution from bystander effect. 13th Symposium on Microdosimetry, Stresa, Italy, May 26-June 1, 2001. *Ra-*

diat Prot Dosim **99**:227-32, 2002.

12. Zhou H, Suzuki M, Geard CR and Hei TK. Effects of irradiated medium with or without cells on bystander cell responses. *Mutat Res* **499**:135-41, 2002.
13. Zhou H, Suzuki M, Randers-Pehrson G, Vannais D, Chen G, Trosko JE, Waldren CA and Hei TK. Radiation risk to low fluences of alpha particles maybe greater than what we thought. *Proc Nat Acad Sci (USA)* **98**:144100-5, 2001.
14. Zhou H, Xu A, Suzuki M, Randers-Pehrson G, Waldren CA and Hei TK. The yin and yan of bystander versus adaptive response: lessons from the microbeam studies. *International Congress Series* **1236**:241-7, 2002.

Gary Johnson, head of the Design and Instrument Shop, working on a CAD-CAM project for RARAF.

RADIATION SAFETY OFFICE 2002

Standing (L-R): Ilya Pitimashvili, Salmen Loksen, Jacob Kamen, Shuntong Guo, Mutian Zhang, Ahmad Hatami, Dae-In Kim, Thomas Juchnewicz. Seated (L-R): Roman Tarasyuk, Raquel Rodriguez, Milvia Perez, Yvette Acevedo, Jason Bergman. Not pictured: Stephen Benson, Brian Chiongbian, Bruce Emmer, Jennifer Kirchherr, Olga Loukhton and Diana Morrison.

PROFESSIONAL STAFF

Salmen Loksen, M.S., CHP, DABR; Director, Radiation Safety Officer
Ahmad Hatami, M.S., DABR, DABMP; Assistant Director
Thomas Juchnewicz, M.S., DABR; Assistant Radiation Safety Officer
Jacob Kamen, Ph.D., NRRPT, CHP; Assistant Radiation Safety Officer
Bruce Emmer, M.S., DABMP, DABR; Physicist
Ilya Pitimashvili, Ph.D.; Radiation Protection Supervisor
Dae-In Kim, M.S.; Junior Physicist
Shuntong Guo, M.S.; Junior Physicist
Mutian Zhang, B.A.; Junior Physicist

TECHNICAL STAFF

Olga Loukhton, M.S.; Chief Technician
Roman Tarasyuk, Technician B
Jennifer Kirchherr, B.S.; Technician B
Brian Chiongbian, B.S.; Technician A

ADMINISTRATIVE AND SECRETARIAL STAFF

Diana Morrison; Administrative Assistant, assigned to the JRSC
Yvette Acevedo, A.A.S.; Administrative Aide
Raquel Rodriguez; Clerk B
Milvia Perez, A.A.S.; Clerk B
Jason Bergman, B.S.; Clerk A
Stephen Benson, B.A.; Administrative Assistant

TABLE OF CONTENTS

RADIATION SAFETY OFFICE 2002

INTRODUCTION

On May 19, 1957, the President of Columbia University distributed a memo entitled "Directive to All University Departments Having a Source of Ionizing Radiation," advising all parties of the expanded function of the Radiation Safety Committee.

Later, a notice entitled "Radiation Safety Guide for Columbia University," dated February 10, 1959, named Philip M. Lorio as the Health Physics Officer for University Departments and Laboratories other than the College of Physician & Surgeons, where Dr. Edgar Watts was the named Health Physics Officer. The Chairman of the Radiation Safety Committee was Dr. Gioacchino Failla, who initiated the Radiological Research Laboratory in the Department of Radiology of Columbia-Presbyterian Medical Center (CPMC).

By agreement between The Presbyterian Hospital in the City of New York (PH) and Columbia University (CU), the Radiation Safety Office (RSO) was established as an autonomous unit in 1962 for the purpose of maintaining radiation safety. The Joint Radiation Safety Committee (JRSC), appointed by the Medical Board of the Presbyterian Hospital in the City of New York and the Vice President for Health Sciences of Columbia University, is charged with the responsibility of defining and ensuring enforcement of proper safeguards in the use of sources of ionizing radiation.

Dr. Harald H. Rossi, Director of the Radiological Research Laboratories, was appointed Chairman of the Joint Radiation Safety Committee. Under his direction, this committee developed a "Radiation Safety Code and Guide," the administration of which is assigned to the Radiation Safety Officer. Dr. Eric J. Hall, the present Director of the Center for Radiological Research, now chairs the JRSC.

The present Joint Radiation Safety Committee of the Columbia-Presbyterian Medical Center and the New York State Psychiatric Institute came into existence through an agreement made on February 12, 1991 between New York State Psychiatric Institute (NYSPI), the College of Physicians and Surgeons of Columbia University (P&S), and The Presbyterian Hospital in the City of New York (PH). This agreement combined several overlapping clinical and educational programs, including all programs for ensuring radiation safety. The current Director of the Radiation Safety Office and Radiation Safety Officer, Salmen Loksen, C.H.P., D.A.B.R., was appointed on December 16, 1996.

The Radiation Safety Office reports to and advises the Joint Radiation Safety Committee of Columbia-Presbyterian Medical Center and New York State Psychiatric Institute. The Committee meets on a quarterly basis. For administrative purposes, the Radiation Safety Office reports to Dr. Richard Sohn, Associate Dean for Research Administration and Director of Grants and Contracts. The Radiation Safety Office participates in the review of research protocols for the Radioactive Drug Research Committee under the jurisdiction of the U.S. Food and Drug Administration.

Radiation Safety Office staff are Columbia University employees. New York Presbyterian Hospital, Columbia University College of Physicians and Surgeons, and New York State Psychiatric Institute fund the Radiation Safety Office budget via a cost sharing payback arrangement.

A full-asset merger between The Presbyterian Hospital in the City of New York and New York Hospital on December 1, 1997, created a single entity known as New York Presbyterian Hospital with facilities in two major Manhattan locations, Columbia Presbyterian Medical Center at West 168th Street in Washington Heights and New York Weill Cornell Center at East 68th Street on the Upper East Side.

OVERVIEW OF RADIATION SAFETY OFFICE RESPONSIBILITIES

The Columbia-Presbyterian Medical Center hosts a large health sciences campus with extensive teaching, research, and clinical facilities. The basic goal of the Radiation Safety Office is to ensure the implementation of all protective measures necessary to keeping the dose from ionizing radiation to patients, visitors, students, faculty and staff on campus, and to the general community at large As Low As Reasonably Achievable (ALARA). Major entities of the campus supported by the Radiation Safety Office are:

- Columbia University, Health Sciences Campus
- Columbia University, College of Physicians & Surgeons
- New York Presbyterian Hospital
- New York State Psychiatric Institute
- New York Presbyterian Hospital, Allen Pavilion
- Columbia Cyclotron Facility - PET Net Pharmaceuticals, Inc.
- Audubon Biomedical Science and Technology Park (Audubon I)
- Russ Berrie Medical Science Pavilion (Audubon II).

Reporting to the Joint Radiation Safety Committee of Columbia-Presbyterian Medical Center and New York State Psychiatric Institute, the Radiation Safety Officers and the staff of the Radiation Safety Office are responsible for obtaining and maintaining licenses authorizing the possession and use of radioactive materials and obtaining and maintaining registrations and permits for the operation of radiation producing equipment. In addition, the Radiation Safety Office is responsible for obtaining and maintaining those permits necessary for the safe disposal of research or medical wastes containing low levels of radioactivity or their controlled discharge to the environment.

The Radiation Safety Office ensures the compliance of the authorized users of radioactive materials or radiation producing equipment with all governmental regulatory requirements and guidelines by means of: training, education, consultation, and by a program of internal audits and inspections of facilities. Regulatory agencies charged with over-

seeing the possession, use, or disposal of radioactive materials or radiation producing machines are:

- United States Food and Drug Administration
- United States Nuclear Regulatory Commission
- New York State Department of Environmental Conservation
- New York State Department of Health
- New York City Department of Health, Office of Radiological Health.

The New York City Department of Health, the New York State Department of Environmental Conservation, and the United States Food and Drug Administration conduct periodic inspections and audits of the Columbia-Presbyterian Medical Center and New York State Psychiatric Institute facilities operating under their licenses or permits. The Radiation Safety Office works continuously to ensure that regulatory violations are prevented and to ensure those that do occur are swiftly corrected.

The Radiation Safety Office also ensures compliance with institutional policies and procedures published in the "Radiation Code and Guide of Columbia-Presbyterian Medical Center and New York State Psychiatric Institute."

SUMMARY OF RADIATION SAFETY OFFICE OPERATIONS FOR 2002

A representative summary of activities performed and services provided by the Radiation Safety Office is presented below. While inclusive of most major activities and services, the summary is by no means exhaustive, but is intended to provide an overview of departmental operations. An unabridged compilation of Radiation Safety Office activities and services may be found in Minutes of the Quarterly Meeting of the Joint Radiation Safety Committee of Columbia-Presbyterian Medical Center and New York State Psychiatric Institute.

Statistical data presented are from the fiscal year, July 1, 2001 through June 30, 2002. Activities are covered for the period through the end of December 2002.

Maintenance of New York City Department of Health Office of Radiological Health Licenses, Registrations, and Permits, Audits and Inspections

A primary activity of The Radiation Safety Office is the continued maintenance of the City of New York Radioactive Materials Licenses, the Certified Linac Registration, and the Diagnostic X-Ray Permits**.** Currently this includes:

- Radioactive Materials License No. 75-2878-01 (Broad Scope Human Use)
- Radioactive Materials License No. 92-2878-02 (Teletherapy)
- Radioactive Materials License No. 74-2878-03 (Non-Human Use)
- Radioactive License No. 52-2878-04 (Cyclotron Facility)
- Radioactive Materials License No. 93-2878-05 (Gamma Knife)
- City of New York Therapeutic Radiation LINAC Unit Certified Registration No. 77-0000019.
- Columbia-Presbyterian Hospital Radiation Installation Permit H96 0076353 86
- Columbia-Presbyterian NMC-Allen Pavilion Radiation Installation Permit H960076383 86.

Significant activities performed in the Year 2002 to maintain the City of New York Licenses, Registrations and Permits include:

1. On September 27, 2002 the Radiation Safety Office filed with the City of New York Department of Health applications for the renewal of two (2) City of New York Radioactive Materials Licenses for an additional five-year period. The Radioactive Materials Licenses due to be renewed were License 52-2878-04 (Cyclotron) and License 93-2878-05 (Gamma Knife). On September 27, 2002, the New York City Department of Health, Office of Radiological Health issued to Columbia-Presbyterian Medical Center letters acknowledging timely filling for renewal. These letters state that the current licenses will not expire until determinations have been made on the applications for renewal. The License Renewal Applications were approved by a quorum of the Joint Radiation Safety Committee on December 17, 2002.

2. In the Year 2002, the Radiation Safety Office submitted a number of License Amendment requests to the New York City Department of Health, Office of Radiological Health. On February 21, 2002, the Radiation Safety Office received an amended License No. 75-28787-01 (Human Use) authorizing an increase in the possession limit of Palladium-103 for brachytherapy implants and also authorizing replacement of the current Gamma-Med HDR Iridium-192 source by a newer model. On September 26, 2002, the Radiation Safety Office received an amended Radioactive Materials License No. 74-2878-03 (Non-Human Use) authorizing possession of SMP Model PET Gallium/Gernanium-68 sealed sources for calibration of a Concorde MicroPET scanner. And on November 1, 2002, the Radiation Safety Office received an amended License No. 75-28787-01 (Human Use) authorizing possession of Strontium-90 in several new models of the Noveste Beta-Cath intravascular brachytherapy device. Each License Amendment request had been approved by the Joint Radiation Safety Committee prior to submission to the New York City Department of Health.

3. On January 7, 2002, a quorum of the Joint Radiation Safety Committee voted to approve a request by Peter Schiff, M.D., Ph.D., Chairman, Department of Radiation Oncology that Gerald Kutcher, Ph.D. DABR, be added as a Therapy Physicist to all Columbia-Presbyterian Medical Center Radioactive Materials Licenses and the Therapeutic Radiation Linac Certified Registration. On April 18, 2002, this amendment request was submitted to the New York City Department of Health, Office of Radiological Health. On November 12, 2002, the Radiation Safety Office received Amendment Number 20 of City of New York Radioactive Materials License No. 75-2878-01 (Human-Use), listing Dr. Kutcher as one of the three Therapy Physicists named on that license. The Radiation Safety Office is still awaiting the addition of Dr. Kutcher to License No. 92-2878-02 (Teletherapy), License No. 93-2878-05 (Gamma Knife) and Linac Certified Registration No. 77-0000019.

4. On September 12, 2002, a quorum of the Joint Radiation Safety Committee voted to approve a request by Peter Schiff, M.D., Ph.D., Chairman, Department of Radiation Oncology that the following board certified medical physicists be added as Therapy Physicists to all Columbia-Presbyterian Medical Center Radioactive Materials Licenses and Therapeutic Radiation Linac Certified Registrations: Yoichi Watanabe, Ph.D., DABR, Tian Liu, Ph.D., DABR, and Dennis Mah, Ph.D., DABR. On August 1, 2002, this amendment request was submitted to the New York City Department of Health, Office of Radiological Health. The Radiation Safety Office is currently awaiting approval of the amendment requests.

5. The Radiation Safety Office provided assistance to Gila Med, operating in the Audubon Biomedical Science Technology Building, in preparing an application for a New York City Department of Health, Office of Radiological Health, Radioactive Materials License for Non-Human Use. The application was submitted on October 8, 2001. The license was approved on December 10, 2001.

6. The New York City Department of Health, Office of Radiological Health conducts periodic unannounced audits of records and inspections of facilities at the Columbia-Presbyterian Medical Center operating under the Radioactive Material Licenses, the Certified Linac Registration, and the Diagnostic X-ray Registrations. In the Year 2002, these audits and inspections included:

- February 28, 2002, Radiation Installation Permit H96 0076353 86
- July 10, 2002 through July 12, 2002, License 93-2878-05 (Gamma Knife)
- August 15, 2002, License 52-2878-04 (Cyclotron & Radioligand)
- September 10, 2002 through November 14, 2002, License 74-2878-03 (Non-Human Use)
- September 18, 2002 through September 24, 2002, License 75-2878-01 (Human Use)
- September 24, 2002, Certified Linac Registration 77-00000019.

7. The New York City Department of Health, Office of Radiological Health reports the results of these audits and inspections to representatives of the Management of Columbia University and the New York Presbyterian Hospital, New York State Psychiatric Institute, and the Radiation Safety Office. All records and activities were deemed to be in compliance with the Rules of the City of New York, Article 175, Radiation Control and the Conditions of the Licenses and Certified Registration with the possible exception of a single calibration performed in the Department of Radiation Oncology. On December 7, 2002, the Radiation Safety Office provided documentation to a New York City Department of Health Administrative Tribunal that this calibration was performed in full compliance with Article 175. The Radiation Safety Office is awaiting the decision of the Department of Health in this matter.

8. In compliance with Office of Radiological Health Information Notice N.2001-1, the Radiation Safety Office is currently preparing a list of all analytical X-ray equipment at Columbia- Presbyterian Medical Center. The list includes equipment such as electron microscopes, analytic X-ray units, X-ray fluorescense units, particle accelerators, and X-ray machines utilized for academic purposes that are non-commercial in nature.

Maintenance of New York State Department of Environmental Conservation Permits, Audits and Inspections

Another primary activity of The Radiation Safety Office is the continued maintenance of New York State Department of Environmental Conservation Radiation Control Permit No. 2-6201-00005/00006.

Under the Conditions of the Radiation Control Permit and in compliance with New York State 6 NYCRR Part 380, Rules and Regulations for Prevention and Control of Environmental Pollution by Radioactive Materials, Columbia-Presbyterian Medical Center conducts medical research and clinical activities that discharge limited and controlled quantities of radioisotopes to the atmosphere and to sewage systems.

The Columbia-Presbyterian Medical Center is sited within a densely populated urban area. The quantities of radioisotopes discharged and the resulting public radiation dose are closely regulated by the New York State Department of Environmental Conservation. Radiation doses to the general public resulting from atmospheric discharges of radioisotopes are required not to exceed the U.S.N.R.C. Constraint Limit of 10 mrem per year.

Columbia-Presbyterian Medical Center and the New York State Psychiatric Institute are currently permitted a total of fifteen (15) atmospheric emission points from which radionuclides are discharged to the atmosphere. Monitoring, analyzing, reporting, and minimizing discharges from these emission points, in order to ensure compliance with the Conditions of the Radiation Control Permit, is one of the major continuing activities of the Radiation Safety Office.

Significant activities performed in the Year 2002 to maintain the New York State Department of Environmental Conservation Radiation Control Permit include:

1. On January 17, 2002, the Radiation Safety Office received approval from the New York State Department of Environmental Conservation of a Permit Modification authorizing installation and use in the Cyclotron Facility of a new chemical processing unit for the synthesis of ^{18}F labeled fluorodeoxyglucose. On February 11, 2002, the Radiation Safety Office received authorization from New York State to place into active service newly installed and calibrated NaI stack monitoring systems to replace older ion chamber based systems. The NaI stack monitoring systems continuously monitor for and record atmospheric discharges of positron emitting radioisotopes from the Cyclotron Facility and the Radioligand Laboratory. The Cyclotron Facility and Radioligand Laboratory are a major source of clinical and research radiopharmaceuticals for the Columbia-Presbyterian Medical Center and other New York Metropolitan Area hospitals.

2. On March 15, 2002, as required by New York State 6 NYCRR Part 380 and the Conditions of the New York State Department of Environmental Conservation Radiation Control Permit, the Radiation Safety Office submitted an Annual

Report summarizing Discharges of Radioactive Effluents to the Environment from the fifteen atmospheric emission points and by controlled sewer disposal. For the Calendar Year 2001, all atmospheric discharges were within the quantities authorized by the Radiation Control Permit, and the resulting public dose was within the U.S.N.R.C. Constraint Limit of 10 millirem per year. All discharges to sewers were well below the Effluent Concentration Limits as required by Part 380-11.7, Table of Concentrations.

3. On September 18, 2002 and September 19, 2002, the New York State Department of Environmental Conservation conducted an unannounced inspection of operations at Columbia-Presbyterian Medical Center authorized under Radiation Control Permit Number 2-6201-0005/0006. The inspection consisted of observations of facility operations, interviews with personnel, measurements, and a selective examination of representative records. On November 7, 2002, the Radiation Safety Office received a letter from the New York State Department of Environmental Conservation stating that, within the scope of the above inspection, operations at Columbia-Presbyterian Medical Center were in compliance with New York State Part 380 and the conditions of the Radiation Control Permit.

4. As required by 6 NYCRR Part 380 and the conditions of the Radiation Safety Office's Radiation Control Permit, the Radiation Safety Office conducts periodic reviews our daily analysis of atmospheric discharges of positron-emitting radioisotopes from the Cyclotron Facility and the Radioligand Laboratory. For the first three Quarters of 2002, all atmospheric discharges from the Cyclotron Facility were well within the Maximum Annual Quantity Authorized. However, in the Fourth Quarter of 2002, releases of Nitrogen-13 and Fluorine-18 compounds from the Cyclotron exhaust stack exceeded the Annual Permit Limit for these radioisotopes. All other atmospheric releases remained well below their Annual Permit Limits.

Investigation of the Nitrogen-13 and Fluorine-18 releases by the Radiation Safety Office revealed that they were the result of the installation of a new model ion-beam target in the Cyclotron. Re-installation of the older model target appeared to solve the discharge problem, and production of radiopharmaceuticals continued with the authorization of the New York State Department of Environmental Conservation. Calculation of the Public Dose resulting from these and all other atmospheric discharges for the year demonstrated that maximum public dose will remain well below the 10 mrem per year U.S.N.R.C. Constraint Limit.

Administration of Radioactive Material: Receipt, Distribution, and Radioactive Waste Disposal

A major program of the Radiation Safety Office is the centralized administration of all authorized radioactive material use at the Columbia-Presbyterian Medical Center and New York State Psychiatric Institute.

Types of radioisotopes, their use, and their possession limits by the member Institutions and by major Departments are authorized by five separate City of New York Radioactive Materials Licenses.

The use of authorized radioisotopes by individual Authorized Users and Responsible Investigators is controlled by the Joint Radiation Safety Committee through the administration of the Radiation Safety Office. Human Use of radioactive materials by Authorized User Physicians is by a review of credentials and a majority vote by a quorum of the Joint Radiation Safety Committee. Non-Human Use of radioactive materials is by a review of credentials and written permission of the Radiation Safety Office. In the Year 2002, no new applications for Authorized User Physician status were submitted. Twenty-two (22) new Responsible Investigators were reviewed and approved for non-human use of radioactive materials, and 111 current Responsible Investigators received renewal of their authorizations.

The Radiation Safety Office maintains the State of South Carolina Transportation Permit for Radioactive Waste necessary for the transfer of Low-Level Radioactive Waste to the disposal site in Barnswell, South Carolina. On October 21, 2002, the Radiation Safety Office filed for renewal of the State of South Carolina Transportation Permit for Radioactive Waste for the year 2003. The renewed Permit was received on December 8, 2002.

Significant activities performed in the Year 2002 to administer, receive, distribute, and dispose of radioactive materials included:

1. The Radiation Safety Office received and distributed 3,025 packages containing radioactive material, excluding Nuclear Medicine and Radiation Oncology shipments. For all shipments, the Radiation Safety Office conducted package surveys and ensured correct distribution to Authorized Users and Responsible Investigators. The Radiation Safety Office maintains inventory control of all radioactive materials received and distributed through the use of a detailed and extensive computerized database.

2. The Radiation Safety Office provides scheduled pick-ups of radioactive waste generated by the activities of the Authorized Users and Responsible Investigators.

3. On January 18, 2002, the Radiation Safety Office shipped a total of thirty-two (32) 30-gallon drums of Liquid Scintillation Vial waste for disposal by Perma-Fix of Gainesville, Florida. Total volume of the shipment was 128.41 cubic feet, weighing 4,791 pounds. Total activity shipped was 29.575 mCi, of which 17.40 mCi was Tritium (3H), 1.1 mCi was Carbon-14, and 11.075 mCi was other isotopes. On June 25, 2002, the Radiation Safety Office shipped a total of eighty-seven (85) drums of Dry Active Waste (thirty-seven 55-gallon drums and fifty 30-gallon drums) for disposal by Envirocare of Utah via GTS Duratek Super-Compaction. Total volume of the shipment was 478 cubic feet, weighing 9,300 pounds. Total activity shipped was 153.880 mCi, of which 99.277 mCi was Tritium (H-3) and 30.644 mCi was Carbon-14. On December 11, 2002, the Radiation Safety Office shipped a total of fifty-four (54) 30-gallon drums of Liquid Scintillation Vial waste for disposal by NSSI/Sources and Services of Houston, Texas. Total volume of the shipment was 6.13 cubic meters, weighing 3,681.82 kilograms. The total activity shipped was 14.8 mCi, of which 12.6 mCi was Tritium (Hydrogen-3) and 1.79 mCi was Carbon-14.

4. Low-Level Radioactive Wastes with a half-life of less

than 90 days may be disposed of by decay-in-storage to background levels. The Radiation Safety Office operates a decay-in-storage program that in the Year 2002 disposed of 40.214 cubic meters, weighing approximately 8,800 kilograms. Total activity disposed of by decay-in-storage was 16,650 MBq.

5. In the year 2002, the Radiation Safety Office disposed of 4,950 liters of low-level aqueous radioactive waste through monitored sewer disposal.

6. Sealed sources of radioactivity and isotope generators that are retired from use are maintained in interim storage by the Radiation Safety Office. In the Year 2002, seven (7) depleted Tungsten/Rhenium-188 generators were packaged and returned to the manufacturer, Oak Ridge National Laboratories. The Radiation Safety Office has solicited bids from Radioactive Waste Disposal vendors for the removal and safe disposal of a number of sealed sources in interim storage.

7. In order to prevent the unauthorized removal of any trash or waste contaminated with radioactive materials, the Radiation Safety Office maintains computerized NaI Scintillation Detector Waste Monitoring systems on the loading docks of Presbyterian Hospital Building, Milstein Hospital Building, New York State Psychiatric Institute, and the Allen Medical Pavilion. In May 2002, an additional system was installed in the exit leading to the loading dock of the Russ-Berrie Building. The Radiation Safety Office also conducted a training course for the monitoring of waste handled by the Facilities Management of the Russ-Berrie building.

8. The Radiation Safety Office is presently in the process of selecting a company to serve as a primary waste disposal vendor for the Columbia-Presbyterian Medical Center and the New York State Psychiatric Institute. The two companies currently providing this service are Radiac Research Corp. and Duratek Services, Inc. In the past, each of these vendors has served us in removing specific classifications of radioactive waste, and the removal services have been divided between them. Radiac and Duratek have each submitted new contract proposals for complete waste removal and disposal programs. These were forwarded to risk management for review, comments, and suggestions.

9. On July 17, 2002, personnel from the Radiation Safety Office attended a training session on Hazardous Chemical Waste Management given by a certified Hazardous Material specialist from the Columbia University Environmental Health & Safety Office. At the end of the session all attendees were given a certificate of training.

ALARA Program - Personnel Dosimetry, Bioassay, and Area Monitoring

In accordance with regulatory requirements, the Radiation Safety Office operates an ALARA (As Low As Reasonably Achievable) Program to ensure that the radiation doses to all workers at the Columbia-Presbyterian Medical Center and New York State Psychiatric Institute and the radiation doses to the general public resulting from all operations of Columbia-Presbyterian Medical Center and the New York Psychiatric Institute are within the legal limits and As Low As Reasonably Achievable (ALARA).

The principal methods of monitoring radiation dose are the assignment of personnel radiation dosimeters to individuals, the posting of area and environmental dosimeters, and the monitoring of all discharges containing radioactivity.

Immediate action is taken, as appropriate, in response to unusual or high dosimeter readings. Quarterly ALARA Reports are prepared and submitted to the Joint Radiation Safety Committee. The Quarterly ALARA Report presents: the doses of individual workers that exceed ALARA I Limits; the results of investigation of doses to individual workers that exceed ALARA II Limits; and discussions of significant trends within departments that may experience high individual doses. In addition, the Quarterly Environmental ALARA Report is prepared and submitted to the Joint Radiation Safety Committee. The Quarterly Environmental ALARA Report presents the quantities of radionuclides discharged to the atmosphere and the sewer system and the resulting dose to the general public.

In the Year 2002, all doses to individual workers were less than the legal limits as specified in RCNY Article 175, Radiation Control. All doses to the general public resulting from atmospheric discharges of radionuclides were less than the U.S.N.R.C. constraint limit of 10 mrem per year.

Significant activities performed in the Year 2002 to maintain the ALARA Program were:

1. The Radiation Safety Office distributed approximately 8,900 personnel radiation dosimeters each quarter, including both monthly and quarterly badges. A total of about 35,600 dosimeters were distributed and collected in the Year 2002. To maintain dosimetry records, the Radiation Safety Office uses dedicated computers with internet and direct modem access to the database of the dosimeter supplier, Landauer Inc.

2. The Radiation Safety Office received Annual Occupational Exposure Reports (NRC Form 5) from Landauer Inc. for the year 2001 and forwarded these reports to radiation workers as required by the New York City Department of Health regulations.

3. In the Year 2002, the Radiation Safety Office notified 63 personnel with ALARA Level 1 readings and investigated 33 cases of ALARA Level II readings as reported by Landauer Inc. Particular attention was paid to occupational groups that typically exceed the ALARA limits, i.e., workers and researchers at the Cyclotron Facility, Angiography, the Cardiac Cath Lab, and physicians in the PET Suite.

4. In the Year 2002, the Radiation Safety Office performed 89 thyroid bioassays on radiation workers using radioactive isotopes of iodine including Iodine-123, Iodine – 125, and Iodine-131.

5. During fiscal year 2001-2002, 18 radiation workers completed declaration of pregnancy forms. The Radiation Safety Office provided them with health physics counseling about risk factors and additional monitoring of the fetus during their gestation period while continuing to closely follow their personnel radiation exposure reports.

6. On May 8 and May 14, 2002, the RSO held two meetings for badge coordinators. Attendees were updated on the following issues: the importance of returning badges on

time; regulatory requirements; exposure reports and units; ALARA review and investigation of exposures; previous exposure history; annual occupational dose limits; pregnancy policy and fetal dose limits; and proper use and badge wear, including wear during fluoroscopy procedures. An officer of the Radiation Safety Office answered questions and addressed concerns from the audience. The Radiation Safety Office is in the process of planning for the next meeting in the spring of 2003.

7. As a result of a new annual contract, Landauer Inc. will provide to CPMC, on a trial basis, a newly designed dosimeter (Aurion) that can be read immediately but does not require a battery. This type of dosimeter will initially be used for visitors to the Cyclotron and Radioligand Facilities and, if found suitable, the RSO will expand the use of these dosimeters to other areas, such as by nursing staff during therapy patient procedures. At this time, the Radiation Safety Office is awaiting NAVLAP certification of the dosimeter.

Radiation Safety Compliance – Routing Internal Inspections and Audits

A major activity of the Radiation Safety Office is the routine performance of inspections of facilities and audits of records of clinical departments and research laboratories to ensure that the use of radioactive materials is in accordance with regulatory requirements and as authorized by the Joint Radiation Safety Committee.

Significant compliance activities conducted in the Year 2002 include:

1. In the Year 2002, the Radiation Safety Office performed quarterly inspections and audits of Columbia-Presbyterian Medical Center and New York State Psychiatric Institute clinical facilities using radioactive materials. The inspections and audits are to ensure compliance with City of New York Radioactive Materials License Conditions and with RCNY Article 175, Radiation Control. The facilities inspected include: NYPH Nuclear Cardiology, NYPH Nuclear Medicine, NYPH PET Suite, NYPH Allen Pavilion Nuclear Cardiology, NYPH Allen Pavilion Nuclear Medicine, NYSPI Functional Brain Imaging, Columbia University Cyclotron, and Columbia University Radioligand Laboratory. In addition, quarterly sealed source inventories and annual leak testing were performed by the Radiation Safety Office.

2. In the Year 2002, the Radiation Safety Office performed 690 routine radiation safety inspections and audits of Columbia-Presbyterian Medical Center and New York State Psychiatric Institute research laboratories using radioactive materials. The results were communicated to the Responsible Investigators. A total of 235 deficiencies were followed up by correction of the cited deficiencies.

3. In the Year 2002, the Radiation Safety Office measured air flow rates in 256 fume hoods in areas where volatile radioactive materials are used. In all rooms where radioactive gases or aerosols are used, ventilation rates were measured and Spill Gas Clearance Times were calculated and posted. Adjustments were made as required to air supply and exhaust systems to obtain negative pressure conditions.

4. In addition to the regular inspections of clinical facilities and research laboratories, the Radiation Safety Office investigates major spills, incidents involving radioactive materials, and misadministrations. The Radiation Safety Office ensured that timely notice of reportable incidents was made to the New York City Department of Health, Office of Radiological Health.

Training

In accordance with regulatory requirements the Radiation Safety Office provides initial radiation safety training to all new employees of the Columbia-Presbyterian Medical Center and the New York State Psychiatric Institute prior to their beginning work with radiation equipment or radioactive materials. The Radiation Safety Office provides the required annual refresher training thereafter.

Significant training activities in the Year 2002 included:

1. Pursuant to Article 175 of the New York City Health Code, the following radiation safety courses and training sessions were presented from July 2001 through June 2002:

- 12 initial training seminars for individual researchers
- 12 annual refresher seminars for researchers
- 12 nursing seminars for New York Presbyterian Hospital
- Training sessions for Dental School residents
- Training sessions for Radiology residents
- Training sessions for the Facilities Department.

2. For employees who could not attend the regularly scheduled classes, the Radiation Safety Office designed and implemented a self-study program, including the use of videotapes available at the Health Sciences Library. A passing grade on the quiz administered after viewing the video qualifies an employee working in Non-Human Use applications to be issued a personnel radiation dosimeter and authorizes that employee to begin work with radioactive material or radiation equipment. If the individual's employment involves human use of radioactive material, a passing grade on the quiz results in obtaining a temporary badge until the next regularly scheduled training session is attended.

3. On October 10, 2002, the Radiation Safety Office provided a lecture as a part of the Department of Anesthesiology's series of guest lecturers.

4. The Radiation Safety Office conducted a training course for the monitoring of waste handled by the Facilities Departments of Columbia University, New York Presbyterian Hospital, and the New York State Psychiatric Institute. Copies of the instructions for the monitoring systems have been circulated to the managers of the several Facilities Departments for their review. A laminated copy of the instructions, in English and Spanish, has been posted at the display monitor.

5. On September 18, 2002, the installation of the Radiation Safety Training Course on RASCAL was completed. All of the RSO technical staff were asked to take the course. Additional modifications to the course installation are in progress.

6. On September 24, 2002, Salmen Loksen, CHP, DABR, Director, Radiation Safety Office, attended a meeting in King of Prussia, Pennsylvania titled “Part 35 Work-

shop for External Stakeholders." The meeting was hosted by the U.S. Nuclear Regulatory Commission and focused on the significance of Part 35 changes. The purpose of the workshop was to inform medical licensees of the revisions to Part 35 to facilitate a smooth transition in adopting the new rules.

Professional Radiation Safety and Health Physics Support

The Radiation Safety Office provides professional radiation safety and health physics consultation to clinical departments, research laboratories, Authorized Users, and Responsible Investigators to ensure compliance with technical requirements in the regulations and good practice in the safe use of radioactive materials and radiation equipment.

Specific examples of professional support provided by the Radiation Safety Office in the Year 2002 include:

1. In the Year 2002, the Radiation Safety Office provided radiation safety support for 75 brachytherapy and Iodine-131 radiopharmaceutical therapy patients receiving treatment from the New York Presbyterian Hospital Departments of Nuclear Medicine and Radiation Oncology. This support included: room preparation; distribution of personnel radiation dosimeters; performance of patient and room surveys; posting instructions in patient rooms; entering instructions in patient charts; patient discharge surveys; room decontamination; and removal of patient generated wastes for decay-in-storage and disposal.

2. An officer of the Radiation Safety Office participates as a Member of the Animal Care Protocol Review Committee, reviewing all procedures using radionuclides in animal research.

3. In the Year 2002, the Radiation Safety Office performed 45 routine animal radiation surveys in the Institute of Comparative Medicine in order to minimize contamination in animal facilities and cages, protect Animal Care staff, and ensure proper disposal of animal carcasses containing radioactivity.

4. In the Year 2002, the Radiation Safety Office provided calibration and maintenance services for 501 radiation survey instruments used throughout the Columbia-Presbyterian Medical Center and New York State Psychiatric Institute. The Radiation Safety Office maintains a supply of portable survey instruments available for loan to Responsible Investigators.

5. The Radiation Safety Office provides continuing radiation safety support for the Columbia University Cyclotron Facility and the Columbia University Radioligand Laboratory for the production and synthesis of PET imaging radiopharmaceuticals. This support includes: basic radiation safety services; personnel dosimetry; area radiation monitoring and analysis of radioisotope releases to the atmosphere; review of Authorized User credentials; and review of system modifications.

6. The Radiation Safety Office is involved in providing professional health physics expertise for the planned construction of an additional Cyclotron/Radioligand Facility on the Columbia University Health Sciences campus.

7. In 2002 the RSO purchased a data-logging meteorological station from Vaisala. The meteorological station will be used to record wind speed, wind direction, and atmospheric stability for dose assessment modeling. The meteorological station will enable the RSO to present improved estimates of public radiation dose resulting from atmospheric discharges of positron emitting isotopes from the Cyclotron and Radioligand Facilities. Subsequently, a representative of BLU DOT Inc., under contract to the Radiation Safety Office, visited CPMC to install, calibrate, and perform acceptance testing of the Vaisala meteorological station.

8. The RSO is authorized by the New York City Department of Health, Office of Radiological Health to calibrate radiation survey instruments. Because of a previous lack of staffing and space, an outside vendor, Co-Physics Corporation, had been contracted for this work. During the second quarter of 2002, the Radiation Safety Office re-instituted the in-house calibration program. Since restarting the in-house calibration program, the RSO has calibrated more than 100 survey instruments. Turn-around time for the in-house calibration is much shorter than the time required for the outside vendor. The RSO will continue to send certain specialized radiation survey instruments to outside vendors for calibration and repair as necessary.

9. The RSO continues the process of scanning paper documents into the PaperPort software application. This process is a measure to back-up our paper files with digital copies that may be transferred to CD-ROM or DVD formats. This electronic document system allows for quicker search and retrieval of information, and reduces the quantity of paper documents maintained in the RSO files. As we prepare to complete the move to our new location, we are reviewing files to determine which are to be retained, archived, or disposed of after they are converted into digital files.

10. In preparation for the Joint Commission on Accreditation of Healthcare Organizations (JCAHO) inspection of the New York Presbyterian Hospital, the Radiation Safety Office worked closely with the staff of the Radiology and other NYPH Departments in order to ensure that the process would proceed smoothly. In addition, the Radiation Safety Office inspected the non-Radiology X-ray facilities to insure compliance with JCAHO requirements.

Professional Radiation Safety and Medical Physics Support for Non-Radiology X-ray Activities

The Joint Radiation Safety Committee in agreement with New York Presbyterian Hospital has assigned the Radiation Safety Office responsibility for Radiation Safety and Medical Physics support for those clinical facilities outside the Department of Radiology that use X-ray equipment. A major part of this program is the quality assurance program for dental radiography.

This quality assurance program is designed to optimize the radiological safety and clinical quality of dental radiography, based on recommendations for quality assurance that have been promulgated by a number of professional organizations, including the National Council on Radiation Protection and Measurements (NCRP), the Bureau of Radiological Health of the Food and Drug Administration, the American College of Radiology (ACR), and the American Academy of Dental Radiology Quality Assurance Committee.

The Radiation Safety Office has primary responsibility for preliminary radiation safety shielding evaluation, acceptance testing, diagnostic quality assurance, and radiation safety surveys on all dental X-ray units installed at the following locations:

- Morningside Dental Associates: 9 intraoral units, and 1 panoramic - cephalographic unit at two locations
- Ambulatory Care Networked Corporation (ACNC): 2 intraoral units and 1 panoramic - cephalographic unit
- Babies Hospital OR: 1 portable intraoral unit
- Vanderbilt Clinic Teaching & Research Areas: 1 panoramic unit, 1 panoramic - cephalographic unit, 23 intraoral units, and 1 intraoral - cephalographic unit
- Dentcare Clinic (Intermediate School 183): 1 intraoral unit
- New York State Psychiatric Institute: 1 intraoral unit and 1 panoramic unit
- Columbia Eastside: 6 intraoral units, and 1 panoramic - cephalographic unit
- Columbia North: 5 intraoral units, 1 panoramic unit
- Mobile Dental Facility: 2 intraoral units
- Mannie L. Wilson Health Care Center: 5 intraoral units, and 1Panoramic Unit.

1. In addition, the Radiation Safety Office performed a Preliminary Radiation Safety Shielding Evaluation for the proposed new Project Renewal Dental Clinic.

2. The Radiation Safety Office is in the process of upgrading its current Dental QA equipment. An officer of the RSO met with a representative of RTI at Columbia Morningside Heights Dental Associates (116th St.) to evaluate their new Dental QA equipment as a possible replacement for the Radiation Safety Office's current test equipment. A representative of the RSO met with additional vendors of dental QA equipment at the Radiological Society of North America meeting in Chicago on December 1-5, 2002. Further on site evaluations of dental quality assurance equipment are scheduled on March 13, 2003.

3. Audits of non-radiology X-ray facilities were conducted in July and August 2001. The departments audited included Animal Care, Endoscopy, Interventional Cardiology, Pain Management, Surgery, and Urology. Audit results were sent to the departments involved, and copies were forwarded to Radiology Medical Physics.

4. The RSO is presently coordinating with Radiology Medical Physics procedures for the audit of non-radiology X-ray facilities, policies for personnel dosimetry for fluoroscopy users, and acceptable methods for calculation of EDE, view box-inspections, and radiation safety checks of protective lead equipment.

University and Hospital Emergency Response & Management of Terrorist Events Involving Radioactive Material

On September 11, 2001, the Radiation Safety Office immediately attempted to contact the New York City Health Department, Office of Radiological Health to offer assistance and inquire about the well being of their personnel located in the downtown Manhattan area. The Radiation Safety Office staff was placed on emergency standby in order to render assistance if requested.

Shortly thereafter, the Radiation Safety Office received a list of pager and home telephone numbers of Office of Radiological Health personnel in order to maintain communications in the event of future disruptions.

As a result of these tragic events, the Joint Radiation Safety Committee formed a new Subcommittee for the Management of Radiation Incidents, chaired by David Brenner, Ph.D., to provide the University and Hospital with professional expertise in the area of possible radiological threats and the appropriate response to them. As always, the Radiation Safety Office provides the professional and technical personnel to support the Joint Radiation Safety Committee's policies and recommendations.

Activities in this new area of responsibility include:

1. On December 13, 2002, a meeting was held on the management of terrorist- initiated radiation incidents. Two officers of the Radiation Safety Office attended the meeting. Among those present was Boaz Todmor, M.D., a visiting physician from Israel on sabbatical and presently affiliated with Columbia University, Mailman School of Public Health at the invitation of Dr. Steve Morse, Director of the Center for Public Health Preparedness at the School of Public Health. Dr. Todmor shared his experience with algorithms for emergency response planning and training. Dr. Richard Sohn, Associate Dean and Director of Grants and Contracts, suggested that a draft proposal be created for submittal for potential funding. David Brenner, Ph.D., Chairman, Subcommittee on Management of Radiation Incidents, informed the meeting that he had communicated with Jim Smith, Chief of Radiation Science at the Center for Disease Control (CDC), about the possibility of grants for dealing with radiological incidents.

2. On August 24, 2002, the RSO participated in a Unit Drill on the Health Sciences Campus. The Unit Drill was led by the FDNY (Ladder 34 and Engines 67 and 84 and the Hazardous Materials (HazMat) Division in conjunction with the Columbia University Environmental Health and Safety and Security Departments.

3. On February 16, 2002, the Radiation Safety Office and the Columbia University Environmental Health and Safety Department in conjunction with the Fire Department of New York conducted an instructional tour and fire drill exercise in the Medical Center. The exercise was with the local fire department and firehouses of Engine 67 and 84, Ladder 35 and 34, Battalion 13 and Division 7. Participating in the drill were: 30 fire fighters and their top brass supported by five trucks; four officers from EHS; and one officer from the Radiation Safety Office. One of the purposes of the drill was for the fire fighters to understand the potential hazards in the laboratory environment at Columbia Health Sciences. They were instructed about different radiation labels on the laboratory doors as well as how to use a Geiger counter in emergency situations. They were also given a tour of the radioactive waste storage room and the chemical storage room.

4. On February 27, 2002, several officers of the Radiation Safety Office met with the heads of the security departments of the Columbia University Health Science Division, the New York Presbyterian Hospital, and the New

York State Psychiatric Institute. The purpose of the meeting was to ensure immediate access to radiation facilities in the event of an emergency. Immediate access by security personnel to locations containing radioactive material may be necessary in the event of an emergency.

5. On October 8, 2002, two of the officers of the Radiation Safety Office attended a meeting in Albany on the "Management of Terrorist Events Involving Nuclear Reactors or Radioactive Sources." The meeting was hosted by three local chapters of the Health Physics Society (Northeast chapter, New England Chapter, and Greater New York City Chapter). The meeting focused on: NCRP 138, Management of Terrorist Events Involving Radioactive Material; relative risk; the Office of Domestic Preparedness; radiological emergency response; improving security of regulated radioactive materials; the role of the EPA; security of nuclear power plants; and other topics. Among the presenters were Robert Feinberg, the former chairman of Nuclear Safety at GE, and George Anastas, the president of the Health Physics Society.

6. On May 9-10, 2002, two officers of the Radiation Safety Office attended training on emergency management of radiological casualties organized by the New York City Department of Health through the Armed Forces Radiobiology Research Institute (AFRRI) of the Department of Defense. The training was well received by attendees from the entire New York City area. On May 13-14, 2002, a third officer of the Radiation Safety Office attended this training program.

RSO Personnel and Facilities

Significant personnel and facilities activities in the Year 2002 included:

1. A number of RSO employees were recruited by other departments and facilities at CPMC this year. These include Ms. Jennifer Kirchherr, Technician B in the Radiation Safety Office, who accepted an officer position in the Environmental Health and Safety Office of the Columbia University Health Sciences Division, and Mr. Brian Chiongbian, Technician A in the Waste Department, who has accepted an engineering position with PET Net Pharmaceuticals at the Cyclotron Facility at Columbia University. The RSO congratulates them on their accomplishments and wishes them well in the advancement of their careers.

2. In addition, there were changes in the technical staffing in the RSO. We are fortunate at this time that all of the staff hired met or exceeded all of the requirements for the positions filled. The Radiation Safety Office appointed Ms. Olga Loukhton, who has a Masters Degree in physics, as Chief Technologist. Mr. Shuntong Guo, M.S., and Mr. Mutian Zhang were hired as Junior Physicists. Mr. Stephen Benson, B.A, was appointed to the part time Administrative Assistant position.

3. The RSO has begun the process of moving to a new location on the fourth floor of the Mailman School of Public Health (722 West 168th Street). Since a meeting on June 13, 2002 with Dr. Richard Sohn and Bob Lemieux regarding the time frame for the complete move of the RSO, the scheduled date has been pushed further back because of the immediate needs of the Institutional Animal Care and Use Committee (IACUC) for space in the location assigned to the RSO. At this time, five (5) RSO officers have moved to the new location. The present plan is that the RSO will be completely relocated to the new office space in the spring of 2003.

Professional Affiliations & Activities

BALAJEE, ADAYABALAM S., Ph.D.

Member

American Association for Advancement of Science
Radiation Research Society

Reviewer

Mutation Research
Advances in Space Research
Medical Science Monitor

Honors

Invited to contribute a chapter for a book on "Molecular mechanisms of Werner syndrome"
Invited to set up the DNA chips/cDNA microarray facility at the University of Sao Paolo, Brazil (March, 2003)
Editing a book on "DNA repair and human diseases" for Landes Biosciences, Texas, USA

BELYAKOV, OLEG V., Ph.D.

Member

American Association for Cancer Research
American Society for Therapeutic Radiology and Oncology
Association for Radiation Research
Radiation Research Society

Reviewer

Advances in Space Research
International Journal of Radiation Oncology, Biology, Physics
Mutation Research. Fundamental and Molecular Mechanisms of Mutagenesis

BIGELOW, ALAN, Ph.D.

Member

American Physical Society
Radiation Research Society

BRENNER, DAVID J., Ph.D., D.Sc.

Adjunct Faculty

Univ. of California, Berkeley, Miller Professor (2001)

Member

Columbia University Radiation Safety Committee, *Chairperson*
Columbia University Committee on Response to Radiation Terrorism, *Chairperson*
National Council on Radiation Protection and Measurements (NCRP)
NCRP Committee 1-6 on Risk Linearity
ASTRO Refresher Course, *Program Committee*
Joint Task Force on Vascular Radiation Therapy
Radiation Research Society, *Policy Committee*
International Symposium on Microdosimetry, *Organizing Committee*
International Workshop on Radiation Risk Research in Southern Urals, *Organizing Committee*
International Conference on Radiation Damage and its Modification, *Organizing Committee*
TV and radio appearances on the subject of pediatric CT examinations

CALAF, GLORIA M., Ph.D.

Adjunct Faculty

University of Tarapaca; Faculty of Sciences; Department of Biology and Health, Arica, Chile, *Adjunct Prof.*

Member

Biology Society of Chile
Mastology Society of Chile
Chilean Society of Citology
Chilean Society of Cancer
New York Academy of Sciences
Tissue Culture Association
International Association of Breast Cancer Research
American Association of Cancer Research
Society of Experimental Biology and Medicine
Radiation Research Society

Teaching

University of Tarapaca, Post Degree Course: "Pesticides on cancer," July–August, 2002

Student Mentoring

Autonomous University of Madrid, Spain, Ph.D. Advisor

GEARD, CHARLES R., Ph.D.

Member

American Society of Therapeutic Radiology and Oncology (ASTRO)
Environmental Mutagen Society
Associate Member Radiobiology Advisory Team (AMRAT) of the Armed Forces Radiobiology Research Institute (AFRRI)
Columbia University, Faculty Council, *Voting Member*
Columbia University, Mailman School of Public Health, Division of Epidemiology Ph.D. Committee
Advisory Committee on Radiobiology, Brookhaven National Laboratory
Scientific Peer Review Panel, Breast Cancer
Department of the Army, Research Program
Scientific Instrumentation Review Panel, Research Council, Ontario, Canada

Editorial Work

International Journal of Radiation Biology, Editorial Board

Reviewer

British Journal of Cancer
Mutation Research
Radiation Research

Student Mentoring

Columbia University, resident in Radiation Oncology
Albert Einstein School of Medicine, M.D. candidate

HALL, ERIC J., D.Phil., D.Sc., FACR, FRCR

Member

American Board of Radiology, *Radiotherapeutic Writ-*

ten-Test Committee
American Society of Therapeutic Radiology and Oncology (ASTRO)
Radiation Research Society
American Radium Society
International Association of Radiation Research, *Pres.*
Columbia University, College of Physicians & Surgeons Cancer Center, *Internal Advisory Committee/Executive Committee*
Columbia-Presbyterian Medical Center, Joint Radiation Safety Committee, *Chairman*; Radioactive Drug Research Committee, *Chairman*
National Council on Radiation Protection and Measurements, Committee 1, *Member*

Editorial Work
Intl. Journal of Radiation Oncology Biology Physics
International Journal of Brachytherapy

HANG, HAIYING, Ph.D.
Member
Radiation Research Society
Grant
RSNA scholar grant

HEI, TOM K., Ph.D.
Adjunct Faculty
Department of Radiological Health Science, Colorado State University, Fort Collins, Co., *Adjunct Professor*
Department of Ion Beam Bioengineering, Chinese Academy of Sciences, Hefei, China, *Adjunct Professor and Doctorate Student Mentor*
External Examiner, University of Hong Kong
Member
Chemical Pathology Study Section, 1998-2001
First International Meeting on Ion Beam, Urumqui, China, *Program Chairman*
Pathology C Study Section, *Chairman, Ad Hoc Review Panel*
Radiation Research Society
American Association for Cancer Research
Environmental Mutagen Society
Oxygen Society
Reviewer
Proceedings of the National Academy of Sciences
British Journal of Cancer
Cancer Research
Carcinogenesis
Radiation Research
Environmental Health Perspective
Inhalation Toxicology
Editorial Work
Advances in Space Sciences, section editor
Student Mentoring
Environmental Heath Sciences, Columbia University School of Public Health, doctoral student
New York City High School, science students, for Intel Science project
Okayama Medical School, 3rd year Japanese medical students in laboratory research training
Fudan University, Faculty Advisor for 4th year Chinese medical exchange students

LIEBERMAN, HOWARD, Ph.D.
Member
Summer Research Program for NYC Secondary School Science Teachers, Columbia University, *Advisory Board*
American Association for the Advancement of Science
American Society for Microbiology
Environmental Mutagen Society
Genetics Society of America
Israel Cancer Research Foundation, Scientific Advisory Board
Radiation Research Society, *Chairman*, Web-Site Committee
Sigma Xi
Theobald Smith Society
Reviewer
Grants:
Basic and Preclinical Subcommittee C of the NCI Initial Review Group, *Member*
Joint Center for Radiation Therapy Foundation, Harvard Medical School, *Reviewer*
Israel Cancer Research Fund Grant Review Panel A, *Member*
Manuscripts:
Intl Journal of Radiation Oncology, Biology and Physics
Radiation Research

MARINO, STEPHEN A., M.S.
Member
Columbia University Radiation Safety Committee
Radiation Research Society

MITCHELL, CATHERINE, Ph.D.
Member
Radiation Research Society

MITCHELL, STEPHEN, Ph.D.
Member
Radiation Research Society

PONNAIYA, BRIAN, Ph.D.
Member
Radiation Research Society
Reviewer
International Journal of Radiation Biology
Radiation Research

ZHAO, YONGLIANG, Ph.D.
Member
Radiation Research Society
Grants
RSNA Research Seed Grant.
NIEHS Center Pilot Grant.

Publications

1. **Balajee AS** and Colette ApRhys, Helicase domain containing proteins in human disorders, *Curr Genomics* **2**:305-24, 2001.
2. **Belyakov OV**, Folkard M, Mothersill C, Prise KM and Michael BD. Bystander-induced apoptosis and premature differentiation in primary urothelial explants after charged particle microbeam irradiation. *Radiat Prot Dosimetry* **99**:249-51, 2002.
3. **Belyakov OV**, Folkard M, Mothersill C, Prise KM and Michael BD. Non-targeted effects of radiation: applications for radiation protection and contribution to LNT discussion. In Proceedings of the European IRPA Congress 2002 "Towards harmonisation of radiation protection in Europe," Florence, Italy, 8-11 October 2002.
4. **Bigelow AW**, **Randers-Pehrson G** and **Brenner DJ.** Laser Ion Source Development for the Columbia University Microbeam. *Rev Sci Instrum* **73**:770, 2002.
5. **Bigelow AW**, **Randers-Pehrson G** and **Brenner DJ.** Laser Ion Source for the Columbia University Microbeam, *9th International Conference on Nuclear Microprobe Technology and Applications, ICNMTA 2002*. Manuscript to be published by Elsevier Science B.V. in a special issue of Nuclear Instruments and Methods B.
6. **Brenner DJ**. Estimating cancer risks from pediatric CT: going from the qualitative to the quantitative. *Pediatr Radiol* **32**:228-3; discussion 42-4, 2002.
7. **Brenner DJ** and **Hall EJ**. Microbeams: a potent mix of physics and biology. Summary of the 5th International Workshop on Microbeam Probes of Cellular Radiation Response. *Radiat Prot Dosimetry* **99**:283-6, 2002.
8. **Brenner DJ**, Martinez AA, Edmundson GK, **Mitchell C**, Thames HD and Armour EP. Direct evidence that prostate tumors show high sensitivity to fractionation (low alpha/beta ratio), similar to late-responding normal tissue. *Int J Radiat Oncol Biol Phys* **52**:6-13, 2002.
9. **Brenner DJ** and Sachs RK. Do low dose-rate bystander effects influence domestic radon risks? *Int J Radiat Biol* **78**:593-604, 2002.
10. **Brenner DJ**, Sawant SG, Hande MP, Miller RC, **Elliston CD**, Fu Z, **Randers-Pehrson G** and **Marino SA**. Routine screening mammography: how important is the radiation-risk side of the benefit-risk equation? *Int J Radiat Biol* **78**:1065-7, 2002.
11. **Calaf G** and **Hei TK**. Carcinogenesis por Radiacion, in: *Oncologia Molecular y Celular* (Bonfil RD, Scharovsky OG (ed), Editorial Dunken, Buenos Aires, Argentina, pp, 113-24, 2002.
12. Cornforth MN, Greulich-Bode KM, Loucas BD, Arsuaga J, Vazquez M, Sachs RK, Bruckner M, Molls M, Hahnfeldt P, Hlatky L and **Brenner DJ**. Chromosomes are predominantly located randomly with respect to each other in interphase human cells. *J Cell Biol* **159**:237-44, 2002.
13. De Santis LP, Garci GL, **Balajee AS**, Stefanini M and Palitti F. Transcription coupled repair efficiency determines the cell cycle regulation and apoptosis after UV irradiation in hamster cells. *DNA Repair* **1**:209-23, 2002.
14. Dynlacht JR, Dewhirst MW, **Hall EJ**, Rosenstein BS and Zeman EM. Toward a consensus on radiobiology teaching to radiation oncology residents. *Radiat Res* **157**:599-606, 2002.
15. Elder RT, Song X-q, Chen M, Hopkins KM, **Lieberman HB** and **Zhao Y**. Involvement of *rhp23*, a *S. pombe* orthologue of the human *HHR23A* and *S. cerevisiae RAD23* nucleotide excision repair genes, in cell cycle control and protein ubiquitination. *Nucl Acids Res* **30**:581-91, 2002.
16. **Hall EJ**. Introduction to session I: Helical CT and cancer risk. *Pediatr Radiol* **32**:225-7, 2002.
17. **Hall EJ**. Lessons we have learned from our children: cancer risks from diagnostic radiology. *Pediatr Radiol* **32**:700-6, 2002.
18. **Hang H**, **Zhang Y**, Dunbrack RL Jr, Wang C and **Lieberman HB**. Identification and characterization of a paralog of human cell cycle checkpoint gene *HUS1*. Genomics **79**:487-92, 2002.
19. **Hei TK**, Xu An and **Zhao YL**. Genotoxic and carcinogenic mechanisms of mineral fibers: Role of reactive radical species. *Lung Injury and Disease* (in press 2002).
20. Kessel M, **Liu SX**, Xu A, Santella R and **Hei TK**. Arsenic induces oxidative DNA damage in mammalian cells. *Mol & Cell Biochem* **234**:301-8, 2002.
21. Marples B, Cann NE, **Mitchell CR**, Johnston PJ, Joiner MC. Evidence for the involvement of DNA-dependent protein kinase in the phenomena of low dose hyperradiosensitivity and increased radioresistance. *Int J Radiation Biology* **78**:1139-47, 2002.
22. **Mitchell CR**, Folkard M, Joiner MC. Effects of exposure to low dose-rate ^{60}Co gamma-rays to human tumor cells *in vitro*. *Radiation Research* **158**:311-8, 2002
23. **Mitchell CR**, Joiner MC. The effect of subsequent acute-dose irradiation on cell survival *in vitro* following low dose rate exposures. *Int J Radiation Biology* **78**:981-90, 2002
24. Prise KM, **Belyakov OV**, Folkard M, Ozols A, Schettino G, Vojnovic B and Michael, BD. Investigating the cellular effects of isolated radiation tracks using microbeam techniques. *Adv Space Res* **30**:871-6, 2002.
25. Prise KM, **Belyakov OV**, Newman HC, Patel S, Schettino G, Folkard M and Michael BD. Non-targeted effects of radiation: bystander responses in cell and tissue models. *Radiat Prot Dosimetry* **99**:223-6, 2002.
26. **Roy D, Calaf G** and **Hei TK.** Allelic imbalance at 11p15.5-15.4 correlated with *c-Ha-ras* mutation during radiation-induced neoplastic transformation of human breast epithelial cells**.** *Int J Cancer* (in press 2002).
27. Sawant SG, Zheng W, **Hopkins KM**, **Randers-Pehrson G**, **Lieberman HB** and **Hall EJ**. The radiation-induced bystander effect for clonogenic survival. *Rad Res* **157**:361-4, 2002.
28. Shukla A, Gulumian M, **Hei TK**, Kamp D, Rahman Q,

Aust A and Mossman B. Multiple roles of oxidants in the pathogenesis of asbestos induced diseases. *Free Radical Biology and Medicine* (in press 2002).

29. Worgul BV, **Smilenov L**, **Brenner DJ**, Junk A, Zhou W and **Hall EJ**. Atm heterozygous mice are more sensitive to radiation-induced cataracts than are their wild-type counterparts. *Proc Natl Acad Sci (USA)* **99**:9836-9, 2002.
30. Xu A, **Zhou HN**, Yu D and **Hei TK**. Mechanisms of the genotoxicity of crocidolite asbestos in mammalian cells: Mutation patterns induced by reactive oxygen species. *Environ Hlth Persp* **110**:1003-8, 2002
31. **Zhao YL**, **Piao CQ** and **Hei TK**. Down regulation of betaig-h3 gene is causally linked to tumorigenic phenotype in asbestos treated immortalized human bronchial epithelial cells. *Oncogene* **21**:7471-7, 2002.
32. **Zhao YL**, **Piao CQ** and **Hei TK**. Overexpression of Betaig-h3 gene downregulates integrin $\alpha 5\beta 1$ and suppresses tumorigenicity in radiation induced tumorigenic human bronchial epithelial cells. *British J Cancer* **86**:1923-8, 2002.
33. **Zhao YL**, **Piao CQ** and **Hei TK.** Tumor suppressor function of the Big-H3 gene in radiation carcinogenesis. *Advances Space Research* (in press 2002).
34. **Zhou HN**, **Randers-Pehrson G**, Suzuki M, Waldren C and **Hei TK**. Genotoxic damage in non-irradiated cells: Contribution from bystander effect. *Radiation Protection Dosimetry* **99**:227-32, 2002.
35. **Zhou HN**, **Randers-Pehrson G**, Waldren C and **Hei TK.** Radiation induced bystander effect and adaptive response: implication for low dose radiation risk assessment. *Advances Space Research* (in press 2002).
36. **Zhou HN**, Suzuki M, **Geard C** and **Hei TK**. Effects of irradiation medium with or without cells on bystander cell responses. *Mutation Research* **499**:135-41, 2002.
37. **Zhou HN**, Xu A, Suzuki M, **Randers-Pehrson G**, Waldren C, **Hall EJ** and **Hei TK**. The Yin and Yan of bystander versus adaptive response: lessons from the microbeam studies. *Int Congress Series* **1236**:241-7, 2002.